SEA
GRANT
PROJECT
OFFICE

MATHEMATICAL SIMULATION OF TIDAL TIME-AVERAGES OF SALINITY AND VELOCITY PROFILES IN ESTUARIES

by

John S. Fisher
John D. Ditmars
and
Arthur T. Ippen

Massachusetts Institute of Technology
Cambridge, Massachusetts 02139

Report No. MITSG 72-11
July 31, 1972

MATHEMATICAL SIMULATION OF TIDAL TIME-AVERAGES OF SALINITY AND VELOCITY PROFILES IN ESTUARIES

by

John S. Fisher

John D. Ditmars

and

Arthur T. Ippen

Report No. MITSG 72-11

Index No. 72-311-Ccb

ABSTRACT

A mathematical model is developed using analytical techniques to determine the longitudinal and vertical distributions of velocities and salinities, averaged over a tidal period, for mixed but partially stratified estuaries. The flow field is assumed laterally homogeneous and the estuary width and depth are assumed to be functions of the longitudinal coordinate only. Required inputs to the model include the salt intrusion length, the ocean boundary salinity, the distribution of the depth-averaged salinity and the freshwater discharge.

The governing equations included in the model are the vertical and longitudinal equations of motion, continuity, salt conservation and an equation of state. The key assumption is that the longitudinal salinity gradient is independent of depth. This decouples these equations and thus permits an analytical solution to be found.

Using data from laboratory flume tests from the U.S. Army Waterways Experiment Station and the Delft Hydraulics Laboratory, and field surveys from the James River Estuary, the model solutions are used to find correlations for the mean vertical transfer coefficients of mass and momentum with gross characteristics of the estuary. These correlations, plus the results from a one-dimensional numerical model, permit this analytical model to be used as a predictor of the velocity and salinity profiles in estuaries and to relate changes in freshwater discharge to possible changes in the location of shoaling zones.

ACKNOWLEDGEMENT

Primary support for this study came from the Office of Sea Grant, National Oceanic and Atmospheric Administration, U.S. Department of Commerce, Coherent Area Project Grant GH-88 and 2-35150, under the Estuary Modeling Program underway at the Ralph M. Parsons Laboratory for Water Resources and Hydrodynamics of the Department of Civil Engineering. This program is under the administrative and technical supervision of Professor Arthur T. Ippen and Professor Donald R.F. Harleman (DSR 72602 and DSR 73479). The purpose of the Estuary Modeling Program is to develop analytical and numerical techniques for modeling the behavior of estuaries and coastal embayments in order to extend the basic understanding of estuarine dynamics and the ability to make predictions relating to the estuarine environment.

Dr. Donald R.F. Harleman has carefully followed the development of this work and has provided valuable guidance and assistance. Dr. M. Llewellyn Thatcher has also provided additional advice. The authors also wish to extend their appreciation to Dr. Gerritt Abraham at the Delft Hydraulics Laboratory and to Dr. J. J. Dronkers, Department of Public Works, The Netherlands, for their assistance in making available the data from the Delft salinity flume. Mr. Frank Hermann provided similar assistance in obtaining data from the salinity flume studies at the Waterways Experiment Station, U.S. Army Corps of Engineers sponsored by the Tidal Hydraulics Committee of the Corps.

A major part of the computer work was done at the M.I.T. Information Processing Center. Grateful acknowledgement is due to Mrs. Stephanie M. Demeris for her careful typing of this report. The material contained in this report was submitted by Mr. Fisher in partial fulfillment of the requirements for the degree of Doctor of Philosophy at M.I.T.

TABLE OF CONTENTS

LIST OF FIGURES

LIST OF TABLES

LIST OF SYMBOLS

A	cross-sectional area of the estuary
b	estuary width
C	Chezy resistance coefficient
D, D_y	vertical coefficient of eddy momentum flux, averaged over a tidal period
$\bar{D}$	effective constant value of D_y
d_c	depth from surface to centroid of cross-sectional area
E	longitudinal dispersion coefficient, $E(x,t)$
E_T	longitudinal dispersion coefficient in freshwater region
E_D	estuary number, $\frac{P_T F_D^2}{Q_f T}$
f	Coriolis parameter
F_D	densimetric Froude number evaluated at the entrance to the estuary $= \frac{u_o}{\sqrt{gh\frac{\Delta\rho}{\rho}}}$
g	acceleration of gravity
h, h_o	depth of mean water level
K_x, K_y	horizontal and vertical coefficients of eddy salt flux, averaged over a tidal period
$\bar{K}$	effective constant value of K_y
k_y	eddy diffusivity
K_l	longitudinal dispersion parameter
L_i	salinity intrusion length
L	length of estuary
ℓ, ℓ_α	mixing length (adiabatic)
n	Manning's resistance coefficient

p	instantaneous pressure
$\bar{p}$	mean pressure averaged over a few minutes
P	mean pressure averaged over a tidal period
p_t	tidal component of two-dimensional pressure
p'	turbulent pressure fluctuations
P_T	tidal prism, defined as the total volume of water entering the estuary on the flood tide
$\bar{Q}$	one-dimensional instantaneous local discharge, $Q(x,t)$
Q_f	freshwater discharge
q	lateral inflow to one-dimensional estuary model
R_h	hydraulic radius
R_i	Richardson number
s	instantaneous salinity
$\bar{s}$	mean salinity averaged over a few minutes
s'	turbulent salinity fluctuation
S	mean salinity averaged over a tidal period $S(x,y)$
$\bar{S}$	one-dimensional instantaneous local salinity, $\bar{S}(x,t)$
S_t	tidal component of two-dimensional salinity
S_o	ocean salinity
S_d	time-averaged,depth-averaged salinity, $S_d(x)$
t	time
T	tidal period
u	instantaneous horizontal velocity, $u(x,y,t)$
$\bar{u}$	mean velocity averaged over a few minutes
u'	turbulent component of u
u_t	tidal component of u
U	average of u over a tidal period, $U(x,y)$

$\bar{U}$	one-dimensional instantaneous horizontal velocity $\bar{U}(x,t)$
U_f	freshwater velocity
u_o	maximum flood velocity at estuary entrance
v	instantaneous vertical velocity, $v(x,y,t)$
$\bar{v}$	v, averaged over a few minutes
v'	turbulent component of v
v_t	tidal component of v
V	average of v over a tidal period, $V(x,y)$
w'	turbulent component of lateral velocity
x	longitudinal axis
y	vertical axis
x	lateral axis
α	conversion factor in equation of state (assumed = 0.75)
ε_x	eddy viscosity
η	dimensionless depth, y/h
Θ	dimensionless salinity, S/S_o, $\Theta(\xi,\eta)$
Θ_d	dimensionless depth-averaged salinity, S_d/S_o, $\Theta_d(\xi)$
ξ	dimensionless longitudinal coordinate, x/L_i
ρ	density, $\rho(x,y,t)$
ρ_o	reference density
$\bar{\rho}$	ρ averaged over a few minutes
ρ_t	tidal variation of ρ
ρ_m	ρ averaged over a tidal period, $\rho(x,y)$
Ψ	stream function
ψ	dimensionless stream function Ψ/Q_f

I. Introduction

1.1 Estuaries as Natural Resources

Coastal zones and estuaries, in particular, provide major resources for both the economic and social well-being of modern man. In recognition of these valuable resources, increased efforts are being made to insure and protect them from needless deterioration and neglect. To aid in these efforts a more complete understanding of the complex interrelationships between the biological, chemical and physical mechanisms of estuaries needs to be developed.

Estuaries are being used as sinks for industrial and municipal wastes. When properly balanced with assimilative capacities, this may be a practical use of these water bodies. However, careful attention must be given to the types and amounts of effluents discharged, in order to avoid conflicts with their great potential for biological productivity and recreation by man.

In order to achieve this balance of uses, a thorough understanding of the complex circulation patters of salt and freshwater in the estuaries is needed.

1.2 Estuarine Circulation - A General Description

An estuary is defined as a body of water connecting a source of freshwater with a tidal sea or bay and extends over the length of tidal action. Natural estuaries, with their irregular boundaries, have highly complex patterns of circulation of the salt and freshwater masses contained within them. The compounded influences of the factors involved, i.e., the complex geometry, the tidal flows, the mixing induced b them

and by the density differences makes estuarine behavior a very difficult subject for analytical description.

Figure 1.1 is a representation of a typical estuary as might be found on the eastern seaboard of the United States. This estuary receives freshwater flows from several rivers and streams and terminates in a bay or the ocean. Perhaps the most striking feature is the irregular boundaries. There are turns and embayments as well as a nonuniform expansion from the narrow section at its inland end to the wide section at the sea boundary. Hence, local eddying and flow reversals must be expected throughout the flow field, and in general, the velocity will have time-varying components in the longitudinal, lateral and vertical directions. However, the predominant direction for the velocity is along the longitudinal axis, periodically changing direction with the tide. Certain sections of the estuary can have strong lateral components during portions of a tidal period.

The influence of tides makes the flow in estuaries unsteady in time, both within a tidal period, and during longer lunar phases. The seasonal variation in the rates of freshwater inflow will also contribute an additional long-term dynamic unsteadiness to estuarine flows.

One of the most important factors influencing the complex circulation is the density difference between the river discharge at the head, and the ocean salinity at the mouth. Density currents resulting from these differences are often major components of the total circulation, and must be included in a realistic model of the flow field.

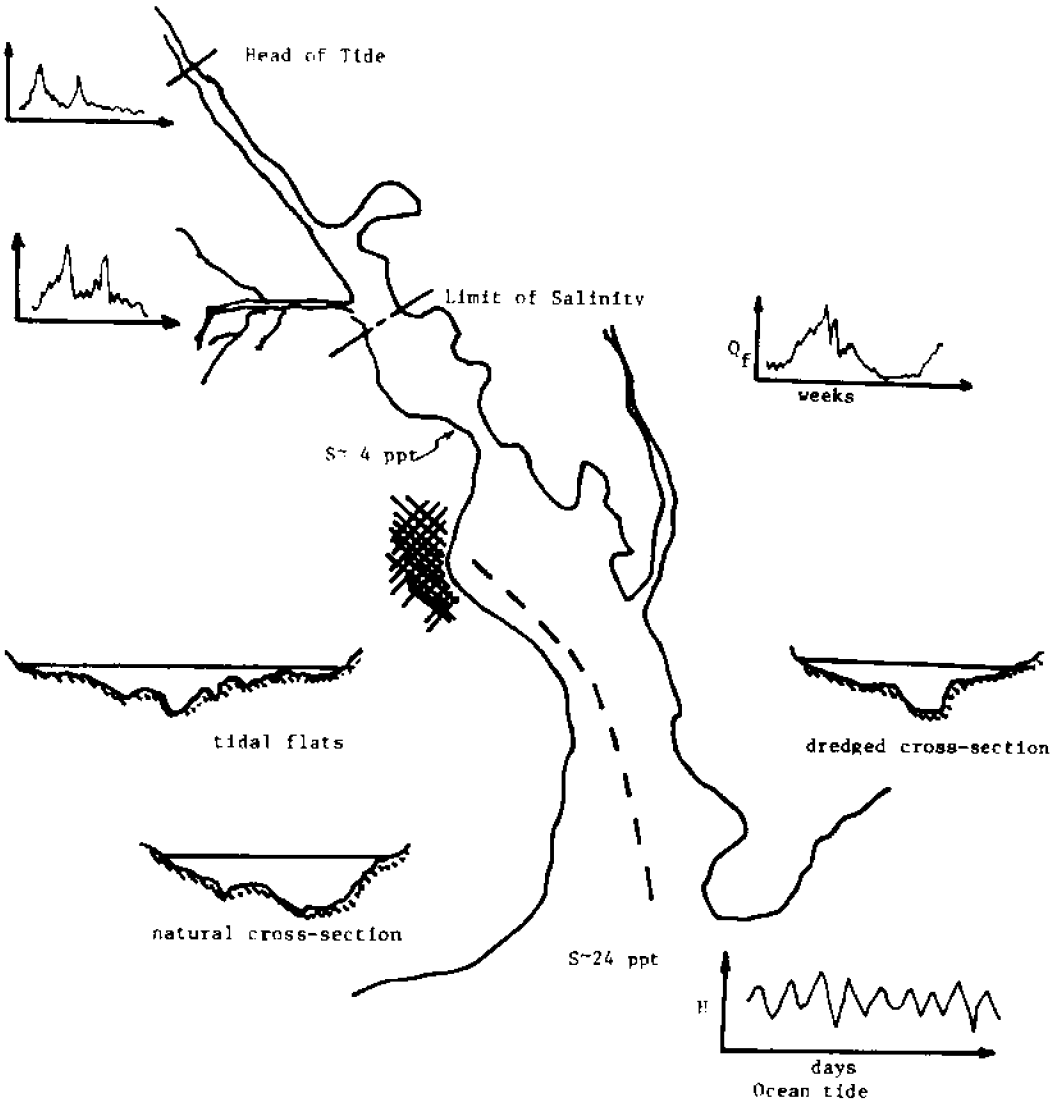

Figure 1.1 Typical estuary, eastern U.S. coast

For some estuaries, the effects of surface winds or Coriolis accelerations may be a significant influence on the circulation. However in general, these factors are of secondary importance when compared with the effects of complex geometry, tidal mixing and density differences and will not be considered further in the present development.

1.3 Estuary Modeling Techniques

The purpose of building models of estuaries is to represent the complex circulation of the prototype in a simplified form which can be tested and studied to determine the possible consequences of modifications of controlling factors on the natural circulation. Examples of such changes could include the dredging of a navigation channel, the diversion of freshwater inflow to other basins, or the placement of a diffuser for the heated condenser water of an electric power station. The former might seriously alter the salinity distribution while the latter could obviously influence normal biological cycles. Recourse to various types of models must be made to provide estimates of the impact of such changes.

There are two main methods for modeling estuaries; physical and mathematical models. Only a very brief review of these techniques is needed here since Tracor (1971) has recently presented a complete survey of this field.

1.3.1 Physical Models

A Physical hydraulic model provides direct visual observation of flow. They can also be carefully instrumented for detailed measurements of the velocity field, water surface elevations and dissolved or

suspended substances. Physical models of estuaries are distorted due to large prototype dimensions. Vertical scales are frequently 1:100 while horizontal scales may be 1:1000. This results in a 1:10 distortion of all cross-sections. General usage has shown that in spite of this distortion, these models can be made to reproduce many details of the circulation as well as of the distribution of salinity.

At the present time, physical models of estuaries are the most important technique for determining the effects of changes in the prototype. Their great expense and slow building and operating times are drawbacks which sophisticated mathematical models may avoid. However, one can expect these physical models to continue to be important tools for estuarine analysis for a long time to come.

1.3.2 Mathematical Models

The movement of water and the distribution of dissolved substances in estuaries are governed by physical laws for which there are known mathematical descriptions. In many cases, where various simplifying assumptions can be made, these mathematical descriptions can be written as equations for which there are known solutions. Depending upon the solution technique, these models are referred to as either numerical or analytical models. A numerical solution implies replacing the governing differential equations with approximate forms which can be solved by computer. An analytical solution is an exact solution of the original equation,by integration, with no subsequent approximations.

The application of analytical models to problems of estuarine circulation is limited by the mathematical complexity of the governing

equations. In order to reduce these equations to a form which can be solved analytically, various assumptions may be introduced which often render the final solutions very limited in application. However, there are several analytical estuary models which can yield meaningful results.

In general, these analytical models describe conditions averaged over one or more tidal cycles. Thus, they serve a limited function if changes within a tidal period are of interest. This will of course depend on the problems being considered. Analytical models are also usually restricted to one or two space dimensions, e.g., to depth and lateral, lateral and longitudinal, or depth and longitudinal directions. Finally, these analytical models are restricted to problems for which simple boundary conditions can be prescribed.

Until the advent of the modern high speed computer, analytical models were the only mathematical technique for describing estuarine circulation. Numerous models of tidal flushing, salinity distribution and tidal motions, had been developed. Many of these models continue to have application today in conjunction with the more powerful numerical methods. These models have also played an important role in clarifying the physical understanding of the important processes and in deriving the proper equations to be included in the newer models.

The greater part of the recent literature on estuarine modeling pertained to numerical mathematical models. These models use advanced computer techniques to find solutions to the governing equations of motion and of mass conservation. One-, two- and three-dimensional models have been developed, the latter however only in a very preliminary form.

An important feature of these models is their ability to handle the unsteady case, i.e., within a tidal period. Thus, the averaging over a tidal period which was required for most analytical models is not required for numerical models.

At the present time, the numerical models available for engineering applications are of either the unsteady one- or two-dimensional type. A one-dimensional model averages all dependent variables over the cross-sectional area, and thus yields changes in mean values with time and along the longitudinal axis. These models can be used to predict water surface elevation, mean currents, and mean salinities. They can also be used with certain reservations to determine the cross-sectional mean concentration of a non-conservative water quality parameter, such as dissolved oxygen or biochemical oxygen demand .

Two-dimensional numerical models usually allow variations along the lateral as well as along the longitudinal axis. In this case, the only averaging is with depth. Again, these models can predict currents, water quality parameters, etc. These models are more complex than the one-dimensional case with regard to the computational techniques required.

1.4 Objectives of this Study

The techniques for estuarine modeling described in the preceeding sections suggest a possible combined approach. Physical models can be used with mathematical models to analyse different scales of circulation problems. Also, analytical models can be used with numerical models to increase the number of spatial dimensions of the solution.

This investigation develops a two-dimensional analytical model of estuarine circulation including vertical and longidudinal distributions of velocity and salinity. All equations are averaged over one or more tidal periods. This model can be coupled with a one-dimensional numerical model which is not time-averaged, but is averaged over a cross-section.

The ability to calculate vertical variations of the important flow parameters is often a useful tool for solving estuarine problems. Vertical salinity stratification is a key element in the circulation pattern of an estuary. Models which can predict the effects of changing geometry, freshwater inflows, etc., on this stratification are of great value. The modeling of vertical velocity profiles is another useful model capability. Many problems of shoaling in estuaries can only be properly studied with a knowledge of the vertical distribution of velocity.

If a model similar to the one described above is to have practical application as a predictive tool, all parameters included in the solution technique must be determinable in advance. Thus, an important part of the objectives of this study is to obtain relationships between the various time-averaged coefficients of turbulent diffusion and eddy viscosity included in the model and the gross parameters of estuarine circulation.

1.5 Synopsis of the Study

The analytical model described in the previous section can be used to find the longitudinal and vertical distributions of velocity and salinity for partially stratified or well mixed estuaries. All model

results are for conditions averaged over a tidal period. Certain coefficients of mixing included in the mathematical equations of the model have been correlated with various parameters for the estuary in question from field and laboratory experiments. Proper application of this model requires a coupling with a one-dimensional unsteady numerical model.

The model has been developed and tested with data from laboratory flumes and field surveys. Results indicate the model has practical application in the prediction of salinity stratification and shoaling changes as might result from the engineering modifications of the factors which control estuarine circulation.

II. Previous Investigations

2.1 Analysis of Recorded Data

The last twenty-five years have been a period of active interest in the description and theoretical analysis of the circulation and mixing characteristics of estuaries. A large body of literature has evolved covering results from field surveys, laboratory experiments and theoretical analysis. These publications are as diverse as the estuaries they discuss, and this chapter will not attempt to review them all. A very excellent survey of this work is presented by Bowden (1966). The present review is restricted to those articles which discuss the vertical distributions of velocity and salinity for partially stratified estuaries.

Pritchard (1952) describes the circulation in the Chesapeake Bay estuarine system, and in particular, in the James River estuary. Data from an extensive program of field surveys are discussed, in which salinities, temperatures and velocities were measured at several depths and stations and averaged over one or more tidal periods. The resulting net circulation and salinity distributions are typical for partially stratified conditions. A basic feature of this net circulation is a reversal in the vertical distribution of the time-averaged horizontal velocity. In the surface region, extending to about middepth, the net flow is towards the ocean, while the bottom region has flow in the opposite direction, towards the river end of the estuary. The depth integral of this velocity is equal to the net discharge of freshwater. Although two regions can be identified for the velocity, the vertical salinity distribution can not be separated into two distinct zones. In

partially stratified estuaries, there is a continuous increase in salinity from the surface to the bottom, without a noticable point of discontinuity.

Pritchard (1952, 1954) also identifies several interesting features of the longitudinal salinity gradient. For all depths, there is an increase in salinity from the freshwater region to the boundary salinity at the ocean end. In addition, over most of the estuary this longitudinal salinity gradient is nearly independent of depth, i.e., vertical position. This latter feature does not hold very near the ocean boundary or where the salinity goes to zero, upstream.

Pritchard (1954) discusses the various terms in the equation of salt conservation and uses the James River data to back-calculate the relative order of these terms. In this analysis, the velocity and salinity are written as the sum of three terms

$$u = U + U_t + u' \qquad 2.1$$

$$s = S + S_t + s' \qquad 2.2$$

where U is a mean velocity for one or more tidal periods, U_t is a one-dimensional tidal velocity (assumed perodic) and u' is a random fluctuation due to turbulence. A similar set of definitions is made for the salinity.

The salt conservation equation averaged over a tidal period is written

$$\frac{\partial S}{\partial t} + U \frac{\partial S}{\partial x} + V \frac{\partial S}{\partial y} = \frac{\partial}{\partial x} \left(K_x \frac{\partial S}{\partial x}\right) + \frac{\partial}{\partial y} \left(K_y \frac{\partial S}{\partial y}\right) \qquad 2.3$$

where U and V are the mean components of velocity in the horizontal and vertical directions, x and y, respectively. K_x and K_y are identified as mean coefficients of eddy diffusivity where $K_x \frac{\partial S}{\partial x}$ represents the cross-product of the turbulent terms $\overline{u's'}$ averaged over a tidal period. Similarly, $K_y \frac{\partial S}{\partial y}$ replaces $\overline{v's'}$. The bar over the products represents the time-average over the tidal period. All other cross-products are assumed uncorrelated, and hence zero. The above equation assumes homogeneous conditions in the lateral direction.

For the period of study, Pritchard found the $\frac{\partial S}{\partial t}$ term to be small, indicating that the freshwater inflows to the James River estuary were nearly steady. The horizontal advection $U \frac{\partial S}{\partial x}$ was found to be much larger than the horizontal eddy diffusion $\frac{\partial}{\partial x} \left(K_x \frac{\partial S}{\partial x}\right)$ and also larger than the vertical advection $V \frac{\partial S}{\partial y}$ except near middepth. With these considerations, a simplified mass balance can be written

$$U \frac{\partial S}{\partial x} + V \frac{\partial S}{\partial y} = \frac{\partial}{\partial y} \left(K_y \frac{\partial S}{\partial y}\right). \qquad 2\text{-}4$$

Pritchard (1956) then developed the equations of motion for a simple partially stratified estuary using the same James River data as cited before. Surface shear due to wind is neglected. The longitudinal conservation of momentum equation, averaged over a tidal period, is

$$U \frac{\partial U}{\partial x} + V \frac{\partial U}{\partial y} + U_t \frac{\partial U_t}{\partial x} = - \frac{1}{\rho} \frac{\partial p}{\partial x} - \frac{\partial \overline{u'u'}}{\partial x} - \frac{\partial \overline{v'u'}}{\partial y} - \frac{\partial \overline{w'u'}}{\partial z} \qquad 2.5$$

where p is the hydrostatic pressure, ρ the density, w' the turbulent fluctuation of the lateral velocity component (z axis). By analogy with the conservation of salt equation, Pritchard argues that only the vertical eddy diffusion of momentun $\frac{\partial \overline{v'u'}}{\partial y}$ needs to be retained. The time-averaged field acceleration terms for the James River data are also small. Finally, the acceleration resulting from the tidal component of the velocity $U_t \frac{\partial U_t}{\partial x}$ is an order smaller than the terms on the right-hand-side of the equation. Using similar arguments, the lateral momentum equation is written

$$0 = - \frac{1}{\rho} \frac{\partial p}{\partial z} + fU - \frac{\partial \overline{w'u'}}{\partial y} \qquad 2.6$$

where f is the Coriolis parameter. Using appropriate boundary conditions, equations 2.5 and 2.6 are solved for the distributions of the turbulent mementum flux terms, averaged over a tidal period. The results indicate that the mean fluxes are zero at the surface and near the bottom, with a somewhat parabolic distribution having a maximum near middepth.

2.2 Analytical Modeling of Circulation

The net circulation averaged over a tidal period described by Pritchard (1952, 1954, 1956) has been used by several investigators as a basis for the development of analytical models. These models have several applications, an important one being the analysis of shoaling zones in estuaries. Simmons (1955) and others have identified a

relationship between locations where the net horizontal velocity at the bottom of a channel reverses direction and zones of high rates of shoaling. Thus, analytical models which can predict the location of this reversal, called a "null point", have practical engineering applications.

Abbott (1960) examines the role of the longitudinal salinity gradient in determining the direction of the net, near bottom drift velocity. Using the assumptions of Pritchard(1956), the longitudinal momentum equation, averaged over a tidal period,is written

$$\frac{1}{\rho}\frac{\partial \bar{\tau}_{xy}}{\partial y} = g\frac{dh_0}{dx} + g\left(\frac{h_0 - y}{\rho}\right)\frac{\partial \rho}{\partial x} \qquad 2.7$$

where $\bar{\tau}_{xy}$ is the mean shear and h_0 is the mean water level. Assuming zero surface stress, this equation is integrated over the depth and the mean stress on the bed is found

$$\bar{\tau}_{xyb} = gh\left(\frac{1}{2}h\left(-\frac{\partial \rho}{\partial x}\right) - \rho\frac{\partial h_0}{\partial x}\right) \qquad 2.8$$

where h(x,z) is the local water depth. Abbott also shows that this bed shear, for an oscillating flow, is in the same direction as the drift velocity

$$\bar{\tau}_{xyb} \sim U \qquad 2.9$$

From 2.8 it is seen that the drift velocity will be either positive or negative when

$$\frac{1}{2}h\left(-\frac{\partial \rho}{\partial x}\right) \gtrless -\rho\frac{\partial h_0}{\partial x}. \qquad 2.10$$

In order to apply this criterion, accurate measurements of the mean surface slope $\frac{\partial h_0}{\partial x}$ and the mean density gradient $\frac{\partial \rho}{\partial x}$ are needed , the former being a difficult parameter to determine in most cases. Abbott assumes the salinity gradient to be independent of depth. Data of this type is used to test the criterion for the Thames and Mersey estuaries. For the Thames, using data reported by Inglis and Allen (1957), no reversal in drift velocity is predicted by this method, although the field studies indicate the existence of a null point. Abbott suggests an additional momentum flux must be present in this case, perhaps a non-linear tidal convection. In the case of the Mersey, a null point is predicted near the location observed in field studies. Here the model appears to reflect the physical processes involved rather well.

Hansen and Rattray (1965) present an analytical model of estuarine circulation averaged over one or more tidal periods. A simultaneous solution of the equations of mass and momentum conservation, assuming geometric similarity of velocity and salinity profiles and lateral homogeniety is developed. The estuary is divided into three regions inner, central and outer, for which different assumptions about salinity gradients and mixing coefficients are made. The equations included in the model are:

momentum $$\frac{\partial p}{\partial x} = \frac{\partial}{\partial y} (\rho D \frac{\partial U}{\partial y}) \qquad 2.11$$

$$\frac{\partial p}{\partial y} = \rho g \qquad 2.12$$

continuity $$\frac{\partial U}{\partial x} + \frac{\partial V}{\partial y} = 0 \qquad 2.13$$

mass $$U\frac{\partial S}{\partial x} + V\frac{\partial S}{\partial y} = \frac{\partial}{\partial x}\left(K_x \frac{\partial S}{\partial x}\right) + \frac{\partial}{\partial y}\left(K_y \frac{\partial S}{\partial y}\right) \qquad 2.14$$

state $$\rho = \rho_o(1 + \alpha S) \qquad 2.15$$

where D is the eddy viscosity and α is a conversion factor for salinity. The boundary conditions include zero velocity at the bottom, known stress at the surface, net flow equal to river discharge and zero net salt flux. Hansen and Rattray do not discuss the differences between the classically defined eddy viscosities and eddy diffusivities and the eddy coefficients which appear in their equations for conditions averaged over a tidal period. These differences are examined in detail in the next chapter of the present analysis. For the purposes of this review, it is important to note that all eddy coefficients introduced into the equations include neglected terms, terms resulting from averaging over a tidal period, as well as the averages of the turbulent cross-products.

For the central or middle region of the estuary, the authors assume that the longitudinal salinity gradient is independent of both depth and longitudinal position. The velocities are assumed only dependent upon depth, and thus similar at different stations. The vertical eddy coefficients, D and K_y are held constant with depth and the horizontal eddy diffusivity K_x is related to the freshwater velocity

$$\frac{d}{dx}(K_x) = U_f. \qquad 2.16$$

With the above assumptions, solutions can be found for the vertical distributions of velocity and salinity. Except for the possible variation in K_x, the solution is independent of longitudinal position. For the condition of zero for the net surface wind stress, two dimensionless parameters determine the vertical velocity and salinity profiles

$$R_a = \frac{g\beta S_o h^3}{DK_{xo}} , \quad M = \frac{K_y K_{xo}}{U_f^2 h^2} \qquad 2.17$$

where S_o and K_{xo} are S and K_x at x = 0 respectively, and U_f is the freshwater velocity. By a proper choice of values for R_a and M, the solution can be fitted fairly well to some of Pritchard's James River data.

For the inner and outer portions of the estuary, near the river and ocean end respectively, different assumptions about eddy coefficients are made. The solutions in these regions still require similarity of velocity and salinity profiles.

Hansen (1966) proposes a non-similarity solution for a similar set of governing equations. Again, the longitudinal dependence of the velocities and salinities is determined by the longitudinal variation of the horizontal eddy diffusivity. However, Pritchard (1952) shows that the longitudinal eddy flux of salt is the smallest term in the time-averaged salt balance. Hansen is thus using the weakest term in the model to provide the longitudinal dependence.

McGregor (1972) develops an analytical model of the net, non-tidal bottom transport velocity for an estuary. This model is similar to

other studies in that a longitudinal force balance includes only the pressure gradient and the vertical eddy stress gradient. For the pressure gradient, both a surface slope and density gradient are evaluated from recorded data for the Humber estuary. The solution technique introduces a number of empirical constants for fitting these distributions, as well as an empirical expression for the mean eddy viscosity. By proper fitting of the numerous constants, McGregor is able to match the net bottom velocity zero points with the shoaling zones for the Humber. The analysis is a good illustration of the roles of the surface slope, salinity gradient and river discharge in determining the zones of high rates of shoaling. However, due to the need to fit several constants to previous data, the model is of limited predictive capability.

2.3 Turbulent Diffusion

As shown in the previous section, mathematical modeling introduces coefficients of turbulent diffusion for mass and momentum. There have been a few investigations which have attempted to measure these coefficients and relate them to the mean properties of the flow field.

Kent and Pritchard (1959) analyse the vertical eddy flux of salt for the James River. A mixing length concept, similar to Prandtl's classic mixing length theory of turbulence, is applied in this analysis. Following Prandtl's arguments, a mixing length can be defined such that

$$\eta^2 \ell^2 = -\frac{\overline{v's'}}{\left|\frac{\partial U}{\partial y}\right| \left|\frac{\partial S}{\partial y}\right|} \qquad 2.18$$

where η is a constant, ℓ is the mixing length, $\overline{v's'}$ is the vertical eddy salt flux, $\frac{\partial U}{\partial y}$ is the vertical gradient of mean velocity and $\frac{\partial S}{\partial y}$ the vertical gradient of mean salinity, all averaged over a tidal period. This ℓ is defined as the observed mixing length, and refers to the actual stratified flow for the estuary. For the unstratified case, an adiabatic mixing length is defined from earlier work by Montgomery (1943)

$$\ell_\alpha = \frac{Ky}{h}(h-y) \qquad 2.19$$

where K is Von Karman's constant and h is water depth. Kent and Pritchard find that the observed and adiabatic mixing lengths can be best related by the expression

$$\ell = \ell_\alpha (1 + \beta R_i)^{-1} \qquad 2.20$$

where β is some unknown proportionality factor and R_i is the local Richardson number

$$R_i = \frac{\frac{g}{\rho}\frac{\partial \rho}{\partial y}}{\left|\frac{\partial U}{\partial y}\right|^2} . \qquad 2.21$$

The observed mixing length is calculated from the extensive James River data. The velocities and salinities are averaged over one or more tidal periods and therefore a tidal mean mixing length is determined. Although agreement between the observed and theoretical mixing length is good, an improvement is found when an additional term for the wind waves is included.

Pritchard (1960) extends the mixing length theory to include the defining of an eddy diffusivity

$$K_y = \ell u^* \qquad 2.22$$

where ℓ is the mixing length developed by Kent and Pritchard (1959) and u^* is a characteristic velocity. u^* is related to the tidal current at middepth, U_t, by similar mixing length arguments

$$u^* = U_t \left(\frac{y(h-y)}{h^2}\right) (1 + \beta R_i)^{-1} \qquad 2.23$$

The eddy diffusivity can therefore be written

$$K_y = \frac{\eta U_t y^2 (h-y)^2}{h^3} (1 + \beta R_i)^{-2} . \qquad 2.24$$

The Richardson number is approximated as

$$R_i = \frac{\frac{g}{\rho}\frac{\partial \rho}{\partial v}}{(0.7 \frac{U_t}{h})^2} . \qquad 2.25$$

For the James River estuary, β was found to be 0.276 and η was 8.59×10^{-3}. An eddy diffusivity computed from the above relationships represents the net, non-tidal eddy processes. No discussions are presented which attempt to relate this net eddy diffusivity to the real time tidal eddy coefficient.

Bowden (1960) analyses velocity and salinity data for the Mersey Estuary. Effective values for the vertical eddy diffusivity and eddy viscosity, averaged over a tidal period, for five depths at a single station are determined. Values for the mean eddy viscosity are

backfigured from a time-averaged longitudinal equation of motion which considers only the pressure gradient and vertical eddy diffusions of momentum. According to Bowden's analysis, for the particular conditions studied, the effective eddy viscosities for the tidal time-average are about one-tenth as large as those expected for a non-stratified flow.

The coefficients of vertical eddy diffusivity are determined from a salt balance equation which considers only the horizontal advection and the vertical eddy diffusion. In this case, estimates of both the time-averaged and tidal varying coefficients are made. The diffusivities averaged over a tidal period are, in general, smaller than the non-averaged coefficients. Again, Bowden concludes that the salinity stratification yielded eddy diffusivities smaller than would be expected for a neutrally stable fluid. In addition, the values for the mean eddy viscosities are found to be greater at all depths than the mean vertical eddy diffusivities.

Bowden (1963) and more recently, Bowden and Gilligan (1971) have studied additional data for the Mersey Estuary. As in the previous studies, mean values for the eddy coefficients are computed from the field data. When the ratio of eddy viscosity to vertical eddy diffusivity is plotted against a local Richardson number, a distribution similar to that of Munk and Anderson (1948) is found. Thus, it appears that although the mean coefficients, averaged over a tidal period, yield smaller values than the non-averaged coefficients, they may still be related empirically to a local Richardson number and therefore the degree of vertical stratification.

Harleman and Ippen (1967) analyse data from a laboratory investigation of estuarine dynamics. A large salinity flume with a tidal and a river control at either end was used to model partially stratified estuaries. Extensive velocity and salinity data were recorded and used to backfigure vertical eddy diffusivities from the time-averaged salt balance equation. In this analysis, the horizontal eddy diffusion is neglected. Both a vertical and horizontal dependence is found for the vertical eddy diffusivity. Maximum values at each longitudinal station occur at about middepth, with a somewhat parabolic decrease towards the surface and bottom. In addition, the coefficients decreased from a maximum at the ocean boundary to a minimum far upstream. Using the relationships of Pritchard (1960), mean vertical eddy coefficients were computed for the same set of flume data. These equations, developed for the James River estuary, yield vertical and longitudinal variations of the eddy coefficients very similar to the backfigured experimental results. Pritchard's equations did, however, produce slightly smaller values at all stations for these eddy diffusivities.

For both the work of Bowden and Harleman and Ippen, eddy coefficients for equations averaged over a tidal period are backfigured from recorded data. Various terms are neglected from the complete set of governing equations in these analyses, and therefore, the resulting coefficients must include the effects of these neglected terms. These coefficients are not simply the averages over a tidal period of the actual eddy coefficients which relate to the turbulent fluctuations. These arguments are developed in greater detail in the following sections of this report.

III Theoretical Considerations

3.1 Statement of the Problem

The analytical models of Abbott (1960), McGregor (1971) and Hansen and Rattray (1965), although limited by the solution techniques, point out the possible advantages from proceeding in a parallel manner to model time-averaged vertical velocity and salinity distributions. These models include, for the longitudinal equation of motion, only the pressure gradient, which contains the salinity gradient, and the eddy transport of momentum. The velocity distributions determined from this equation include all of the important features of measured net velocities. It may therefore be concluded that this simplified balance of forces describes the essential mechanisms of time-averaged circulation.

There are two important disadvantages of the Hansen and Rattray model. The first is the necessity of dividing an estuary into several regions, each having a unique mathematical model and solution. Within each of these regions the solutions maintain geometric similarity. In real estuaries, however, there is a continuous transformation of velocity and salinity profiles along the longitudinal axis. Therefore, a solution without implicit similarity assumptions is a preferable technique.

The second feature of the Hansen and Rattray model which may be considered a weakness is the strong dependence on the coefficient of horizontal eddy diffusivity. Numerous investigators have shown the horizontal eddy flux of salt to be a minor term in the salt balance for estuaries. Eddy coefficients are difficult parameters to measure, and even more difficult to predict, especially when averaged

over a tidal period. Thus, until a more detailed understanding of eddy processes in stratified fluids is achieved, it seems reasonable to include only the most important of these eddy flux terms in estuary models.

The objective of the present study is to develop an analytical model of time-averaged estuarine circulation which will avoid the less tractable features of the previous models described above. The governing equations are similar to Hansen and Rattray's model, which was originally suggested by Pritchard's analysis of the James River estuary. A solution technique which is continuous over the entire length of an estuary is desired and which makes no assumptions about similarity of velocity or salinity profiles. Only the vertical eddy flux of salt and momentum are included, and thus only two eddy coefficients need to be specified. In order to provide the analytical solution with a predictive capabality, empirical correlations for these two parameters with gross characteristics of the flow field are sought, as a fundamental feature of the complete solution.

3.2 Governing Equations

3.2.1 Introduction

The model equations describing the circulation and distribution of salinity are the equations of motion, of continuity, of conservation of salt and an equation of state. The model is reduced to the longitudinal and vertical dimensions by assuming lateral homogeneity. Figure 3.1 is a definition sketch showing the orientation of the coordinate system with the x - axis positive towards the head of the

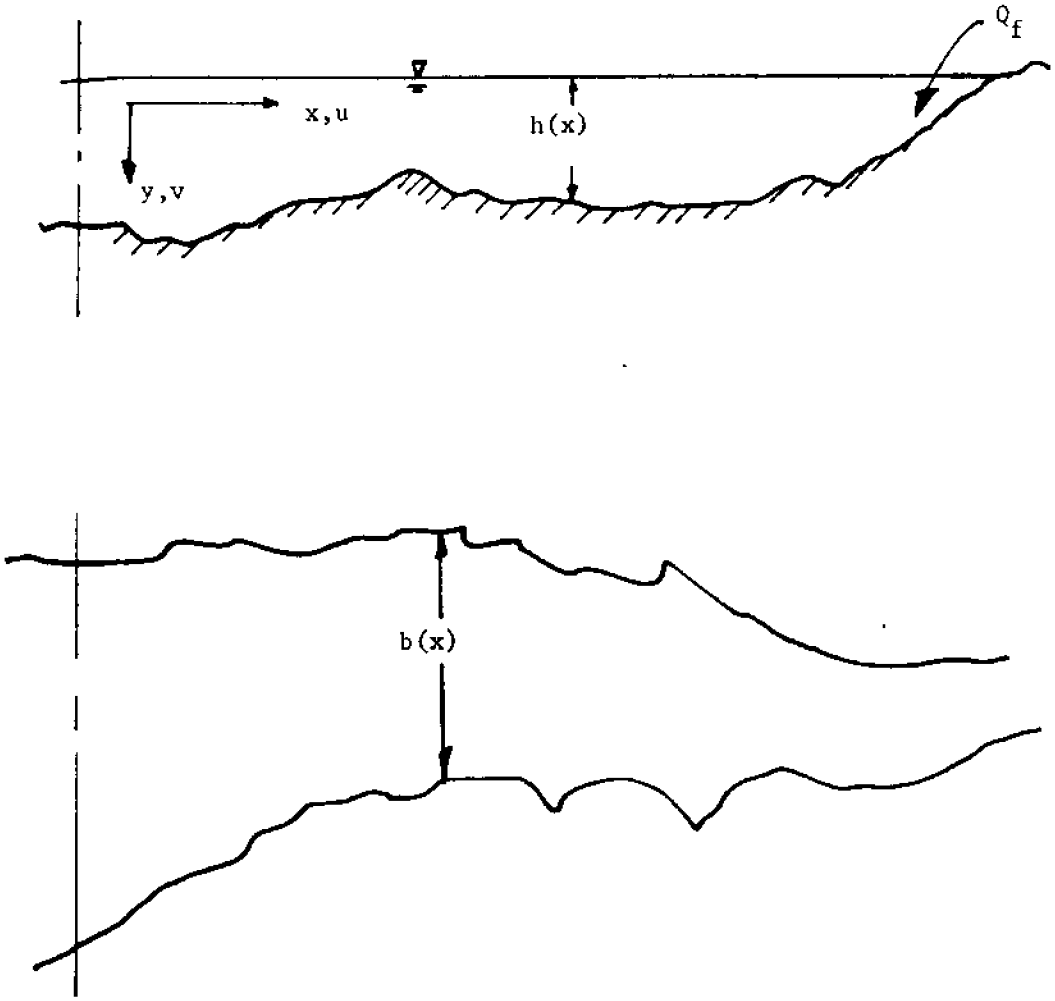

Figure 3.1 Definition sketch for model equations

estuary (upstream) and the y - axis positive downward. An additional simplification is made restricting the width b(x) and the mean water level h(x) to be functions of the longitudinal coordinate only. An inflow of freshwater Q_f occurs at the far upstream end.

3.2.2 Equations of Motion

For the conditions described, the conservation of momentum for the longitudinal direction can be written

$$\frac{\partial ub}{\partial t} + \frac{\partial u^2 b}{\partial x} + \frac{\partial uvb}{\partial y} = -\frac{1}{\rho}\frac{\partial p}{\partial x} b \qquad 3.1$$

where u = velocity in longitudinal direction

v = velocity in vertical direction

t = time

ρ = density

p = pressure

x = longitudinal direction

y = vertical direction

b = width

This equation is a balance of forces for the estuary at any time in a tidal period, i.e., before time-averaging. The viscous frictional terms and Coriolis forces have been neglected. In addition, the approximation of Boussinesq has been applied to neglect density variations in all but the bouyancy terms. The pressure is for the fluid only, atmospheric pressure being assumed zero.

For the conservation of momentum in the vertical direction, hydrostatic conditions are assumed. Thus, inertial and convective

accelerations are neglected. The vertical equation of motion can therefore be written

$$0 = -\frac{1}{\rho}\frac{\partial p}{\partial y} + g \qquad 3.2$$

where g is the acceleration of gravity.

3.2.3 Equations of Water and Salt Conservation

For incompressible flow, the two-dimensional equation of continuity is

$$\frac{\partial ub}{\partial x} + \frac{\partial vb}{\partial y} = 0. \qquad 3.3$$

The conservation of salt equation, before time-averaging, and neglecting molecular diffusion is

$$\frac{\partial sb}{\partial t} + \frac{\partial usb}{\partial x} + \frac{\partial vsb}{\partial y} = 0 \qquad 3.4$$

where s is the salinity and is a function of x, y, and t.

3.2.4 Time-Averaging of Equations

There are three time scales of interest for the model being considered. Turbulent fluctuations of the dependent variables may be assumed to take place within a few minutes. These variables also have a diurnal or semi-diurnal component due to the tidal motion. Finally, slow variations over several tidal periods can result from the changing freshwater inflows and monthly changes in tidal amplitude. Following the classical methods, the dependent variables are written as the sum of a mean and turbulent component, i.e., within the first time scale mentioned,

$$u = \bar{u} + u'$$

$$v = \bar{v} + v'$$

$$s = \bar{s} + s'$$

$$\rho = \bar{\rho} + \rho' \qquad 3.5$$

$$p = \bar{p} + p'$$

where the prime refers to the turbulent component. These equations are substituted into the governing equations 3.1 - 3.4 and averaged

$$\frac{\partial \bar{u}b}{\partial t} + \frac{\partial \bar{u}^2 b}{\partial x} + \frac{\partial \bar{u}\bar{v}b}{\partial y} = -\frac{1}{\rho}\frac{\partial \bar{p}}{\partial y} b - \frac{\partial \overline{u'^2 b}}{\partial x} - \frac{\partial \overline{u'v'b}}{\partial y} \qquad 3.6$$

$$0 = -\frac{1}{\bar{\rho}}\frac{\partial \bar{p}}{\partial y} + g \qquad 3.7$$

$$\frac{\partial \bar{u}b}{\partial x} + \frac{\partial \bar{v}b}{\partial y} = 0 \qquad 3.8$$

$$\frac{\partial \bar{s}b}{\partial t} + \frac{\partial \bar{u}\bar{s}b}{\partial x} + \frac{\partial \bar{v}\bar{s}b}{\partial y} = -\frac{\partial \overline{u's'b}}{\partial x} - \frac{\partial \overline{v's'b}}{\partial y}. \qquad 3.9$$

The eddy fluxes of momentum and salt, $\overline{u'^2}$, $\overline{v'u'}$, $\overline{u's'}$, and $\overline{v's'}$ are usually written as the product of an eddy coefficient and the mean gradient of the quantity being transported. For example, $\overline{u'^2}$ may be replaced by $\epsilon_x \frac{\partial \bar{u}}{\partial x}$, where ϵ_x would be a horizontal eddy viscocity. However, for the purpose of the present analysis the introduction of eddy coefficients will be postponed until time-averaging over a tidal period is introduced.

In order to facilitate the tidal time-averaging, the mean dependent variables are divided into two components, a tidal mean, and a tidal varying term

$$\bar{u} = U + u_t$$

$$\bar{v} = V + v_t$$

$$\bar{s} = S + s_t \qquad 3.10$$

$$\bar{\rho} = \rho_m + \rho_t$$

$$\bar{p} = P + p_t$$

where U is the mean horizontal velocity for a tidal period and u_t is the harmonic component for the same tidal period, etc. As with the turbulent components, the average of a harmonic term, e.g., u_t, s_t, over a tidal period is zero by definition. Equations 3.10 are substituted into equations 3.6 - 3.9 and averaged over a tidal period

$$\frac{\partial Ub}{\partial t} + \frac{\partial Ub}{\partial x} + \frac{\partial \langle u_t^2 \rangle b}{\partial x} + \frac{\partial UVb}{\partial y} + \frac{\partial \langle u_t v_t \rangle b}{\partial y} =$$

$$\frac{-1}{\rho_m} \frac{\partial P}{\partial x} b - \frac{\partial \langle \overline{u'^2} \rangle b}{\partial x} - \frac{\partial \langle \overline{u'v'} \rangle b}{\partial y} \qquad 3.11$$

$$0 = -\frac{1}{\rho_m} \frac{\partial P}{\partial y} + g \qquad 3.12$$

$$\frac{\partial Ub}{\partial x} + \frac{\partial Vb}{\partial y} = 0 \qquad 3.13$$

$$\frac{\partial Sb}{\partial t} + \frac{\partial USb}{\partial x} + \frac{\partial \langle u_t s_t \rangle b}{\partial x} + \frac{\partial VSb}{\partial y} + \frac{\partial \langle v_t s_t \rangle b}{\partial y} =$$

$$- \frac{\partial \langle \overline{u's'} \rangle b}{\partial x} - \frac{\partial \langle \overline{v's'} \rangle b}{\partial y} \qquad 3.14$$

where < > indicates averaging over a tidal period.

From the analysis of the James River data, Pritchard (1954, 1956) argues that the dominant terms in the longitudinal equation of motion 3.11 are the pressure gradient and the vertical eddy flux of momentum, all other terms being of second order. This assumption is included in the present development. In a later section it will be shown that the neglected terms are indeed small for the cases studied. For the salt balance 3.14 the tidal cross-products and horizontal eddy flux are neglected by similar arguments. The reduced equations are further simplified by introducing mean eddy coefficients for the remaining turbulent terms

$$- \frac{\partial \langle \overline{u'v'} \rangle}{\partial y} \equiv \frac{\partial}{\partial y} \left(D_y \frac{\partial U}{\partial y} \right) \qquad 3.15$$

$$- \frac{\partial \langle \overline{v's'} \rangle}{\partial y} \equiv \frac{\partial}{\partial y} \left(K_y \frac{\partial S}{\partial y} \right) \qquad 3.16$$

These definitions for D_y and K_y are convenient with regard to reducing the mathematical complexity of the model. However, they are strictly artificial in that they do not preserve the mechanisms of turbulent mixing, i.e., tidal activity, in their formulation. In particular, equation 3.15 relates the net turbulent momentum flux $\langle \overline{u'v'} \rangle$ to the

net, non-tidal velocity U. By purely physical arguments this flux should be related to the tidal velocity u_t. This apparent inconsistancy is partially resolved in Chapter V where D_y is correlated with the tidal velocity. The equations are now written

$$0 = -\frac{1}{\rho_m}\frac{\partial P}{\partial x} + \frac{1}{b}\frac{\partial}{\partial y}\left(bD_y\frac{\partial U}{\partial y}\right) \qquad 3.17$$

$$0 = -\frac{1}{\rho_m}\frac{\partial P}{\partial y} + g \qquad 3.18$$

$$\frac{\partial Ub}{\partial x} + \frac{\partial Vb}{\partial y} = 0 \qquad 3.19$$

$$\frac{\partial Sb}{\partial t} + \frac{\partial bUS}{\partial x} + \frac{\partial bVS}{\partial y} = \frac{\partial}{\partial y}\left(bK_y\frac{\partial S}{\partial y}\right). \qquad 3.20$$

The value and distributions of the mean eddy coefficients are unknown. If a solution to the above set of equations can be shown to match recorded data by proper fitting of D_y and K_y, one must assume that either all the neglected terms are zero, or more probably, that these neglected terms have been absorbed into these coefficients. A comparison of equations 3.15 and 3.16 with the classical definitions of eddy viscosity and eddy diffusivity clearly shows the difference in the meaning of these terms

$$\frac{\partial}{\partial y}\left(<\varepsilon_y\frac{\partial \bar{u}}{\partial y}>\right) \neq \frac{\partial}{\partial y}\left(D_y\frac{\partial U}{\partial y}\right) \qquad 3.21$$

$$\frac{\partial}{\partial y}\left(\langle k_y \frac{\partial \bar{s}}{\partial y}\rangle\right) \neq \frac{\partial}{\partial y}\left(K_y \frac{\partial S}{\partial y}\right). \qquad 3.22$$

More specifically, D_y and K_y are not simply ϵ_y and k_y averaged over a tidal period.

3.2.5 Equation of State

The effect of temperature on the relationshp between density and salinity is not included in this model. A simple linear empirical expression is used

$$\rho = \rho_o(1 + \alpha s) \qquad 3.23$$

where ρ_o is a reference density and α is a conversion constant. The range of temperatures encountered in estuaries does not require a more complex expression, in light of other model assumptions.

3.3 Additional Assumptions

The governing equations developed in the preceeding sections can not be solved analytically in their present form. Previous investigators have introduced similarity assumptions for the velocity and salinity distributions as well as restrictions on the longitudinal salinity gradient. As stated in a preceeding section, the present investigation seeks to avoid the limitations of a similarity solution. However, as will be developed in the following sections, the longitudinal salinity gradient will be modified to allow an analytical solution to be found.

The Pritchard (1952, 1954) investigation of the James River revealed that for the stations and conditions of the survey, the

longitudinal salinity gradient did not vary appreciably with vertical position. Harleman and Ippen (1967) showed a similar pattern for the analysis of data from a laboratory flume. Taken to the extreme, this observed feature suggests that the longitudinal salinity gradient may be assumed independent of its vertical position, i.e.,

$$\frac{\partial S}{\partial x} = \frac{\partial S}{\partial x}\,(x) \qquad 3.24$$

although

$$S = S(x,y).$$

Introducing equation 3.24 into the set of governing equations 3.17 - 3.20 results in equations, which although now solvable analytically, no longer describe exactly the presumed physical mode of the net circulation. A close fit of velocity or salinity profiles between field or experimental data and the theoretical solutions can suggest the validity of the above assumption only within the context of all the other assumptions made in developing these equations.

The longitudinal salinity gradient $\frac{\partial S}{\partial x}$ is replaced in equations 3.17 - 3.20 with the longitudinal gradient of a depth averaged salinity S_d. Next, a steady-state condition is assumed for the initial development of the solution. This condition will be removed in later sections, and an unsteady solution will be presented. In addition, the two mean eddy coefficients D_y and K_y are assumed independent of vertical position. These coefficients have been shown to represent the rather complex effects of time-averaging and of the neglecting of terms

considered of smaller order. The vertical dependence of these coefficients is not known, although several investigators have attempted to analyse these terms from experimental and field observations, as discussed in Chapter II. Thus, D_y and K_y are assumed to be independent of y, and are replaced with effective coefficients for the entire depth of flow, D and K, respectively.

3.4 Synthesis of Governing Equations

The synthesis of the original model equations, modified by the assumptions discussed in section 3.3 begins with the equation of hydrostatic pressure

$$0 = -\frac{1}{\rho_m}\frac{\partial P}{\partial y} + g. \qquad 3.12$$

Equation 3.12 is intergrated in y

$$P = \int_{h_0}^{y} \rho_m g \, dy \qquad 3.25$$

and differentiated in x

$$\frac{\partial P}{\partial x} = -g\rho_m \frac{\partial h_0}{\partial x} + g\int_{h_0}^{y} \frac{\partial \rho_m}{\partial x} dy \qquad 3.26$$

applying Leibnitz' rule and the Boussinesq approximation. Equation 3.26 is next substituted into the longitudinal equation of motion which now has assumed that $D_y(x,y)$ can be replaced with $D(x)$

$$\frac{1}{\rho_m}\frac{\partial P}{\partial x} = D\frac{\partial^2 U}{\partial y^2} \qquad 3.27$$

After substitution of 3.26

$$- g \frac{\partial h_0}{\partial x} + \frac{g}{\rho_m} \int_{h_0}^{y} \frac{\partial \rho_m}{\partial x} \, dy = D \frac{\partial^2 U}{\partial y^2} \qquad 3.28$$

and differentiation in y, yields

$$\frac{g}{\rho_m} \frac{\partial \rho_m}{\partial x} = D \frac{\partial^3 U}{\partial y^3} . \qquad 3.29$$

The equation of state 3.23 is next introduced into equaiton 3.29

$$g\alpha \frac{\partial S}{\partial x} = D \frac{\partial^3 U}{\partial y^3} . \qquad 3.30$$

The steady-state salt conservation equation, with $K_y(x,y)$ replaced with K(x) can be written

$$\frac{\partial USb}{\partial x} + \frac{\partial VSb}{\partial y} = bK \frac{\partial^2 S}{\partial y^2} \qquad 3.31$$

This equation can also be written

$$U \frac{\partial S}{\partial x} + V \frac{\partial S}{\partial y} = K \frac{\partial^2 S}{\partial y^2} \qquad 3.32$$

since

$$S \left(\frac{\partial Ub}{\partial x} + \frac{\partial Vb}{\partial y}\right) = 0 \qquad 3.33$$

from continuity 3.19.

Equation 3.32 is further simplified by introducing the assumption that the longitudinal salinity gradient $\frac{\partial S}{\partial x}$ can be replaced with a gradient of the depth averaged salinity $\frac{\partial S}{\partial x}d$. The same procedure is applied to equation 3.31. The resulting system of governing equations

can be written

$$g\alpha \frac{\partial S_d}{\partial x} = D \frac{\partial^3 U}{\partial y^3} \qquad 3.34$$

$$\frac{\partial Ub}{\partial x} + \frac{\partial Vb}{\partial y} = 0 \qquad 3.35$$

$$U \frac{\partial S_d}{\partial x} + V \frac{\partial S}{\partial y} = K \frac{\partial^2 S}{\partial y^2} \qquad 3.36$$

A stream function satisfying the equation of continuity 3.35 is defined

$$U = -\frac{1}{b} \frac{\partial \Psi}{\partial y} , \quad V = \frac{1}{b} \frac{\partial \Psi}{\partial x} \qquad 3.37$$

and thus the equations are reduced to

$$g\alpha \frac{\partial S_d}{\partial x} = -\frac{D}{b} \frac{\partial^4 \Psi}{\partial y^4} \qquad 3.38$$

$$-\frac{\partial \Psi}{\partial y} \frac{\partial S_d}{\partial x} + \frac{\partial \Psi}{\partial x} \frac{\partial S}{\partial y} = bK \frac{\partial^2 S}{\partial y^2} \qquad 3.39$$

3.5 Boundary Conditions

The set of governing equations, (3.38 and 3.39) includes a fourth order equation for the stream function requiring four boundary conditions and a second order equation for salinity, subject to two boundary conditions. These governing equations describe the dynamics of an estuary averaged over a tidal period. The boundary conditions,

as well, should be mean conditions for this averaged system. With the assumption of steady-state, any control volume defined by two vertical boundaries, the mean water surface, and the bottom must maintain a constant quantity of salt and have a net through-flow of water equal to the freshwater discharge. No flux of water or salt can occur at a horizontal boundary, i.e., the surface or bottom. Frictional stresses can be applied at both the surface and bottom and the condition of no slip of the horizontal velocity on the bottom should also be considered. These various boundary conditions are examined in the following paragraphs and a set of conditions is selected for inclusion in the analytical model.

Considering first the equation of conservation of momentum 3.34, four boundary conditions are needed. Surface wind stresses are neglected, and since the mean eddy coefficient D has a finite value at the surface by assumption, the vertical gradient of the net horizontal velocity $\frac{\partial U}{\partial y}$ must be made zero for zero surface stress. At the bottom $y = h$, two possible conditions for the horizontal velocity are considered. A no-slip or $U = 0$ condition must apply for a precise model of the actual flow. However, for the rough natural bottoms, or even in laboratory flumes, the turbulent velocities are very large near the bed, going to zero in a very thin layer which can be neglected in the analytical model. If the net velocity is to have its maximum value just above this thin layer, a condition of zero gradient, $\frac{\partial U}{\partial y} = 0$, at the bottom is the appropriate model boundary condition. An analysis of the laboratory flume tests in Chapter IV will show that this latter

condition of negligible stress results in a closer fit of the mathematical model to experimental and field velocities. However, for the purpose of examining the behavior of these two possible approaches, solutions for both are developed in this chapter.

The remaining two conditions for the stream function are specified by the requirement that the integral of the net horizontal velocity over the depth must equal the freshwater discharge per unit width, $Q_{f/b}$. By assigning the stream function a zero value at the bottom, its surface value must equal Q_f.

These boundary conditions for the equation of motion 3.38 may be summarized as follows:

$$y = 0,\ \frac{\partial U}{\partial y} = 0,\ -\frac{\partial^2 \psi}{\partial y^2} = 0 \qquad \text{zero surface stress}$$

$$y = h,\ U = 0,\ \frac{\partial \psi}{\partial y} = 0 \qquad \text{zero bottom velocity}$$

or

$$y = h,\ \frac{\partial U}{\partial y} = 0,\ -\frac{\partial^2 \psi}{\partial y^2} = 0 \qquad \text{zero bottom stress}$$

$$Q_{f/b} = \int_0^h U\, dy = -\frac{1}{b} \int_0^h \frac{\partial \psi}{\partial y}\, dy = \frac{1}{b}\{-\psi_o + \psi_h\}$$

therefore

$$y = h,\ \psi = 0$$

$$y = 0,\ \psi = Q_f \qquad \text{conservation of freshwater}$$

Two boundary conditions are needed to satisfy the salt balance equation 3.39. Ideally, these conditions should specify a zero flux of salt at the surface and the bottom. As the vertical velocity V is zero at these boundaries, the flux reduces to $K\frac{\partial S}{\partial y}$ where K is non-zero. Thus, a condition that $\frac{\partial S}{\partial y}$ is zero at the surface and bottom will satisfy the zero flux requirements. The form of the solution of equation 3.39, however, does not permit the specification of the gradient of the salinity at two boundaries. This restriction will be fully explained in section 3.7. The consequence of this limitation is that a condition of zero gradient is specified at either of the two boundaries and a second non-gradient condition for salinity is introduced. If the salt balance equation is an accurate description of the physical processes, a computed gradient at the other boundary, which has no specified condition, should also be zero.

The alternate boundary condition for the salt balance is a statement that the depth averaged salinity must equal a prescribed value, S_d. This mean salinity S_d also appears in the modified longitudinal salinity gradient. $\frac{\partial S_d}{\partial x}$. This condition, with either a zero gradient at the surface or at the bottom, completes the boundary conditions for the model. These final conditions are written

$$y = 0, \quad \frac{\partial S}{\partial y} = 0 \qquad \text{zero flux at surface}$$

or

$$y = h, \quad \frac{\partial S}{\partial y} = 0 \qquad \text{zero flux at bottom}$$

$$\frac{1}{h}\int_0^h S\,dy = S_d. \qquad \text{specification of mean salinity}$$

3.6 Non-Dimensionalization of Equations

As with most problems of fluid dynamics, it is convenient to develop analytical solutions in a non-dimensional form in order to permit generalized discussions of results. The choice of terms introduced to non-dimensionalize the various dependent and independent variables, although somewhat arbitrary, should recognize the possible difficulties in quantifying these new parameters. The following defintions will be shown to satisfy this condition:

$$\eta \equiv \frac{y}{h} \qquad \xi \equiv \frac{x}{L_i}$$

$$\psi \equiv \frac{\psi}{Q_f} \qquad \theta \equiv \frac{S}{S_o} \qquad 3.40$$

$$\theta_d \equiv \frac{S_d}{S_o}$$

where L_i is the mean intrusion length, defined as the distance from the ocean boundary to a point where the time-averaged, depth averaged salinity is one percent of the ocean salinity. S_o is the ocean salinity, h is the depth of the mean water level and Q_f is the fresh-water discharge, as previously noted.

These quantities are introduced into equations 3.38 and 3.39

$$\frac{g\alpha S_o}{L_i}\frac{\partial \theta_d}{\partial \xi} = -\frac{DQ_f}{h^4 b}\frac{\partial^4 \psi}{\partial \eta^4} \qquad 3.41$$

$$\frac{Q_f}{h}\frac{\partial\psi}{\partial\eta}\frac{S_o}{L_i}\frac{\partial\theta_d}{\partial\xi} + \frac{Q_f}{L_i}\frac{\partial\psi}{\partial\xi}\frac{S_o}{h}\frac{\partial\theta}{\partial\eta} = \frac{bKS_o}{h^2}\frac{\partial^2\theta}{\partial\eta^2} \quad . \qquad 3.42$$

The set of boundary conditions developed in section 3.5 is represented by

$$\eta = 0, \; -\frac{\partial^2\psi}{\partial\eta^2} = 0$$

$$\eta = 1, \; -\frac{\partial\psi}{\partial\eta} = 0$$

or 3.43

$$\eta = 1, \; -\frac{\partial^2\psi}{\partial\eta^2} = 0$$

$$\eta = 1, \quad \psi = 0$$

$$\eta = 0, \quad \psi = 1$$

and

$$\eta = 0, \; \frac{\partial\theta}{\partial\eta} = 0$$

or

$$\eta = 1, \; \frac{\partial\theta}{\partial\eta} = 0$$

$$\int_0^1 \theta \; d\eta = \frac{S_d}{S_o} \qquad 3.44$$

3.7 Analytical Solution for Steady-State Conditions

The steady-state equations of motion and salt conservation, in dimensionless form are

$$\left\{\frac{g\,S_o h^4 b}{L_i\,DQ_f}\right\}\frac{\partial\theta_d}{\partial\xi} = -\frac{\partial^4\psi}{\partial\eta^4} \qquad 3.45$$

$$-\frac{\partial\psi}{\partial\eta}\frac{\partial\theta_d}{\partial\xi}+\frac{\partial\theta}{\partial\eta}\frac{\partial\psi}{\partial\xi}=\frac{bKL_i}{Q_f h}\frac{\partial^2\theta}{\partial\eta^2} \qquad 3.46$$

wherein ψ, θ, θ_d, ξ and η are all dimensionless variables. These equations can be further simplified by defining two coefficients,

$$C_1(\xi)=\frac{g\alpha S_o h^4 b}{L_i D Q_f} \qquad 3.47$$

$$C_2(\xi)=\frac{KL_i b}{Q_f h}\,. \qquad 3.48$$

Equation 3.45 can be solved for the stream function Ψ by integrating with y four times

$$\psi=-C_1\frac{\partial\theta_d}{\partial\xi}\frac{\eta^4}{24}+a_1\frac{\eta^3}{6}+a_2\frac{\eta^2}{2}+a_3\eta+a_4$$

where a_1, a_2, a_3, and a_4 are all functions of ξ, and are evaluated from the boundary conditions. This determination will be presented for two cases, depending upon the choice of boundary conditions.

case 1: zero bottom velocity

For this case, the boundary conditions are

$$\frac{\partial^2\psi}{\partial\eta^2}=0,\ \psi=1,\ \eta=0 \qquad 3.50$$

$$\frac{\partial\psi}{\partial\eta}=0,\ \psi=0,\ \eta=1$$

and therefore

$$a_1 = 3 + \frac{3}{8} C_1 \frac{\partial \theta_d}{\partial \xi} \qquad a_2 = 0$$

$$a_3 = -\frac{3}{2} - \frac{1}{48} C_1 \frac{\partial \theta_d}{\partial \xi} \qquad a_4 = 1 \; . \tag{3.51}$$

Substituting these values into 3.49 yields

$$\psi = \frac{\partial \theta_d}{\partial \xi} \frac{C_1}{24} (-\eta^4 + 2\eta^3 - \eta) - \eta + 1 + \frac{\eta}{2} (\eta^2 - 1)(1 - \frac{\partial \theta_d}{\partial \xi} \frac{C_1}{24}) \tag{3.52}$$

case 2: zero bottom stress

For this case, the boundary conditions are

$$\frac{\partial^2 \psi}{\partial \eta^2} = 0, \quad \psi = 1, \quad \eta = 0$$

$$\frac{\partial^2 \psi}{\partial \eta^2} = 0 \quad \psi = 0, \quad \eta = 1 \tag{3.53}$$

and therefore

$$a_1 = \frac{1}{2} C_1 \frac{\partial \theta_d}{\partial \xi} \qquad a_2 = 0$$

$$a_3 = -\frac{C_1}{24} \frac{\partial \theta_d}{\partial \xi} - 1 \quad a_4 = 1. \tag{3.54}$$

Substituting these values into 3.49 yields

$$\psi = \frac{\partial \theta_d}{\partial \xi} \frac{C_1}{24} \{-\eta^4 + 2\eta^3 - \eta\} - \eta + 1. \tag{3.55}$$

The difference between the stream function for the two cases is

$$\frac{\eta}{2} (\eta^2 - 1)(1 - \frac{\partial \theta_d}{\partial \xi} \frac{C_1}{24}).$$

The solution of the salt balance equation 3.46 is dependent upon the stream function ψ and therefore on the choice of case 1 or case 2. However, the general solution can also be developed in terms of an unspecified stream function. A dummy variable $f(\xi,\eta)$ is defined

$$f(\xi,\eta)=\frac{\partial\theta}{\partial\eta} \qquad 3.56$$

and substituted into a modified form of equation 3.46

$$\frac{\partial f}{\partial\eta} - \frac{B(\xi,\eta)}{C_2(\xi)} f = \frac{A(\xi,\eta)}{C_2(\xi)} \qquad 3.57$$

where

$$A(\xi,\eta) = - \frac{\partial\psi}{\partial\eta}\frac{\partial\theta_d}{\partial\xi}$$

$$B(\xi,\eta) = \frac{\partial\psi}{\partial\xi}$$

$$C_2(\xi) = \frac{KL_i b}{Q_f h} .$$

Equation 3.57 is multiplied by an intergration factor

$$\exp\left(\int - \frac{B}{C_2}\, d\eta\right)$$

and the solution for 3.57 is shown by Wylie (1960) to be

$$f(\xi,\eta) = \exp\left(\int \frac{B}{C_2} d\eta\right) \int \frac{A}{C_2} \exp\left(\int - \frac{B}{C_2} d\eta\right) d\eta + b_1(\xi) \exp\left(\int \frac{B}{C_2} d\eta\right) \qquad 3.58$$

wherein $b_1(\xi)$ must be evaluated from the boundary condition. At this point it is clear that only one gradient condition for salinity may be included, as noted in section 3.5. There is no reason to expect that the choice of boundary for specifying $\frac{\partial \theta}{\partial \eta} = 0$, i.e., $f(\xi,\eta) = 0$, is important. Thus, for convenience this condition will be applied at the surface, $\eta = 0$, and this determines that $b_1(\xi) = 0$.

A second condition is needed to specify the salinity from equation 3.56,

$$S(\xi,\eta) = \int f(\xi,\eta)\, d\eta + b_2(\xi). \qquad 3.59$$

This condition, stated in equations 3.44, is that the depth average of the salinity must equal a known value, θ_d ,

$$b_2(\xi) = \theta_d - \int_0^1 \int f(\xi,\eta)\, d\eta\, d\eta \qquad 3.60$$

and thus

$$\theta(\xi,\eta) = \int f(\xi,\eta)\, d\eta + \theta_d - \int_0^1 \int f(\xi,\eta)\, d\eta\, d\eta. \qquad 3.61$$

Equation 3.61, although awkward in appearance if written in terms of the stream function, may be evaluated easily by numerical intergration using a digital computer.

3.8 Inputs for Solution

In the development of the solutions for the stream function and salinity, several parameters have been introduced and assumed known a priori. These parameters are reviewed in this section and possible sources of quantitative evaluation are discussed.

The depth average of the salinity, averaged over a tidal period, S_d and its longitudinal gradient $\frac{\partial S_d}{\partial x}$ must both be specified in the solutions. For the purpose of evaluating the model from recorded data, these parameters can be simply backfigured from the measurements. However, in order for the analytical model to have a predictive capability, these terms must be predictable themselves. There have been numerous semi-empirical fits for this one-dimensional salinity distribution, Harleman and Ippen (1961), McGregor (1972) and others. However, a recently developed numerical model by Thatcher and Harleman (1972) permits one to compute a one-dimensional unsteady salinity distribution. This approach results in a general, non-empirical analysis for this input parameter. A summary of their model, and the details of its coupling with the analytical two-dimensional solution are presented in Chapter V The intrusion length can also be evaluated by their technique.

The freshwater inflow and ocean boundary salinity are considered to be fundamental quantities, as are the depth and width distributions.

The remaining two quantities needed to evaluate the analytical solution are the eddy coefficients, K and D. Nothing can be said about these terms prior to their evaluation from recorded data. The procedure for their determination is to fit the analytical solutions for velocity and salinity with flume and field data and to pick the best fit values for K and D by trial and error. Since the stream function is dependent only on D, this procedure is not too cumbersome, even though the salinity is dependent on both D and K. This process of back- calculating D and K from recorded data is repeated for several data sets.

The resulting distributions of these coefficients are then correlated with parameters characteristic of the flow conditions, as is shown in Chapter IV.

In summary, the parameters needed to evaluate the analytical solutions for velocity and salinity, except for the coefficients D and K, may be determined either from recorded data or a numerical model. The former method is used first to appraise the model and to back-figure values for D and K. The latter method, a coupling with a numerical model demonstrates the predictive capabilities of the analytical model.

3.9 Theoretical Velocity and Salinity Profiles

3.9.1 Velocity Profiles

For the condition of zero horizontal velocity at the bottom, the dimensionless stream function, equation 3.52, is

$$\psi = \frac{\partial \theta_d}{\partial \xi} \frac{C_1}{24} (- \eta^4 + 2\eta^3 - \eta) - \eta + 1 + \frac{\eta}{2} (\eta^2 - 1)(1 - \frac{\partial \theta_d}{\partial \xi} \frac{C_1}{24}) \qquad 3.52$$

where

$$C_1 = \frac{g\alpha S_o h^4 b}{L_i D Q_f} .$$

The horizontal velocity, normalized by the freshwater velocity $U_f = \frac{Q_f}{bh}$ is

$$\frac{U}{U_f} = - \frac{\partial \psi}{\partial \eta} = - \frac{\partial \theta_d}{\partial \xi} \frac{C_1}{24} (- 4\eta^3 + 6\eta^2 - 1) - 1 - \frac{1}{2} (1 - \frac{\partial \theta_d}{\partial \xi} \frac{C_1}{24})(3\eta^2 - 1) \qquad 3.62$$

and the vertical velocity normalized by this same factor is

$$\frac{V}{U_f} = \frac{L_i}{h}\frac{\partial \psi}{\partial \xi} = \frac{L_i}{h}\frac{C_1}{24}\frac{\partial^2 \theta_d}{\partial \xi^2}(-\eta^4 + 2\eta^3 - \eta) - \frac{\eta}{2}(\eta^2 - 1)\frac{\partial^2 \theta_d}{\partial \xi^2}\frac{C_1}{24}. \qquad 3.63$$

Table 3.1

Model Parameters for Figures 3.2 - 3.4

S_o	29.2	ppt
L_i	160	ft
h	.5	ft
b	.75	ft
α	.75	
θ_d	.66	
$\frac{\partial \theta_d}{\partial \xi}$	- .97	
$\frac{\partial^2 \theta_d}{\partial \xi^2}$	-2.86	
D	$.24 \times 10^{-3}$	ft^2/sec
K	$.18 \times 10^{-3}$	ft^2/sec

The broken lines in figures 3.2 and 3.3 illustrate these velocity profiles for representative values of input parameters listed in Table 3.1. The horizontal velocity profile, figure 3.2, clearly shows the boundary conditions of zero gradient at the surface and zero velocity at

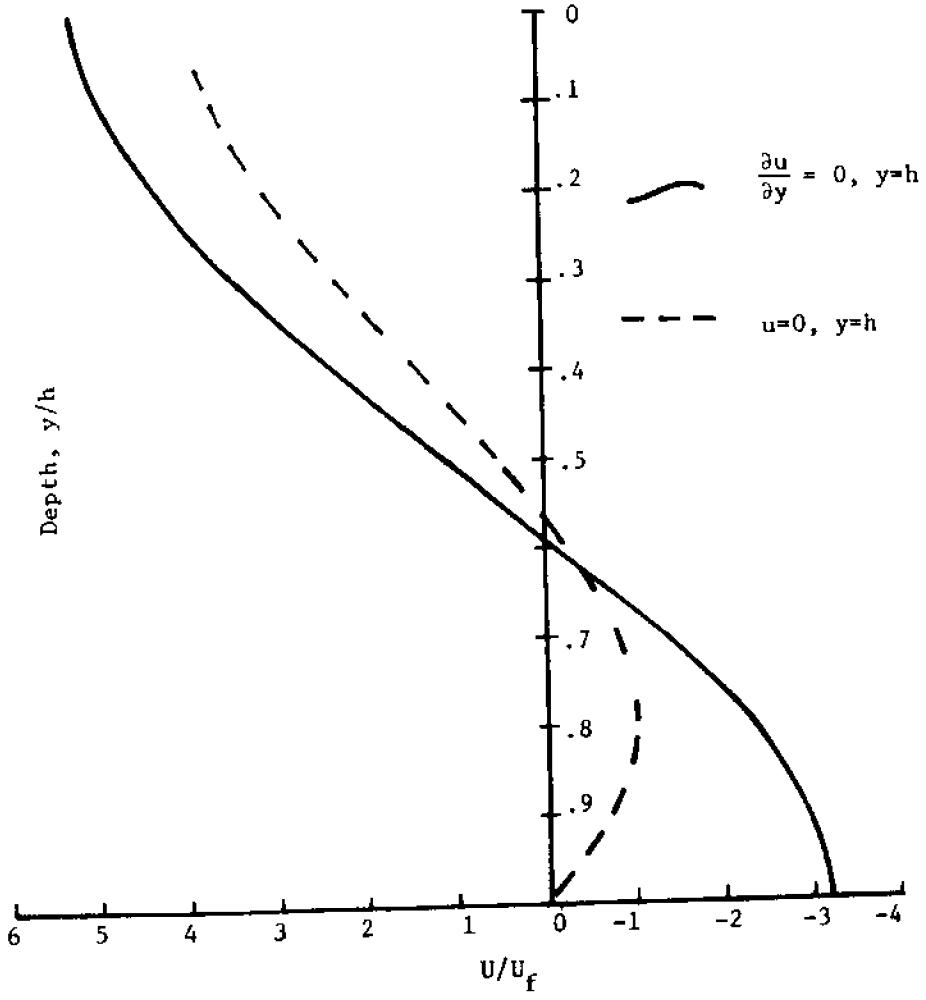

Figure 3.2 Analytic solution for horizontal velocity profile

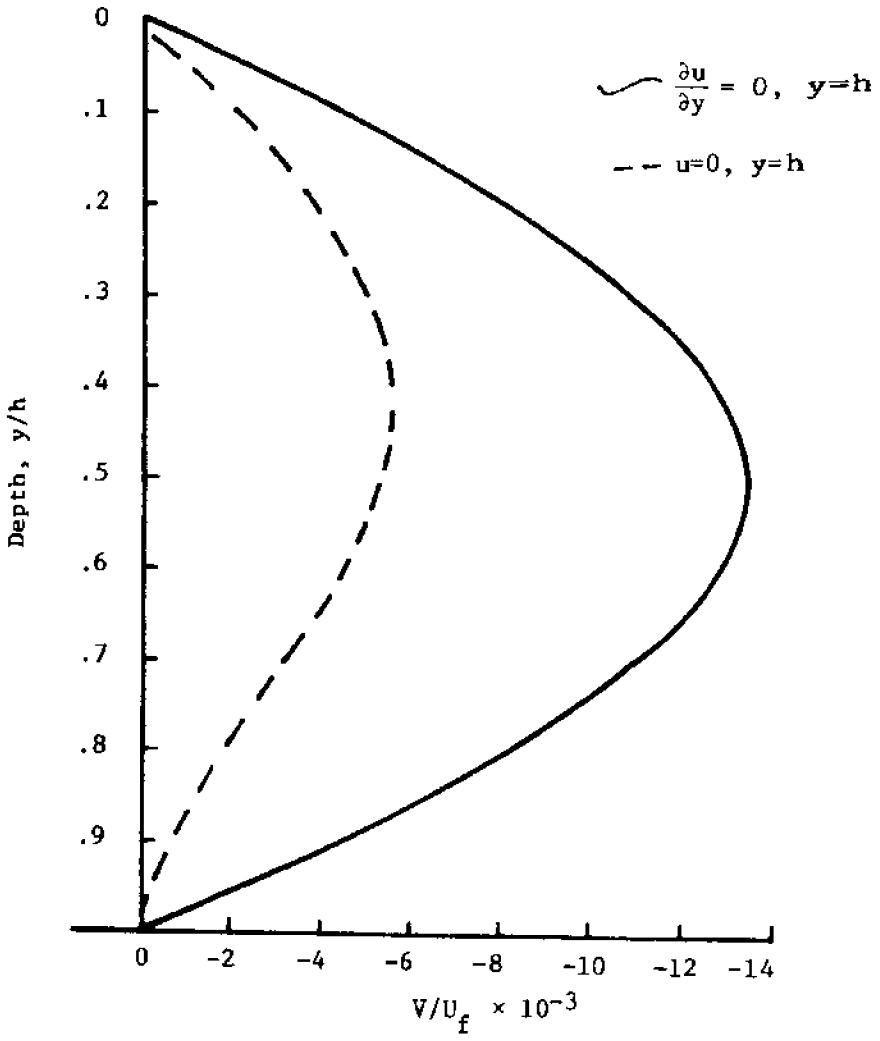

Figure 3.3 Analytic solution for vertical velocity profile

the bottom. The flow reversal, with seaward flow in the top region and landward flow in the bottom region is also demonstrated. The intergral of this profile is equal to 1.0 which is a net discharge of the freshwater inflow. Figure 3.3 shows the vertical velocity profile for the same conditions. This velocity is zero at the surface and bottom, and directed downward throughout the depth. From the form of equation 3.63 it is apparent that the direction of the vertical velocity depends on the sign of the second derivative of the salinity gradient $\frac{\partial^2 \theta_d}{\partial \xi^2}$ a point which will be further discussed in section 4.2.2. The maximum value of this velocity occurs near mid-depth.

The second case for the bottom boundary condition is that the vertical gradient of the horizontal velocity is zero, as stated in equation 3.55.

$$\psi = \frac{\partial \theta_d}{\partial \xi^2} \frac{C_1}{24} \{- \eta^4 + 2\eta^3 - \eta\} - \eta + 1. \qquad 3.55$$

Proceeding in a similar manner,

$$\frac{U}{U_f} = - \frac{\partial \psi}{\partial \eta} = - \frac{\partial \theta_d}{\partial \xi} \frac{C_1}{24} \{ - 4\eta^3 + 6\eta^2 - 1 \} - 1 \qquad 3.64$$

and

$$\frac{V}{U_f} = \frac{L_i}{h} \frac{\partial \psi}{\partial \xi} = \frac{L_i}{h} \frac{C_1}{24} \frac{\partial^2 \theta_d}{\partial \xi^2} \{- \eta^4 + 2\eta^3 - \eta\}. \qquad 3.65$$

These profiles are shown as solid lines on figures 3.2 and 3.3. For this case, both the horizontal velocity U and the vertical velocity V are symetric about the mid-depth, y/h = 0.5. In addition, the horizontal velocity is symetric about a vertical coordinate of $U/U_f = 1.0$.

The mean eddy coefficient D, as well as all other input parameters, is the same for both cases plotted in figures 3.2 and 3.3. Thus, for the same value of D, the boundary condition of zero bottom velocity results in a significant reduction in both the horizontal and the vertical velocities over most of the depth. This means that the choice of boundary condition will influence the best-fit values of D for a given set of experimental or field data.

3.9.2 Salinity Profiles

The model solution for the vertical salinity distribution is given as

$$\theta(\xi,\eta) = \int f(\xi,\eta)\, d\eta + \theta_d - \int_0^1 \int f(\xi,\eta)\, d\eta\, d\eta \qquad 3.61$$

where

$$f(\xi,\eta) = \exp\left\{\int \frac{\partial \psi}{\partial \xi}\frac{1}{C_2}\, d\eta\right\}\int - \frac{\partial \psi}{\partial \eta}\frac{\partial \theta_d}{\partial \xi}\frac{1}{C_2} \exp\left\{\int - \frac{\partial \psi}{\partial \xi}\frac{1}{C_2}\, d\eta\, d\eta\right.$$

and

$$C_2(\xi) = \frac{K(\xi)\, L_i b(\xi)}{Q_f\, h(\xi)} \qquad 3.62$$

Using the same data from Table 3.1, as in the example for the velocity profile, figure 3.4 illustrates the salinity profile for zero bottom velocity (broken line) and zero bottom stress (solid line). It is clear from these figures that the choice of velocity boundary condition also influences the vertical salinity distribution if the same value of K is used.

In obtaining equation 3.61 for the salinity distribution, an assumption of zero vertical gradient at the surface was made. Figure

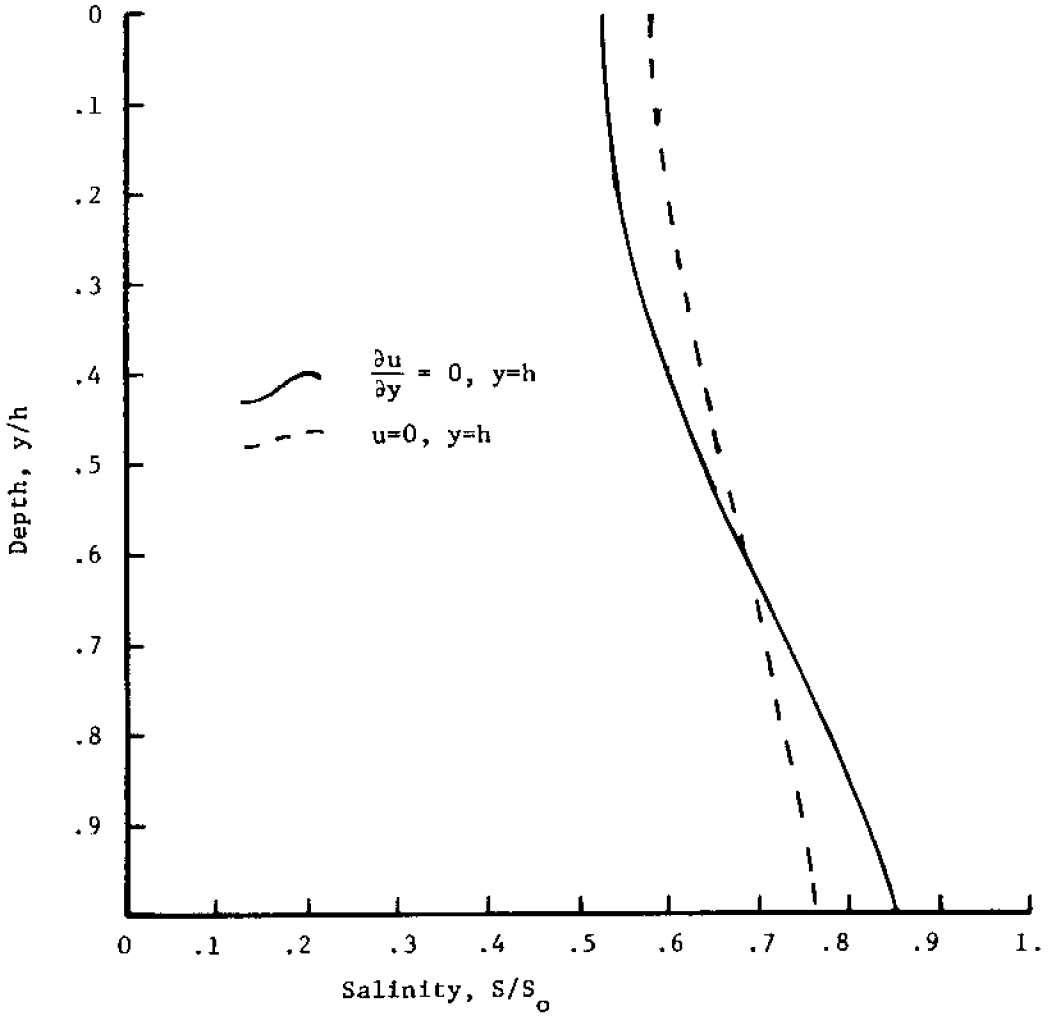

Figure 3.4 Analytic solution for salinity profile

IV Evaluation of Steady-State Solution

4.1 Introduction

The analytical solution for velocity and salinity distribution developed in Chapter II is evaluated with laboratory data from the Vicksburg salinity flume, the Delft Hydraulic Laboratory salinity flume and the James River field study. This combined set of data covers a wide range of flow conditions and degrees of salinity stratification, some of which may partially invalidate model assumptions. These latter studies help to define the limits of model application. For each case studied, a best-fit value for the two mean eddy coefficients is found at each longitudinal station. All of these cases are assumed to be in a steady-state condition, i.e., values for velocity and salinity for successive tidal cycles are assumed the same. This assumption is valid for the flume studies by experimental design. For the James River study, steady-state can only be an approximate condition, depending upon the freshwater hydrograph.

4.2 W.E.S. Flume

4.2.1 Description of Flume

The laboratory flume of the Corps of Engineers, U.S. Army, Vicksburg Waterways Experiment Station (WES), is described in detail in a WES report (1955). The flume, schematically shown in figure 4.1, is a lucite channel 327 ft. long, 0.75 ft. wide and 1.5 ft. in total depth. At the ocean end there is a tidal reservoir which can maintain a constant salinity and a periodic surface level. The opposite end has a freshwater reservoir. Roughness is achieved by 1/4 inch strips attached to the side walls on 2 inch centers. Different estuarine conditions are modeled by varying the freshwater inflow, the tidal amplitude and the basin salinity.

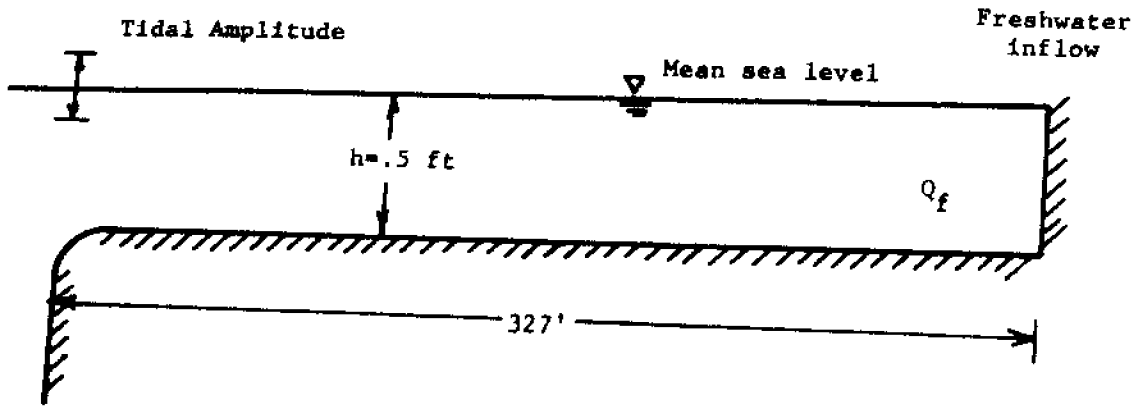

Figure 4.1 Schematic diagram of WES tidal flume

Detailed one-dimensional results are presented by Ippen and Harleman (1961) for numerous tests and conditions. Harleman and Ippen (1967) present two-dimensional analysis of three tests showing the average over a tidal period of the vertical velocity and salinity profiles for several longitudinal stations. Table 4.1 summarizes the flume conditions for these three runs.

4.2.2 Evaluation of Bottom Boundary Condition - WES 16

The depth-averaged time-averaged longitudinal salinity distribution and its first and second derivatives is a required input to the analytical model. For the purpose of evaluating the model solutions and determining the eddy coefficients, this salinity distribution is determined from the recorded data. An analytical function is passed through the data points, and its first and second derivatives computed using a spline computer program, outlined in appendix 2. Figure 4.2a shows the depth-averaged, time-averaged longitudinal salinity distribution for WES 16. The experimental points are the depth-averages of the vertical profiles shown in Plate 11 of Harleman and Ippen (1967), and the smooth curve is the fitted spline function. The first and second derivatives for this function are plotted in figures 4.2b and 4.2c respectively. As stated previously, the inflection point shown in figure 4.2c determines the longitudinal position where the vertical velocity changes its direction.

Harleman and Ippen (1967) backfigured vertical velocities using graphical intergration of the equation of continuity. Figure 4.2d shows these vertical velocities with the corresponding velocities from the analytical solution. The agreement in direction, and more significantly, location of the reversal in direction (between 40 and 80) confirms the

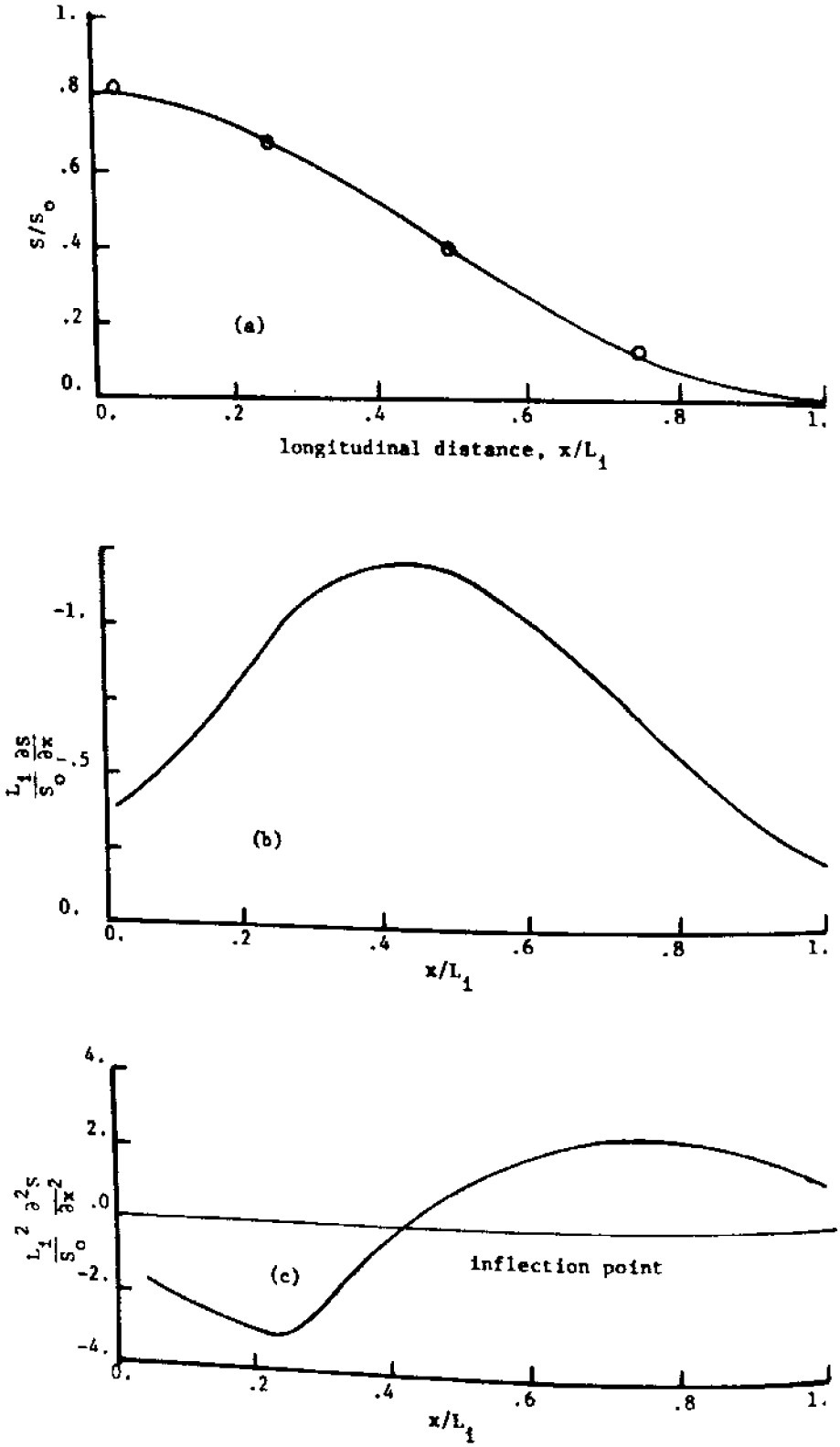

Figures 4.2 a,b,c Longitudinal salinity and derivatives, WES 16

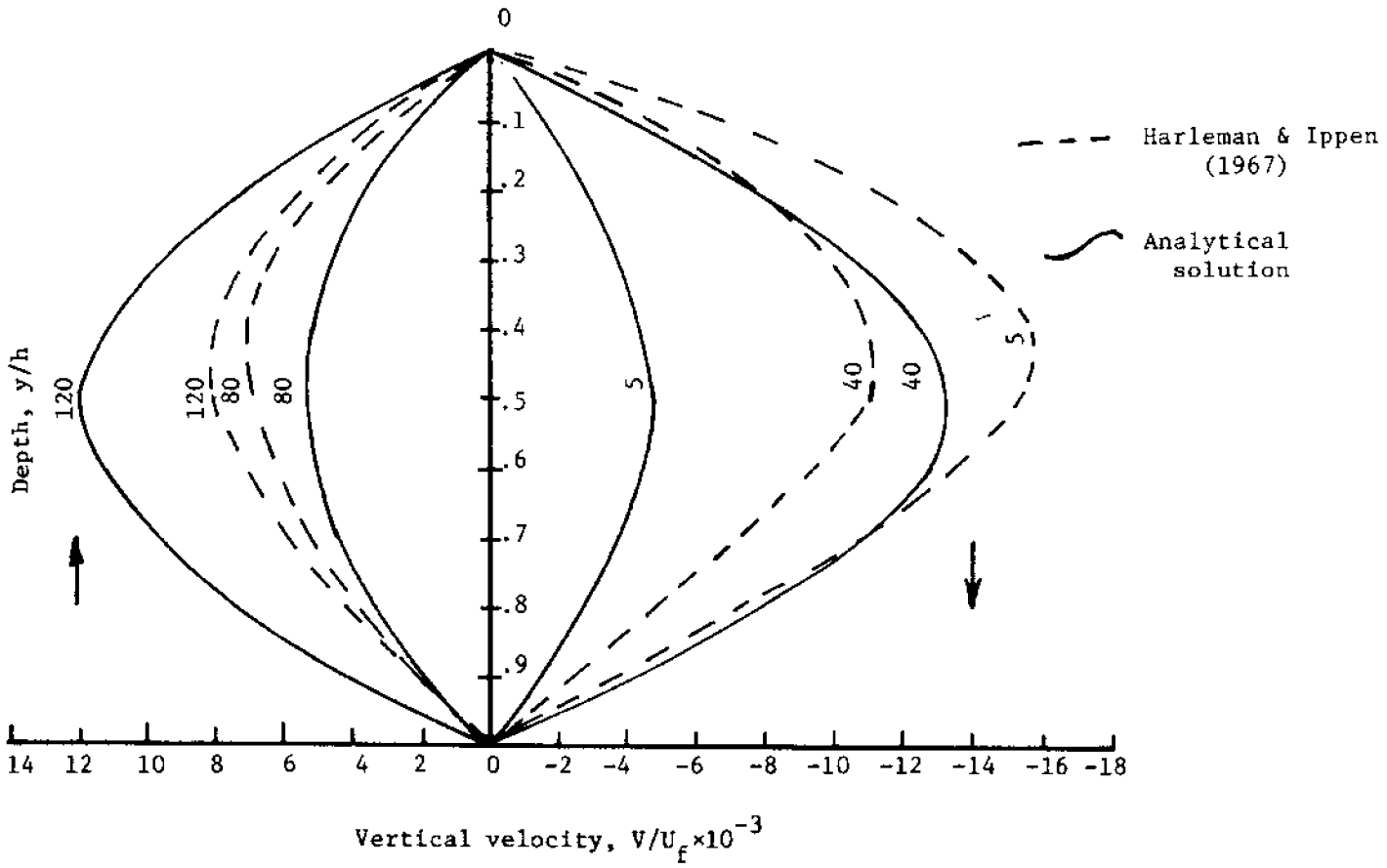

Figure 4.2d Distribution of vertical velocity, WES 16

Table 4.1

Summary of WES Salinity Flume Conditions

Flume depth at msl = 0.5 ft. Tidal Period = 600 sec

Length of Flume = 327 ft. Flume Width = 0.75 ft.

Test No.	Tidal Basin Salinity, ppt	Tidal Basin Amplitude, ft.	Freshwater Velocity, ft^2/sec	Intrusion Length, ft.
11	26.4	0.05	0.056	140.
14	29.7	0.10	0.020	180.
16	29.2	0.05	0.020	160.

observation that the inflection point of the first derivative of the salinity determines this location. The large difference in magnitude between the vertical velocities at station 5 is probably due to the fact that in both the graphical technique of Harleman and Ippen and the spline function of the present analysis, difficulty is encountered at the end points, where extrapolation becomes necessary. Consequently, all analytical results at the upstream or downstream ends of observed or predicted salinity distributions must be viewed with a considerable degree of caution.

Having found the longitudinal salinity distribution function and using the values for the other input parameters from table 4.1, the analytical model can be evaluated for different values of the eddy coefficients. Two solutions sets are shown, depending upon the choice of bottom boundary condition for the horizontal velocity. The computations are carried out on a digital computer, as is outlined in appendix 1.

Case 1 - Zero Bottom Velocity

The equations for the model solutions for velocity and salinity are given in Chapter III. Figure 4.3a and figure 4.3b show the best-fit comparisons of model and experimental velocity profiles for 5 stations, 5, 40, 80, 120 and 160 feet from the ocean end for WES test 16. At each station, a different value for the eddy coefficient D is used, as listed in table 4.2. At station 5, very close to the ocean reservoir of the flume, entrance effects, as well as the influence of extrapolated gradients, probably are responsible for the higher values of D for both cases. At the remaining stations, the values of the eddy coefficients do not vary much with the longitudinal position. From the figures, 4.3a - 4.3b, it is seen that the condition of zero bottom stress,

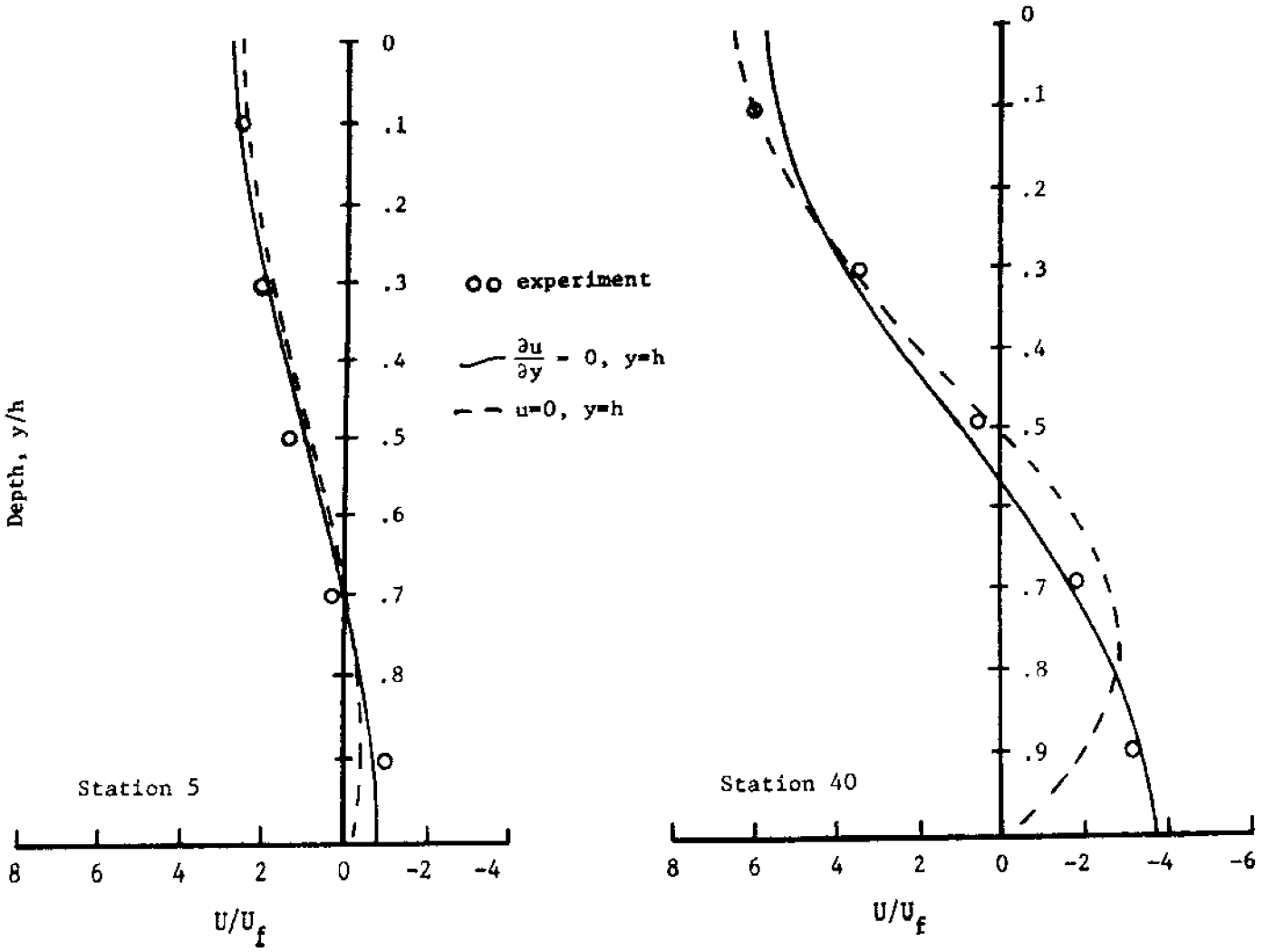

Figure 4.3a Horizontal velocity profiles, WES 16, stations 5, 40

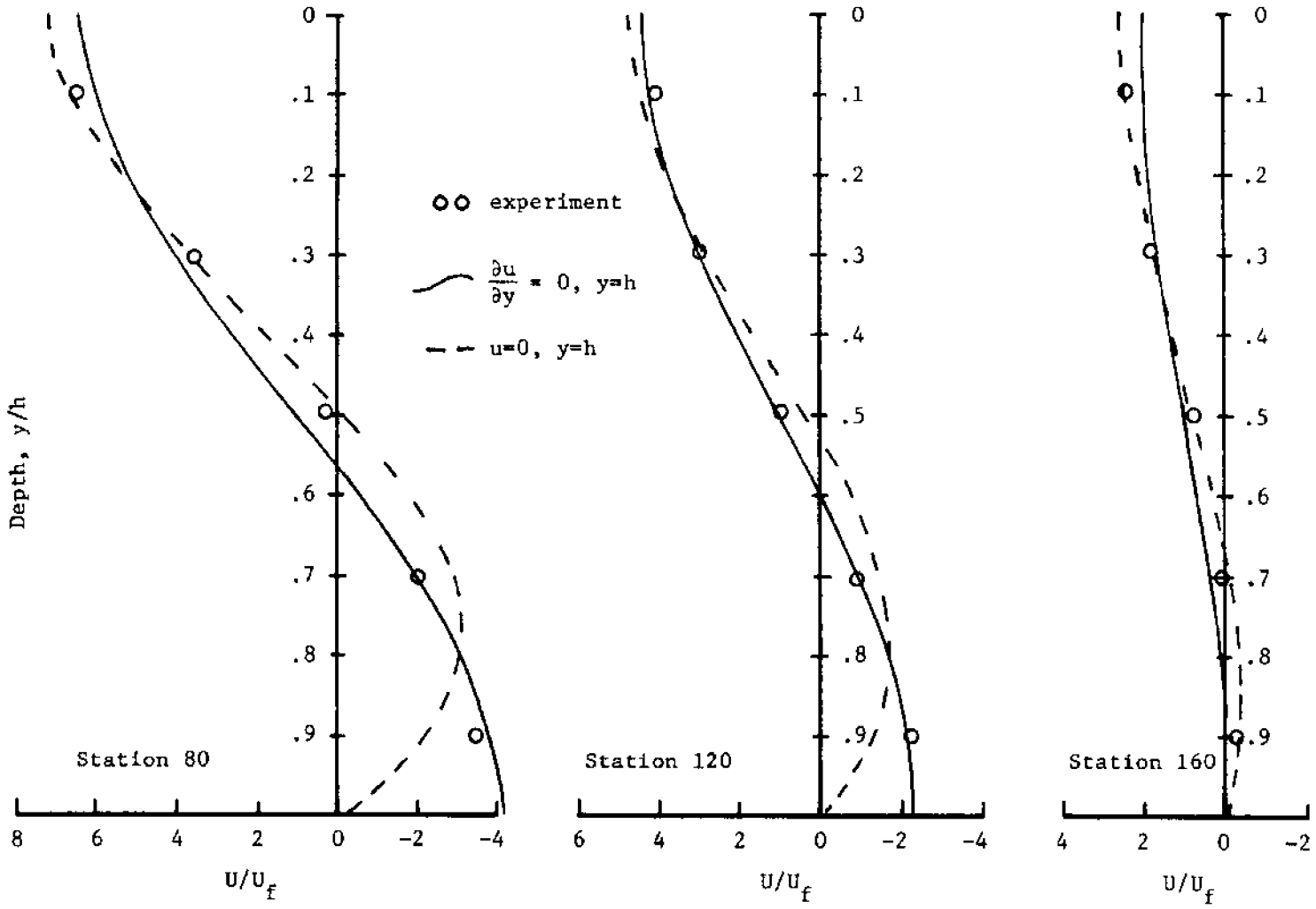

Figure 4.3b Horizontal velocity profiles, WES 16, stations 80, 120 and 160

case 2, gives a better fit to the experimental data. Figures 4.3c - 4.3d show the comparisons of salinity profiles for the same flume test. Clearly, the choice of velocity boundary condition has little effect on the salinity profiles. Table 4.3 lists the best-fit values of the eddy coefficient of salt K for the WES test No. 16 for the two cases. Again, except for station 5, 5 feet from the flume entrance, the eddy coefficients do not vary much along the length of the flume.

Based upon an evaluation of figures 4.3a - 4.3d as well as similar plots for other WES tests, case 2, which states that at the bottom the vertical gradient of the longitudinal velocity is zero, was chosen as the most suitable boundary condition. In making this selection, certain emphasis was placed on modeling the net velocities just above the bed (which this case handles better than the condition of zero bottom velocity) for the purposes of analyzing sediment transport problems. All remaining comparisons of experimental and analytical velocity and salinity profiles are for this zero gradient condition, case 2. Table 4.4 illustrates the comparison of computed and experimental velocity and salinity distributions for WES test 16 for the zero gradient boundary condition. All data in this table except the values for D and K are dimensionless, the latter having units of ft^2/sec. Appendix 3 contains the complete tabulated summary of WES test 16, as well as the data for the other tests analysed in this study.

4.2.3 WES Test 14 and 11

The other two WES tests used to evaluate the analytical model are examples of a more stratified flow, test 11, and a less stratified flow, test 14. Figures 4.4a - 4.4b illustrate experimental and model agreement

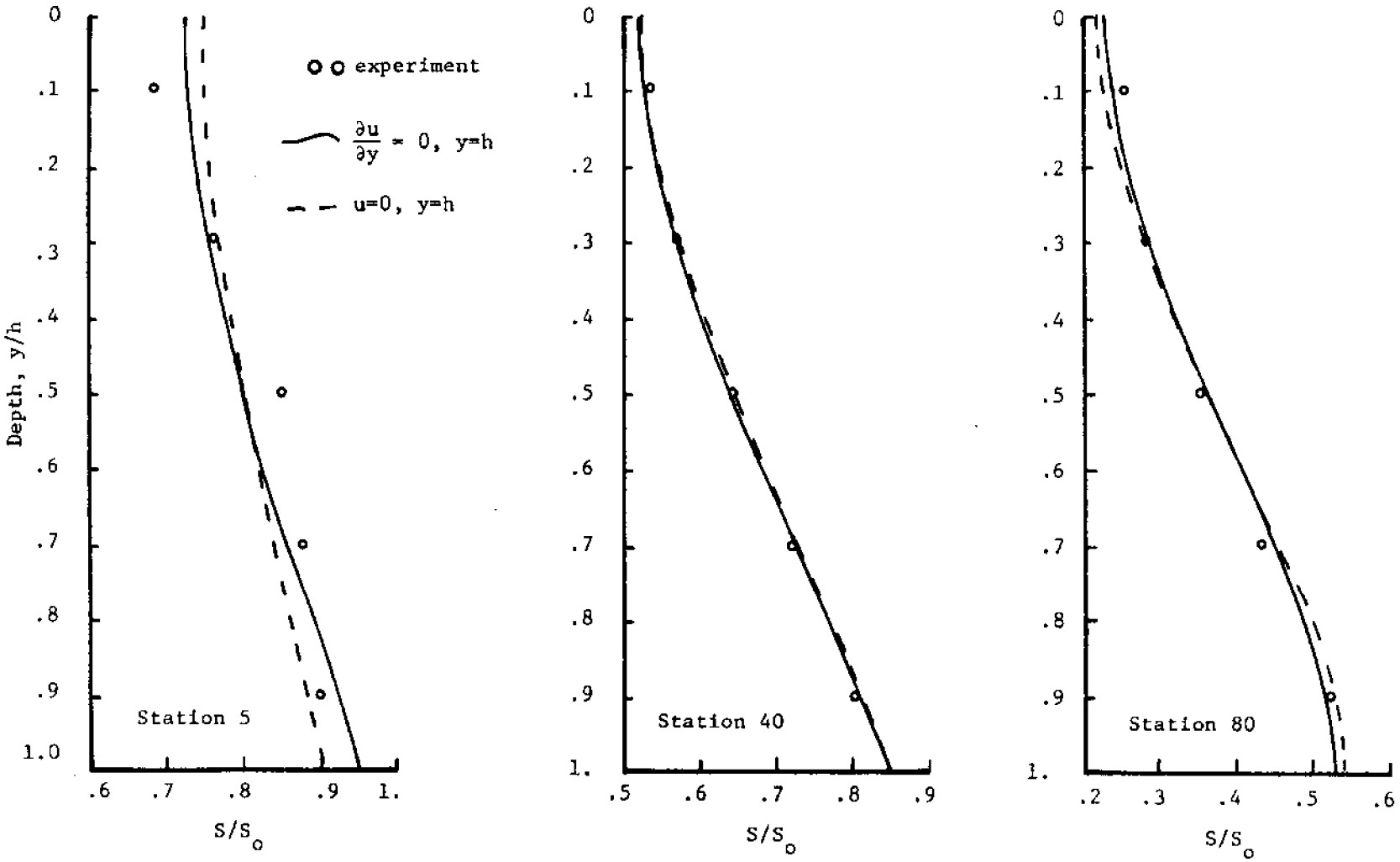

Figure 4.3c Salinity profiles, WES 16, stations 5, 40 and 80

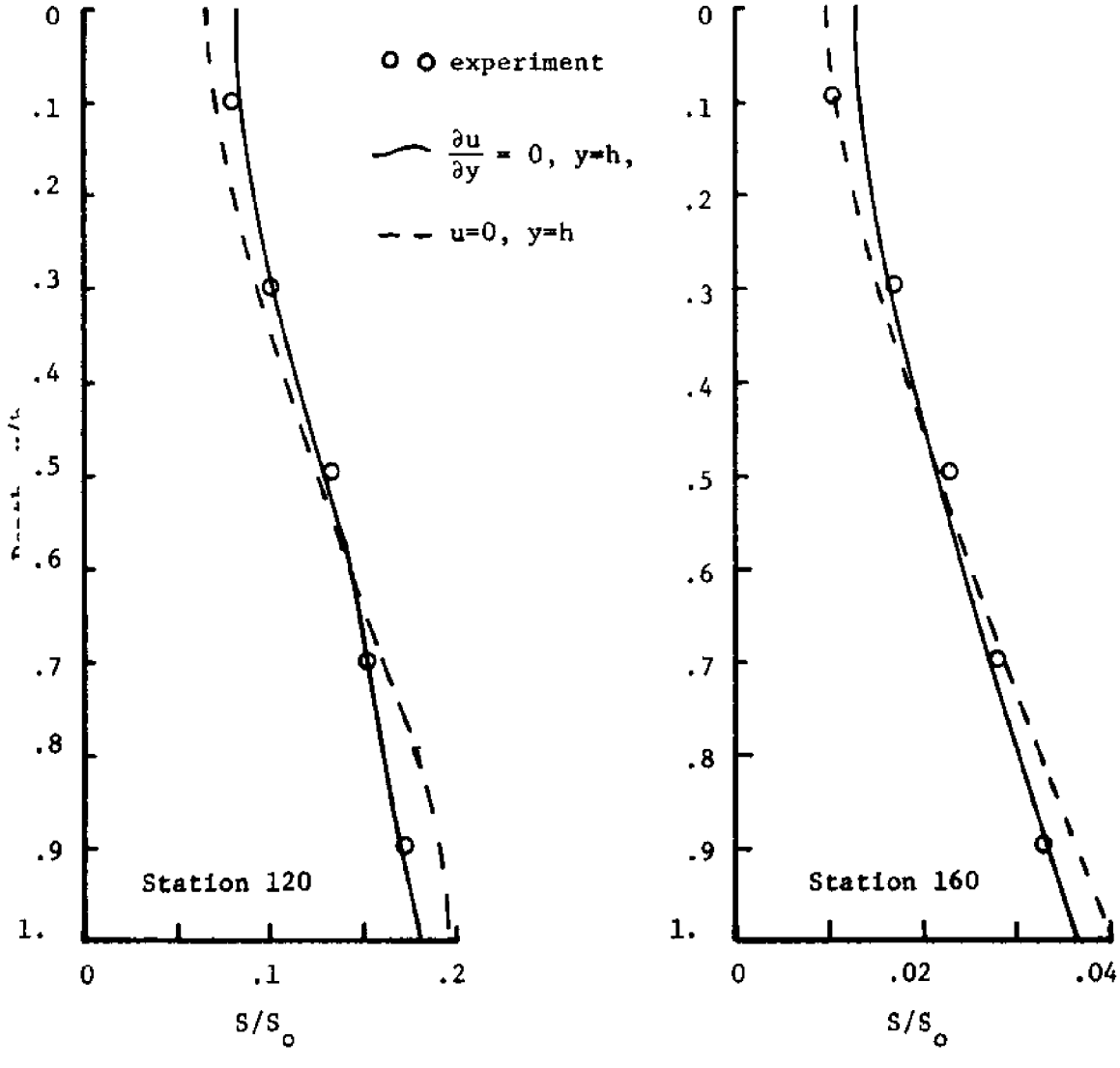

Figure 4.3d Salinity profiles, WES 16, stations 120 and 160

Table 4.2

Best-Fit Values for D for WES-16

Station	Case 1	Case 2
	$u=0,\ y=h$	$\frac{\partial u}{\partial y}=0,\ y=h$
	D, $Ft^2/sec \times 10^{-3}$	D, $Ft^2/sec \times 10^{-3}$
5	.2	.35
40	.11	.24
80	.12	.26
120	.12	.24
160	.12	.22

Table 4.3

Best-Fit Values for K for WES-16

Station	Case 1	Case 2
	$u=0,\ y=h$	$\frac{\partial u}{\partial y}=0,\ y=h$
	K, $Ft^2/sec \times 10^{-3}$	K, $Ft^2/sec \times 10^{-3}$
5	.07	.18
40	.17	.18
80	.15	.17
120	.15	.21
160	.15	.18

TABLE 4.4

COMPUTED AND EXPERIMENTAL VELOCITY AND SALINITY DISTRIBUTIONS

WES TEST 1A

X/LI = 0.50

S MEAN= 0.367 DS/DX MEAN= -1.145 DS2/DX2 MEAN= 1.275

U= 0.20E-03 SQ FT/SEC K= 0.17E-02 SQ FT/SEC

Y/H	EXP U/UF	COMP U/UF	EXP S/SO	COMP S/SC
0.000	7.20	6.14	0.24	0.23
0.100	6.50	5.87	0.25	0.24
0.200	5.20	5.05	0.26	0.26
0.300	3.50	3.93	0.28	0.28
0.400	1.00	2.53	0.31	0.42
0.500	0.30	1.00	0.35	0.36
0.600	-1.00	-0.53	0.39	0.40
0.700	-2.00	-1.93	0.43	0.44
0.800	-3.00	-3.09	0.47	0.48
0.900	-3.40	-3.97	0.52	0.50
1.000	-3.90	-4.16	0.54	0.52

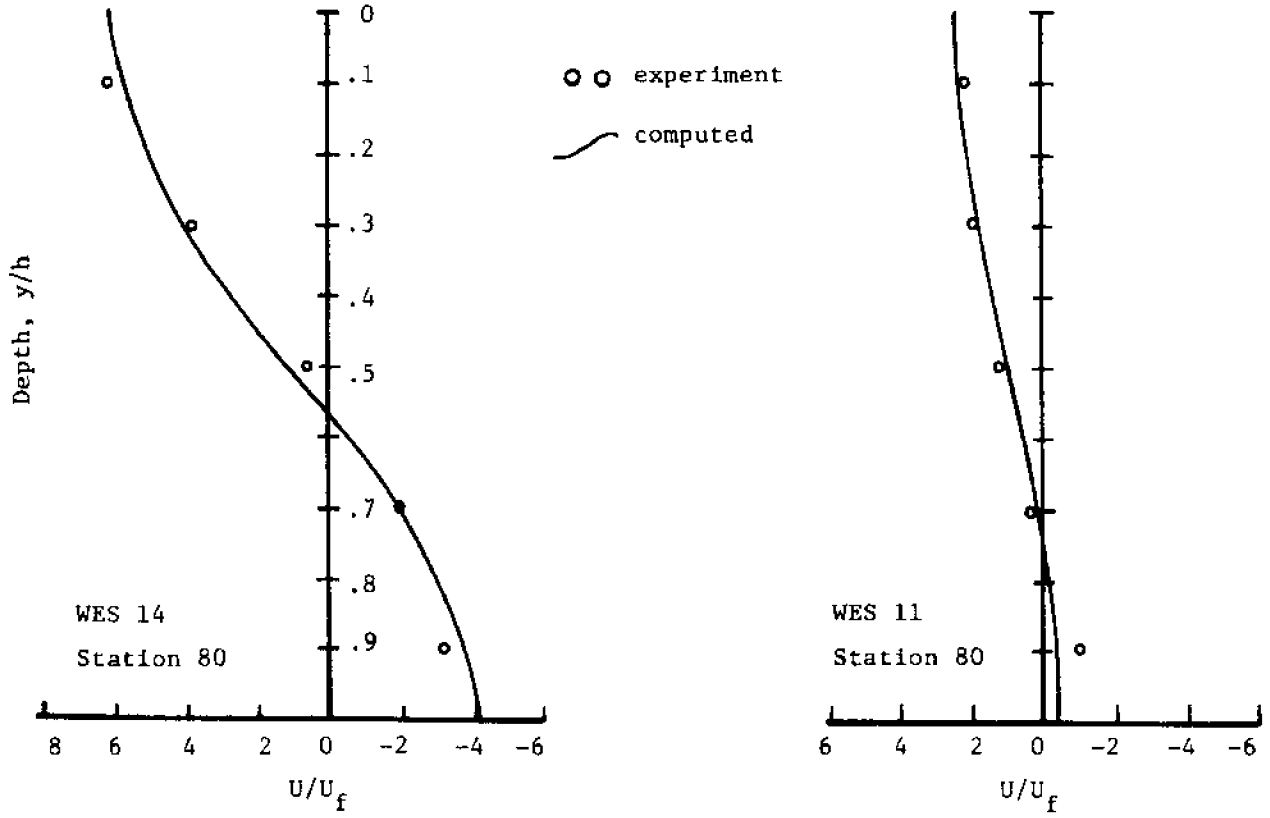

Figure 4.4a Horizontal velocity profiles, WES 11 & WES 14, station 80

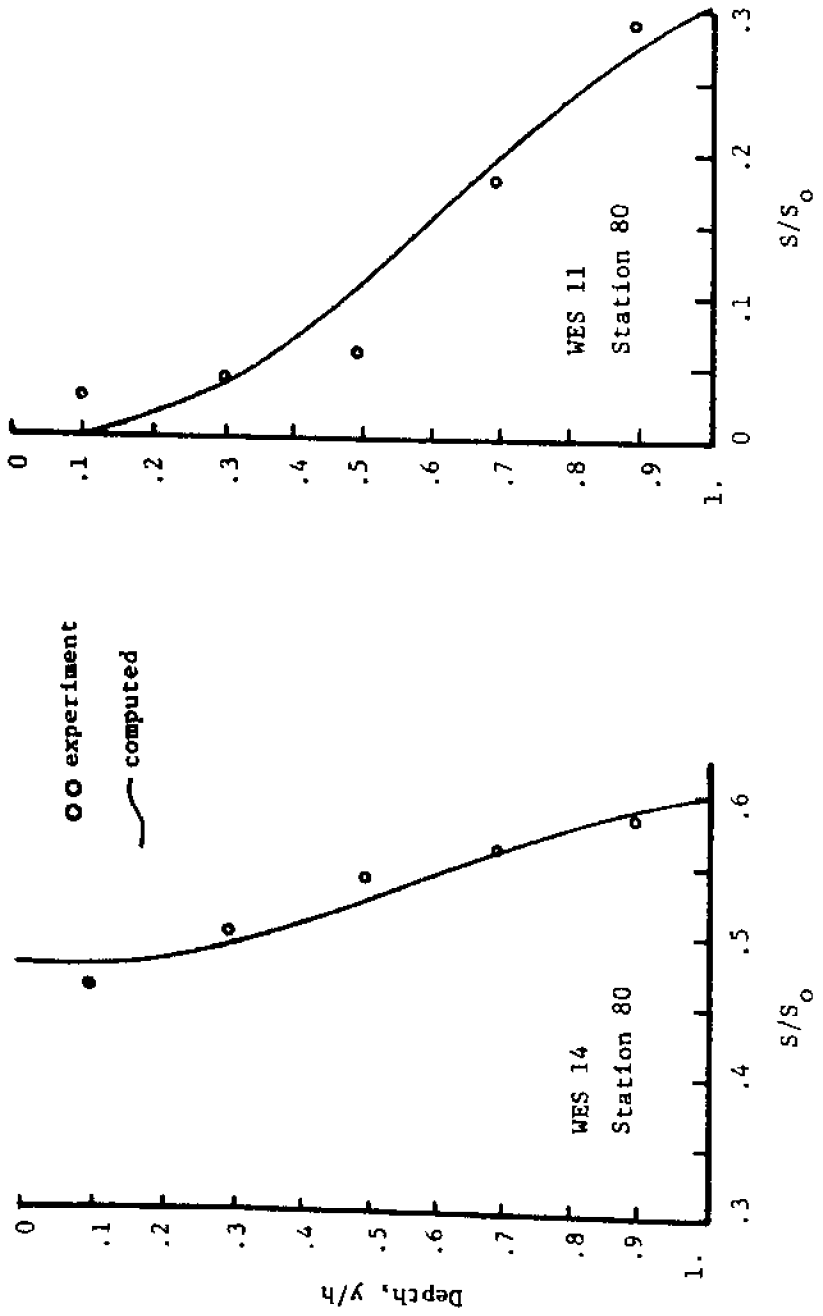

Figure 4.4b Salinity profiles, WES 11 and Wes 14, station 80

for velocity and salinity at station 80 for both tests. In figure 4.4b (test 11) the salinity gradient at the botton y/h = 1.0 has an appreciable slope, indicating that perhaps the model assumptions are not as valid for this degree of stratification. The tables in appendix 3 summarize the results for these two tests.

4.3 Delft Flume

4.3.1 Description of Flume

At the Delft Hydraulics Laboratory an experimental investigation of salinity intrusion in estuaries similar to the Vicksburg studies has been carried out. The details of flume design and measurement technique are reported in Delft (1970). Table 4.5 lists the basic Delft flume dimensions with those of the Vicksburg flume for comparison. For the Delft

Table 4.5

Delft and Vicksburg Flume Dimensions

	Delft	Vicksburg
Length, ft.	546	327
Depth, ft. (msl)	.7	.5
Width, ft.	2.0	.75
Roughness	(bottom)	(side)

test the bottom roughness was achieved by vertical bars .5 x .5 cm^2 in cross-section attached to the flume bottom. By changing the number of bars the roughness could be varied for different runs.

Four Delft tests were analysed with the analytical model. All the tests were for steady-state conditions and the longitudinal salinity

distribution was backfigured from the recorded data as was done for the WES tests. Table 4.6 summarizes the flow conditions for these four tests. Tabulated detailed results can be found in appendix 3 which document the agreement between experimental data and best-fit analytical solutions for these Delft tests. Figures 4.5 - 4.8 illustrate these results at a central section of the salinity regime.

4.4 James River Estuary

The Chesapeake Bay Institute 1950 survey of the James River estuary is described by Pritchard and Kent (1953). Velocity and salinity data, averaged over several tidal periods, are presented for three longitudinal stations, shown in figure 4.9. Table 4.7 summarizes the flow conditions for the three periods of the survey.

Table 4.7

James River Estuary - Flow Conditions

Date	Q_f, m^3/sec	L_i, m	S_o, ppt
18-23 June	124.	90,900	24
26 June-9 July	104.	94,127	24
17-21 July	130.	90,000	24

The data in the field survey report did not include sufficient longitudinal salinity stations for direct estimates of the intrusion lengths and ocean salinity (Chesapeake Bay salinity). The ocean salinity was estimated from an unpublished report by the U.S. Army, Waterways Experiment Station, describing the salinity verification of a hydraulic model of the James River estuary. The intrusion lengths were determined from Lee (1970), figure 14.10 which plots intrusion length as a function of

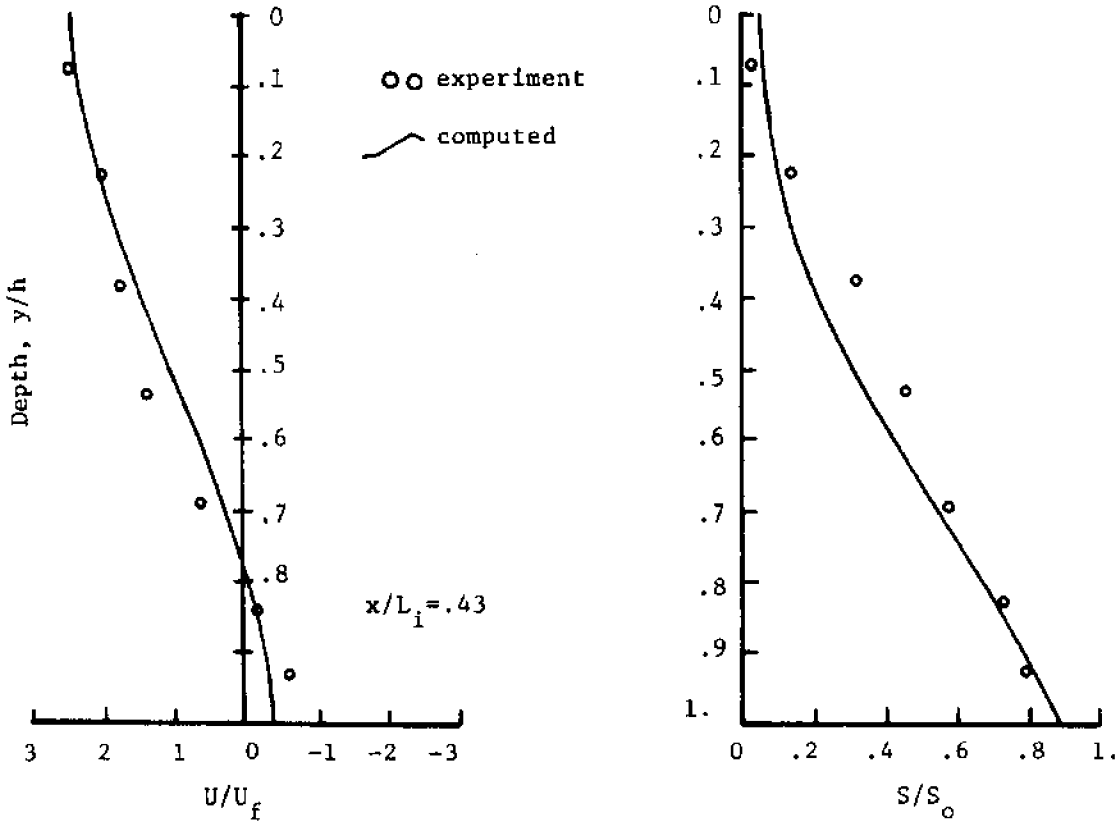

Figure 4.5 Horizontal velocity and salinity profiles, Delft 117

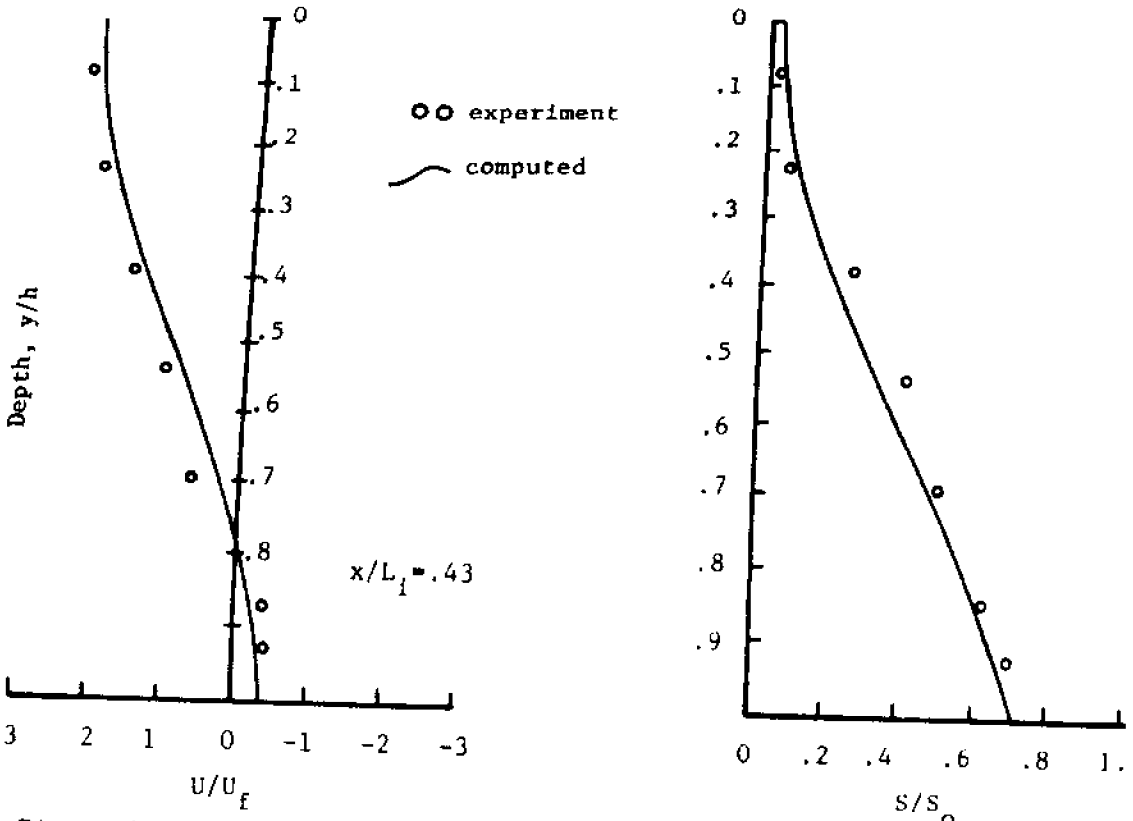

Figure 4.6 Horizontal velocity and salinity profiles, Delft 116

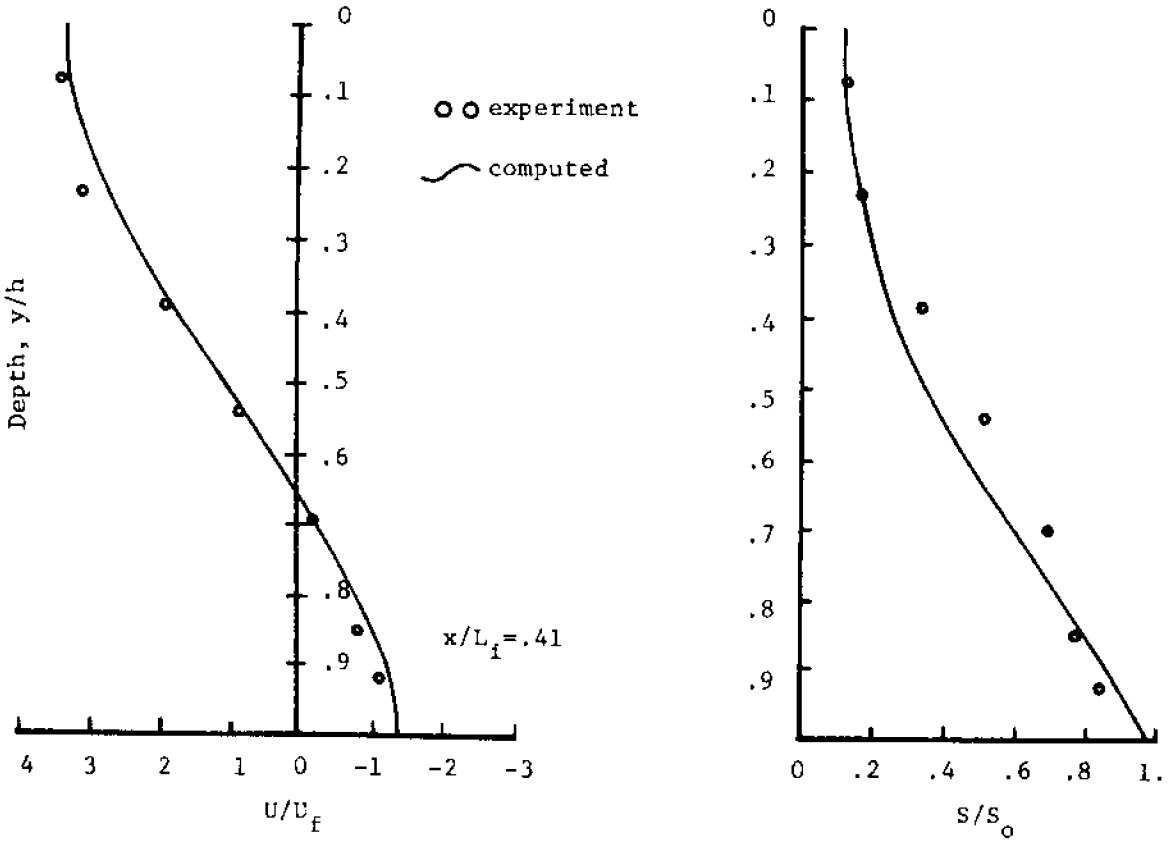

Figure 4.7 Horizontal velocity and salinity profiles, Delft 121

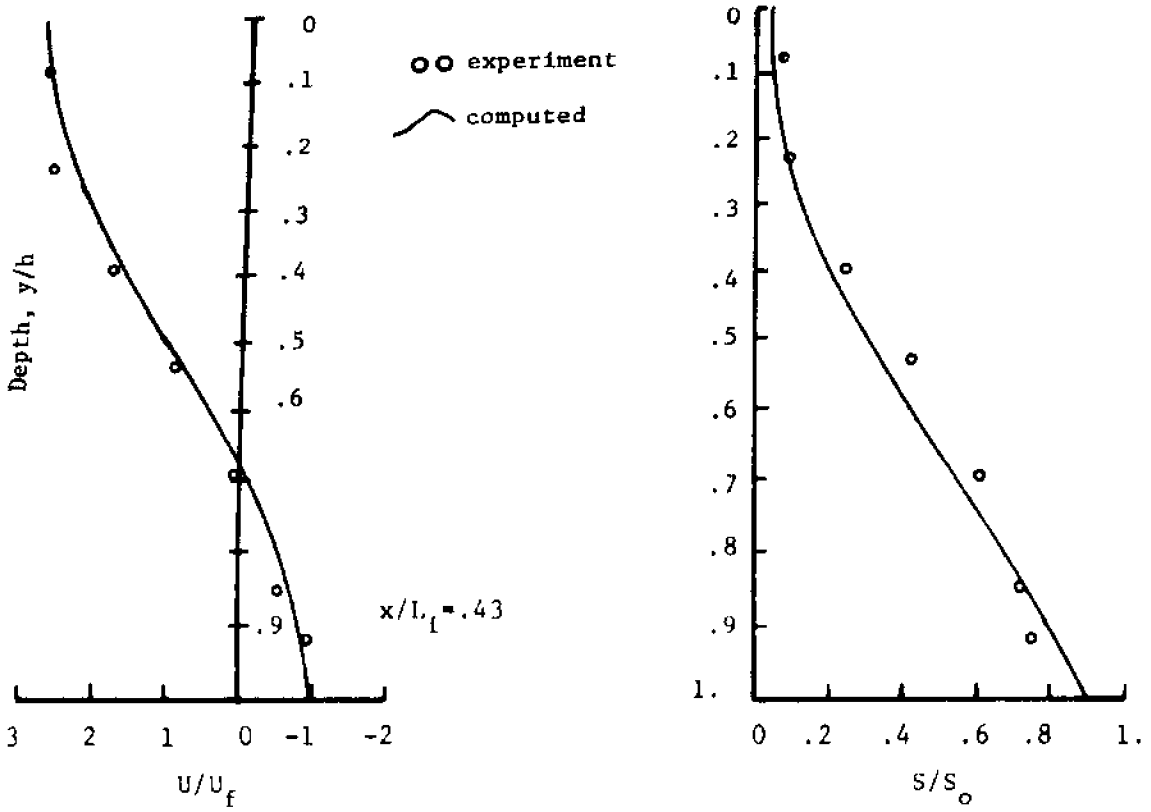

Figure 4.8 Horizontal velocity and salinity profiles, Delft 122

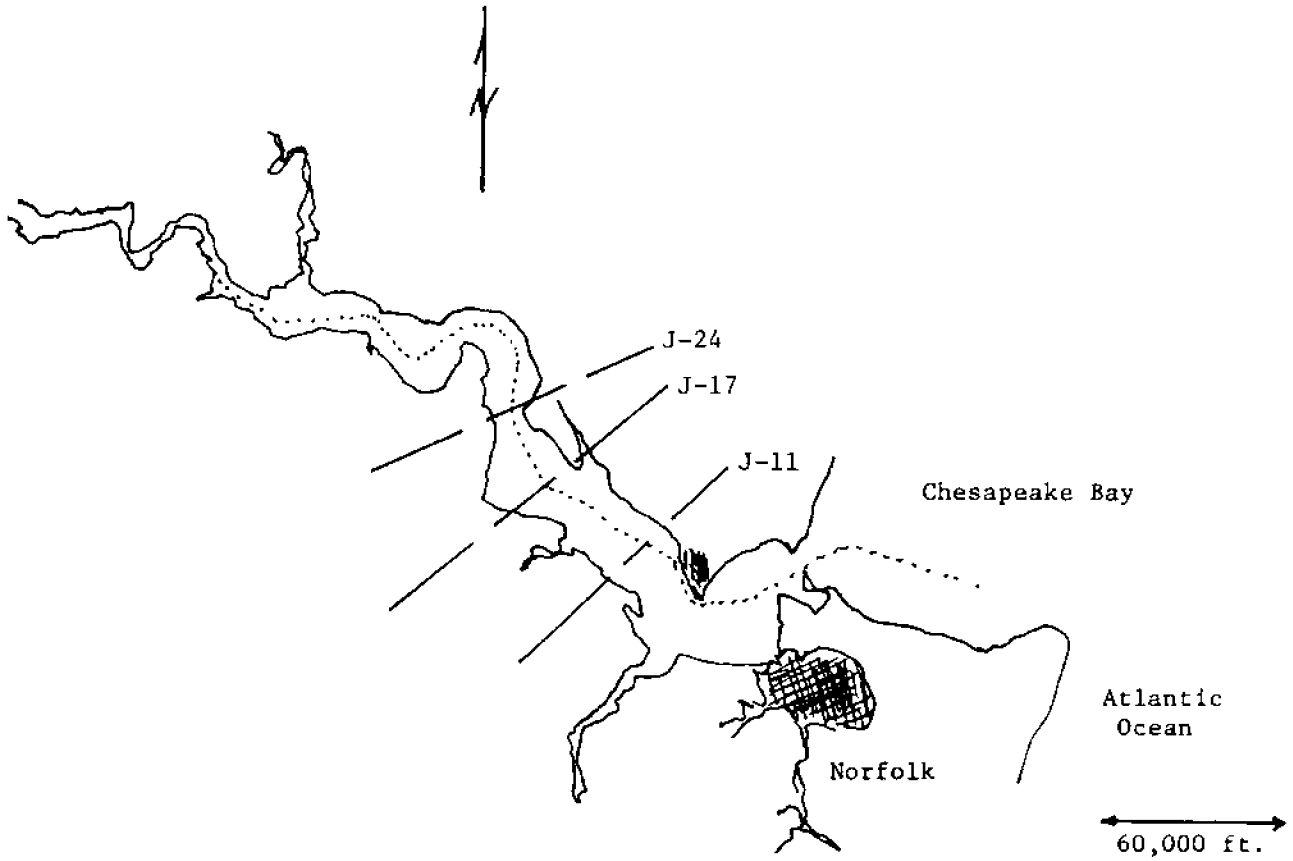

Figure 4.9 Survey sites, James River estuary

Table 4.6

Summary of Delft Salinity Flume Conditions

Flume depth at msl = .216 m

Length of Flume = 179.16 m

Basin Salinity = 30 ppt.

Tidal Period = 560.4 sec

Flume Width = .672 m

Test No.	Roughness $m^{1/2}/sec$	Tidal Amplitude m	Freshwater Discharge m^3/sec	Intrusion Length, m
117	28.5	.0125	- .0029	51.
116	25.3	.0125	- .0029	51.
121	19.0	.0125	- .00145	54.
122	19.0	.0125	- .00181	51.

freshwater discharge.

The depth of mean water was assumed to be 7.5 meters for all three stations, and the mean widths were determined from the CBI report as follows:

station	mean width, m
J-11	3000.
J-17	2350.
J-24	1640.

Tables in appendix 3 present the comparison between field measurement and analytical solution for velocity and salinity with depth. Figure 4.10 illustrates this comparison at J-17 for 26 June-7 July. The difference between computed and actual velocities over most of the depth is probably due to several factors, including the uncertainity of time-averaged field measurements, and more importantly, the simplifying assumption of constant width with depth for the analytic solution. The salinity profiles for this same station show better agreement than the velocities. However, there appears to be a sharp vertical gradient near middepth for the field data which is not observed for the analytical solution. This difference may be a result of the same factors cited before for the velocity profile.

In general, the analytical model, although clearly capable of reproducing flume conditions more exactly, does not appear to break down for the prototype conditions and scales exemplified by the James River estuary.

4.5 Comments on Neglected Terms and Other Model Assumptions

In the development of the governing set of model equations, the time-averaged convective terms have been neglected from the longitudinal

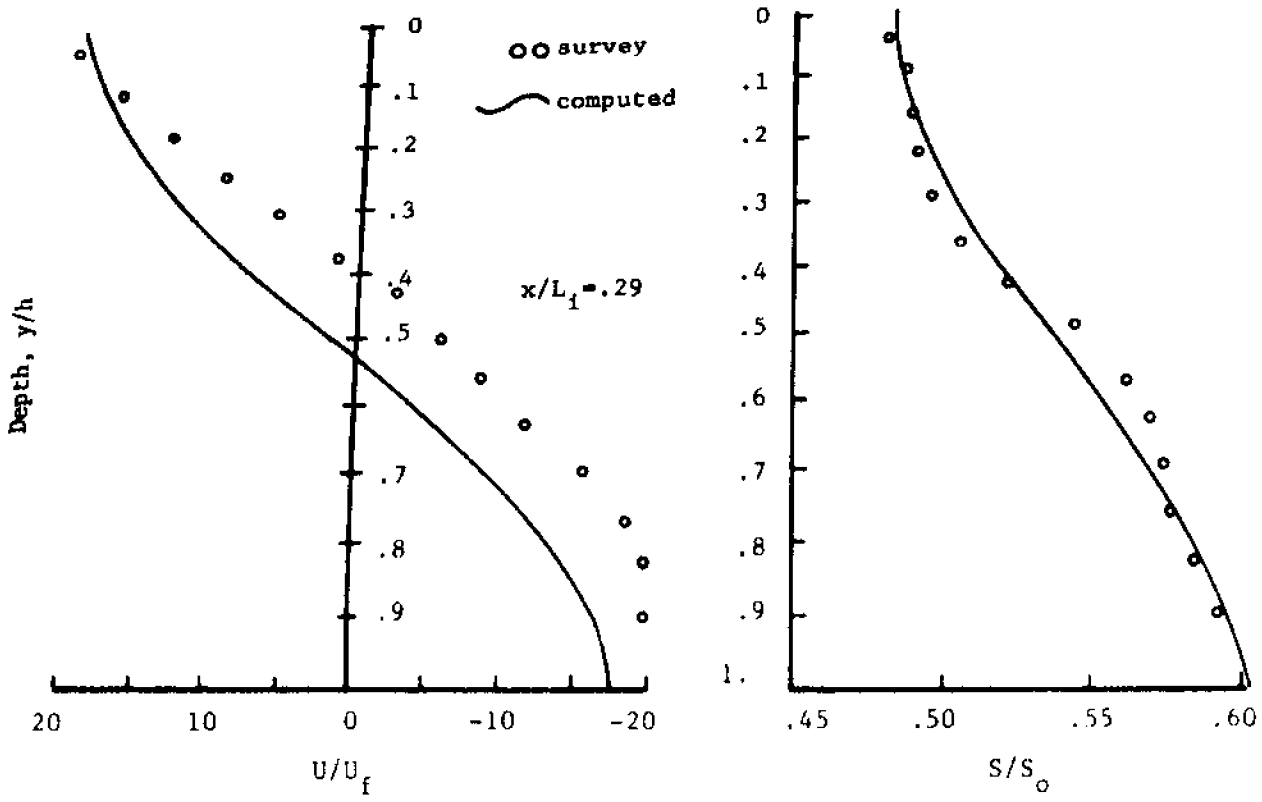

Figure 4.10 Horizontal velocity and salinity profiles, James River, 26 June - 7 July

equation of motion, leaving the pressure gradient balanced by the vertical eddy diffusion of momentum

$$\underbrace{U \frac{\partial U}{\partial x} + V \frac{\partial U}{\partial y}}_{\text{neglected}} = - \frac{1}{\rho} \frac{\partial P}{\partial x} + D \frac{\partial^2 U}{\partial y^2} \qquad 4.1$$

These neglected terms can now be computed from equations 3.64 and 3.65 and compared with the remaining terms to determine the reasonableness of the assumtpion. This comparison is shown in table 4.8 for WES test No. 16. At all stations and depths the neglected terms are smaller than the remaining terms, but there are several places, e.g., stations 40 and 80 at middepth where these terms, and especially the vertical convection $V \frac{\partial U}{\partial y}$ is of relatively important size. The non-neglible order of these terms indicates that the mean eddy coefficient D is an ambiguous parameter, including both convective and diffusive components. Table 4.9 shows a similar comparison of the order of the convective terms for Delft test 116 and the James River estuary, 26 June-7 July. Again, the neglected terms are consistently smaller than the pressure gradient-turbulent diffusion terms, but of significant size at about middepth.

A second important model assumption is that the longitudinal salinity gradient $\frac{\partial S}{\partial x}$ is independent of its vertical position, and thus longitudinal salinity profiles at different depths are assumed parallel. Figures 4.11, 4.12, and 4.13 illustrate these profiles for WES 16, Delft 116 and James River 26 June-7 July, respectively. This assumption appears to be quite reasonable from about $x/L_i = .25$ to $x/L_i = .60$ and rather questionable upstream and downstream of this region. However, the tabulated analysis of

Table 4.8

Comparison of Size of Neglected Terms from Longitudinal Equation of Motion for WES Test 16

(all values x 10^{-4} ft/sec^2)

x/L_1 = 0.03

y/h	$U\frac{U}{x}$	$V\frac{U}{y}$	$D\frac{^2U}{y^2}$
0.	.3	.0	6.
.2	.2	.07	3.
.4	.05	.2	1.
.6	-.02	.2	-1.
.8	.03	.07	-3.
1.0	.08	.0	-6.

x/L_1 = 0.25

0.	2.	.0	10.
.2	1.	.6	6.
.4	.2	1.	2.
.6	.04	1.	-2.
.8	.7	.6	-6.
1.	1.	.0	-10.

x/L_1 = 0.5

y/h	$U\frac{U}{x}$	$V\frac{U}{y}$	$D\frac{^2U}{y^2}$
0.	-.9	.0	12.
.2	-.6	-.3	8.
.4	-.1	-.6	3.
.6	-.02	-.6	3.
.8	-.3	-.3	-8.
1.	-.6	.0	-12.

x/L_1 = 0.75

0.	-1.3	.0	8.
.2	-.9	-.4	5.
.4	-.2	-.8	2.
.6	.002	-.8	-2.
.8	-.4	-.4	-5.
1.	-.7	.0	-8.

Table 4.9

Comparison of Size of Neglected Terms for Longitudinal Equation of Motion for James River and Delft Flume

James River 26 June - 7 July $x/L_i = .29$				Delft Flume T-116 $x/L_i = .29$			
y/h	$U\frac{\partial U}{\partial x}$	$V\frac{\partial U}{\partial y}$	$D\frac{\partial^2 U}{\partial y^2}$	y/h	$U\frac{\partial U}{\partial x}$	$V\frac{\partial U}{\partial y}$	$D\frac{\partial^2 U}{\partial y^2}$
	($\times 10^{-6}$ m^2/sec)				($\times 10^{-4}$ m^2/sec)		
0.	1.1	.0	16.2	0.	.1	.0	4.8
.2	.7	.4	9.7	.2	.07	.02	2.9
.4	.1	.9	3.2	.4	.02	.05	1.
.6	.08	.9	-3.2	.6	.0	.05	-1.
.8	.6	.4	-9.7	.8	.0	.02	-2.9
1.	1.	.0	-16.2	1.	.02	.0	-4.8

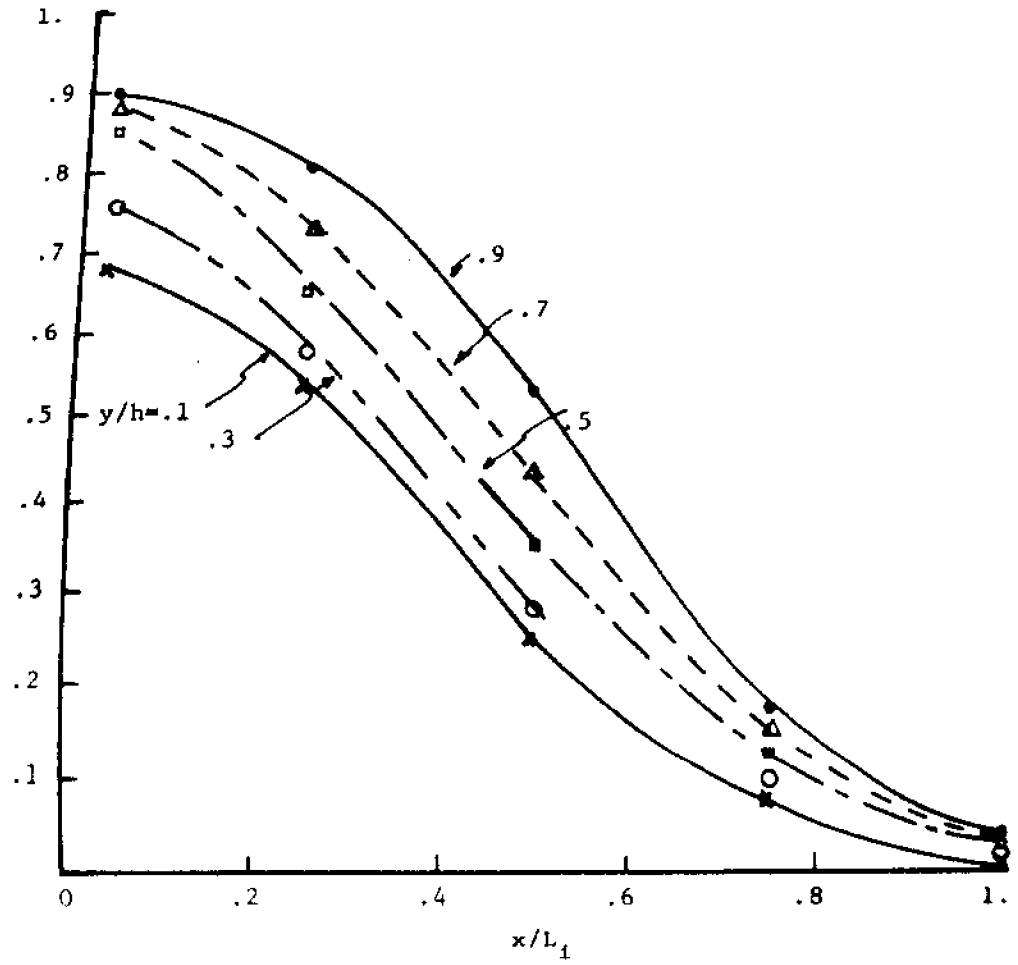

Figure 4.11 Depth variation of longitudinal salinity distribution, WES 16

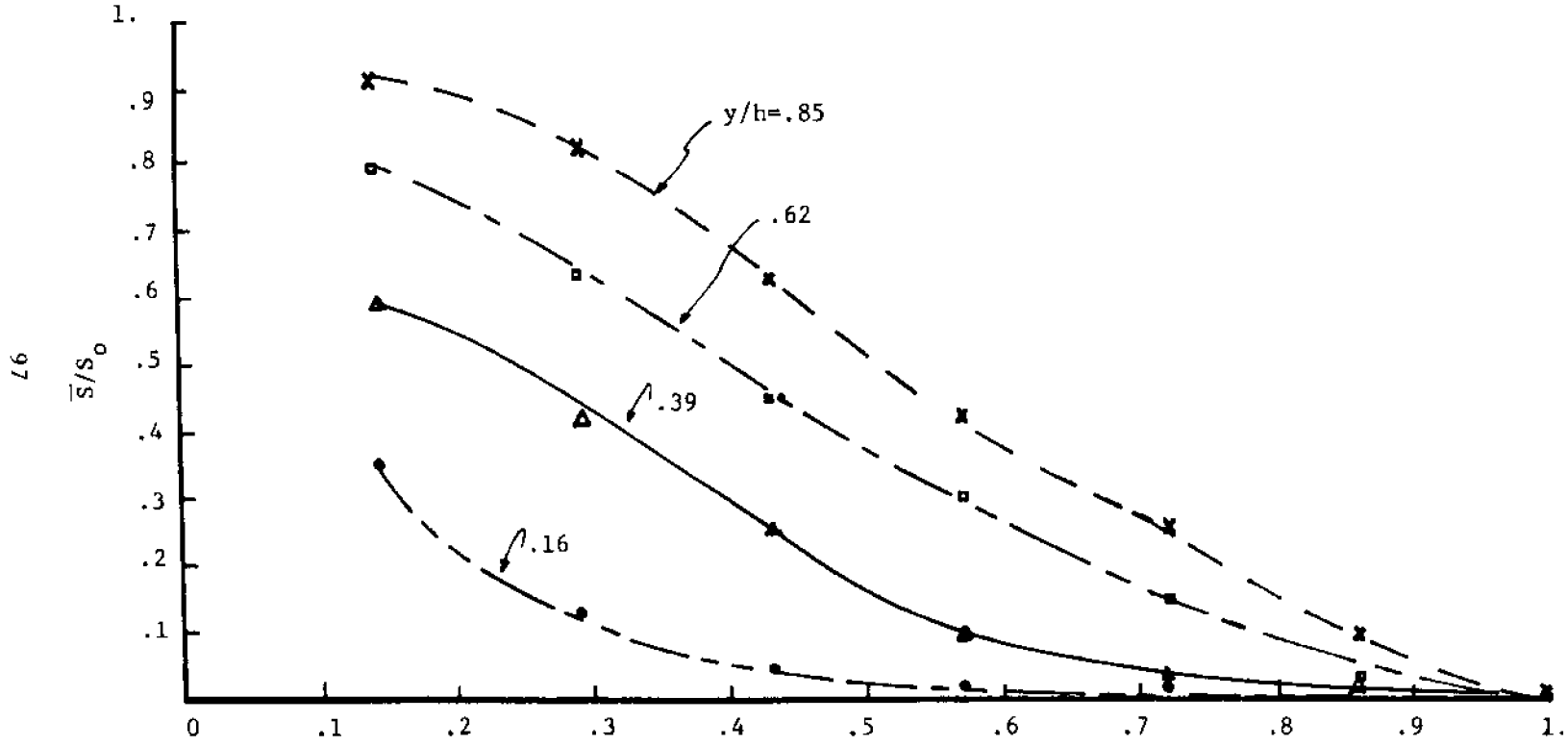

Figure 4.12 Depth variation of longitudinal salinity distribution, Delft 116

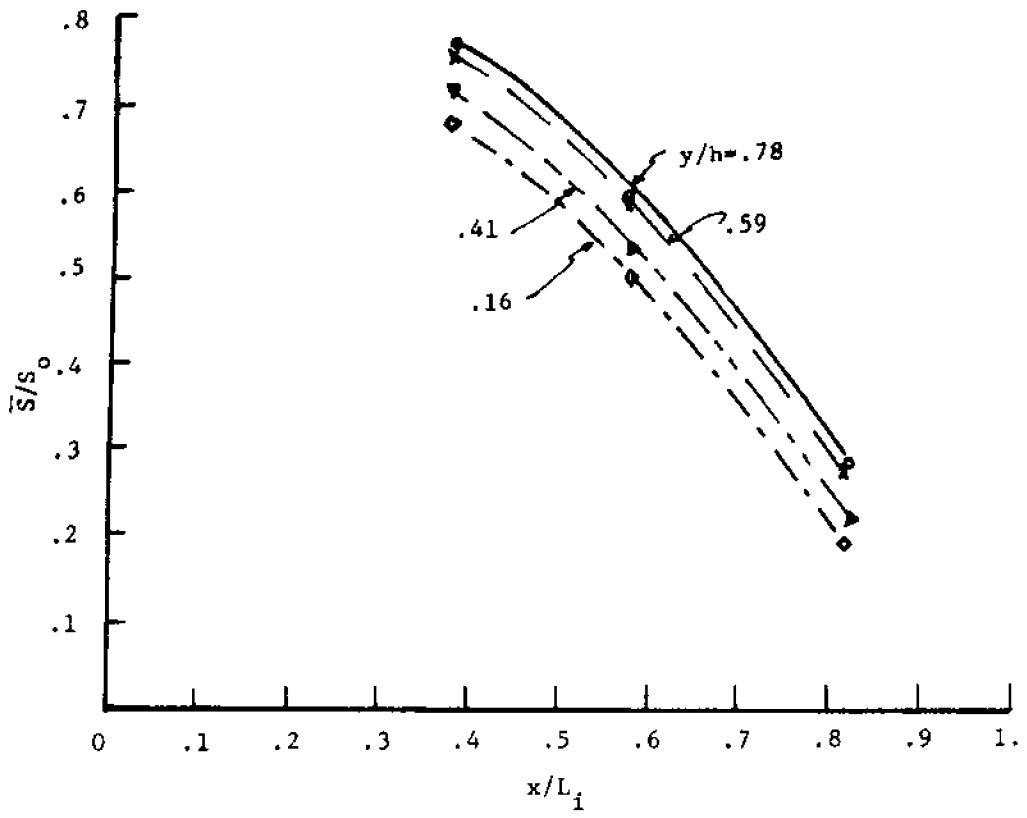

Figure 4.13 Depth variation of longitudinal salinity distribution, James River, 26 June - 7 July

the various flume tests seem to indicate that the analytical solution is not very sensitive to violations of this assumption, since good experimental-analytical comparisons are found over the entire salinity region.

4.6 Analysis of Time-Averaged Eddy Coefficients

In the preceeding section best-fit values for the time-averaged eddy coefficients D and K were determined for 10 tests including 3 prototype field studies. These tests covered a wide range of density stratifications and hydraulic conditions. The coefficients of mean momentum flux and mean salt flux for these tests show a varying degree of longitudinal variation as summarized in table 4.10. As is discussed in section 4.2.2, the upstream and downstream ends of the salinity distribution have been eliminated from this table. This procedure removes errors introduced by faulty analytical extrapolation of the spline function used to compute first and second derivatives of the longitudinal salinity distribution. To facilitate cross-comparisons between flume tests, the units of the eddy coefficients are all given in the MKS system in this table.

The longitudinal variations of the mean eddy coefficients shown in table 4.10 suggest that although D and K are functions of x, this dependence is of secondary importance. By introducing the additional assumption that these mean eddy coefficients may be replaced with effective constant values for the entire longitudinal distance of the salinity regime, correlations of these coefficients are greatly simplified. Table 4.11 lists the arithemetic mean values for the various tests analysed, defined as $\bar{D}$ and $\bar{K}$. The ratio of freshwater velocity U_f to

Table 4.10

Longitudinal Variation of Mean Eddy Coefficients

Test/Station	x/L_i	$D, m^2/sec \times 10^4$	$K, m^2/sec \times 10^4$
WES 11	.29	.29	.12
WES 14	.22	.19	.35
	.44	.26	.48
	.66	.28	.26
WES 16	.25	.22	.17
	.50	.24	.16
	.75	.22	.20
DELFT 117	.29	.56	.15
	.43	.60	.17
	.57	.68	.13
	.71	.64	.18
	.86	.84	.22
DELFT 116	.29	.64	.20
	.43	.64	.15
	.57	.84	.13
	.71	.68	.18
	.86	.92	.34
DELFT 121	.28	.72	.06
	.41	.76	.15
	.54	.84	.06
	.67	.80	.15
	.81	1.12	.11
	.94	1.04	.15
DELFT 122	.29	.72	.11
	.43	.76	.15
	.57	.76	.06
	.71	.84	.18
James River			
18-23 June	.30	7.5	2.1
26 June-7 July	.30	6.5	3.1
17-21 July	.30	6.5	2.1

Table 4.11

Mean Values of Eddy Coefficients

Test		$\bar{D}$ $m^2/sec \times 10^{-4}$	$\bar{K}$ $m^2/sec \times 10^{-4}$	U_f/u_o
WES	11	.29	.12	.13
	14	.24	.36	.029
	16	.23	.18	.047
DELFT	117	.66	.17	.14
	116	.74	.20	.15
	121	.88	.11	.09
	122	.77	.13	.11
James River				
18-23 June		7.5	2.1	.0085
26 June-7 July		6.5	3.1	.007
17-21 July		6.5	2.1	.009

maximum flood velocity at the ocean boundary u_o is also shown in table 4.11. This velocity ratio is a significant parameter for defining flow conditions and degrees of stratification, as will be shown in the following discussion.

Figure 4.14 demonstrates the effect of using $\bar{K}$ and $\bar{D}$ in the place of the local best-fit values for Delft test 116. It is clearly seen in this example that the constant coefficients yield quite useful results for the velocity and salinity distributions. This example is typical of the influence of this new assumption, and similar results can be shown for the other tests analysed.

The significance of being able to use constant values for D and K, i.e., $\bar{D}$ and $\bar{K}$, is that only two unknown parameters need now be specified in order to apply the analytical model to a given set of estuarine conditions, i.e., freshwater discharge, ocean salinity, depth, etc. All other model parameters can be readily determined with the possible exception of the longitudinal salinity distribution. This latter input can be computed with the aid of a one-dimensional numerical model, as previously discussed in Chapter III. The determination of $\bar{K}$ and $\bar{D}$ for input to the model is made by using an empirical correlation of these constant coefficients with the gross characteristics of the estuarine system.

The set of governing equations developed in Chapter III can be written

$$C_1(\xi) \frac{\partial \theta_d}{\partial \xi} = - \frac{\partial^4 \psi}{\partial \eta^4} \qquad 4.2$$

and

$$- \frac{\partial \psi}{\partial \eta} \frac{\partial \theta_d}{\partial \xi} + \frac{\partial \psi}{\partial \eta} \frac{\partial \theta}{\partial \xi} = C_2(\xi) \frac{\partial^2 \theta}{\partial \eta^2} \qquad 4.3$$

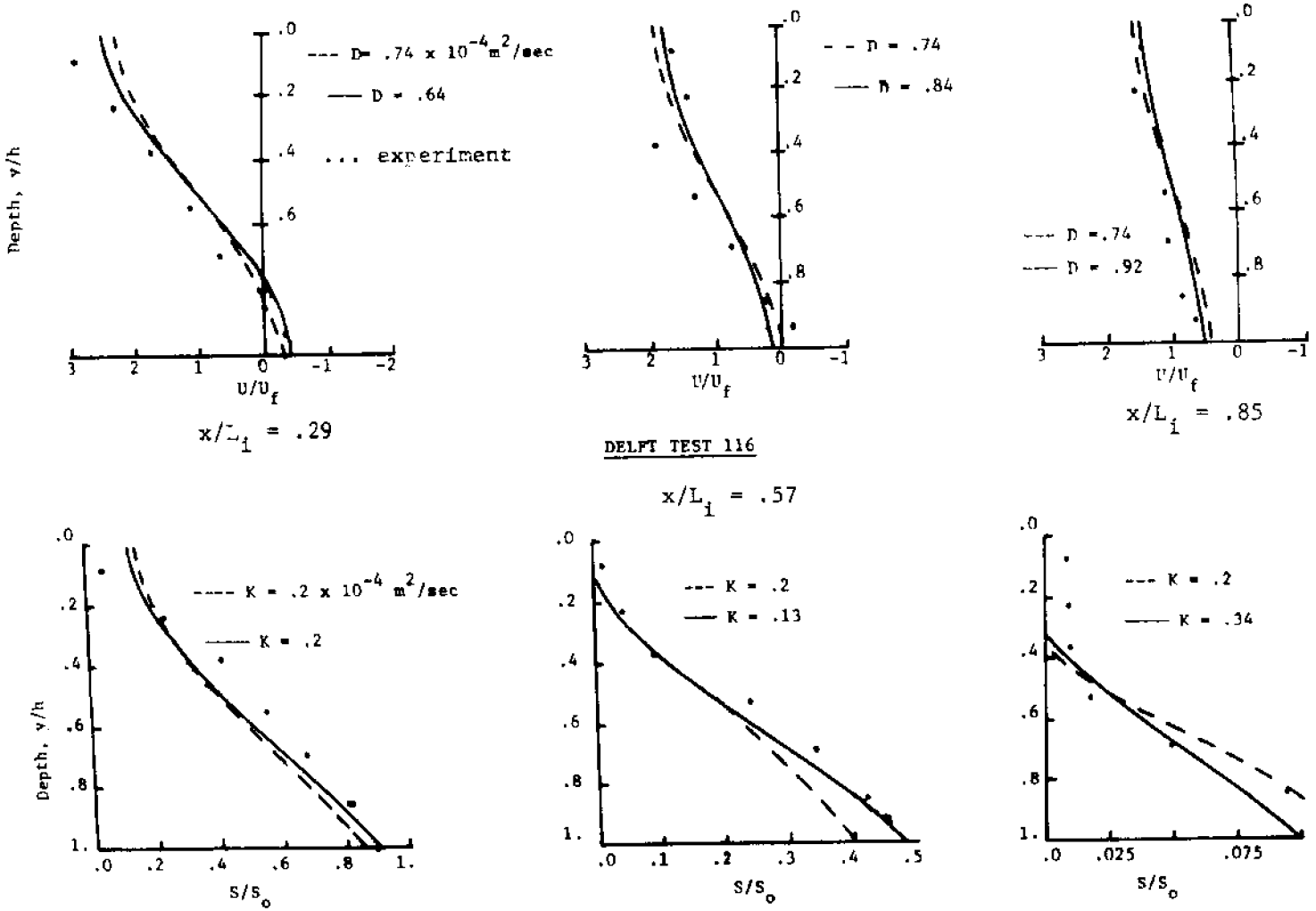

Figure 4.14 Effects of using constant eddy coefficients

where C_1, C_2, h, b, Q_f, D, and K are all functions of the longitudinal coordinate ξ.

Following the arguments presented above for using constant values of $D(\xi) \simeq \bar{D}$ and $K(\xi) \simeq \bar{K}$, the dimensionless form of the governing equations suggests that a possible pair of useful parameters for correlating $\bar{K}$ and $\bar{D}$ is

$$\bar{C}_1 = \frac{g\alpha S_o h_o^4 b_o}{L_i Q_{fo} \bar{D}} \qquad 4.4$$

and

$$\bar{C}_2 = \frac{\bar{K} L_i b_o}{Q_{fo} h_o}$$

where the zero subscript, e.g., b_o, h_o, refers to the downstream limit or ocean boundary of the estuary. All terms in these new terms are assumed constant over the longitudinal and vertical dimensions, and the only unknown parameters are $\bar{K}$ and $\bar{D}$.

The values of $\bar{K}$ and $\bar{D}$ should be a function of the degree of mixing of the flow field which is in turn a function of the tidal activity. In recognition of this dynamic relationship of the physical system being modeled, $\bar{C}_1$ and $\bar{C}_2$ have been correlated with a characteristic non-time-averaged tidal velocity. To be consistent with the definitions above, this velocity is specified as the maximum entrance flood velocity u_o, non-dimensionalized by the freshwater velocity at this same boundary $\frac{Q_{fo}}{h_o b_o}$,

$$\bar{C}_3 = \frac{Q_{fo}/b_o h_o}{u_o} = \frac{U_{fo}}{u_o} \qquad 4.5$$

The value of the maximum flood velocity is considered to be a depth averaged term, as might be estimated from a table of tide currents, or some other similar hydrographic reference.

Tables 4.12a, 4.12b, and 4.12c summarize the computations of $\bar{C}_1$, $\bar{C}_2$, and $\bar{C}_3$ for the estuaries included in this development. Figures 4.15 and 4.16 show the correlation of $\bar{C}_1$ with $\bar{C}_3$ and $\bar{C}_2$ with $\bar{C}_3$. In general, this straight forward technique of using dimensionless groups defined by the equations, yields seemingly significant correlations. No explanation is readily available to explain the point for WES 16 on figure 4.15, although the complex manipulation of the data could easily have introduced an improper value for one of the component parameters.

It is significant in figures 4.15 and 4.16 that both laboratory flume tests and prototype field surveys follow the same correlations. In addition, the range of degrees of stratification include the highly stratified Delft tests 121 and 122 as well as the nearly well mixed middle reaches of the James River estuary. Thus, this empirical approach to evaluating the effective coefficients of mean eddy flux, $\bar{D}$ and $\bar{K}$ is apparently applicable to naturally occuring estuarine conditions.

By a simple rearrangement of terms, the unfamiliar parameters $\bar{C}_1$ and $\bar{C}_2$ can be shown to be equivalent to the products of several more conventional quantities.

$$\bar{C}_1 = \frac{\alpha g S_o h_o^4 b_o}{Q_{fo} L_i \bar{D}} = \left(\frac{\alpha S_o g h_o}{u_o^2}\right)\left(\frac{h_o}{L_i}\right)\left(\frac{h_o u_o}{\bar{D}}\right)\left(\frac{u_o}{U_{fo}}\right) \qquad 4.6$$

and

Table 4.12 a

Computation of Correlation Constants for WES Tests

$g = 32.2\ ft^2/sec$ $\quad b_o = 0.75$ ft. $\quad \bar{C}_1 = \dfrac{\alpha S_o g h_o^4 b_o}{L_i Q_{fo} \bar{D}}$ $\quad \bar{C}_2 = \dfrac{\bar{K} L_i b_o}{Q_{fo} h_o}$ $\quad \bar{C}_3 = \dfrac{U_{fo}}{u_o}$

$\alpha = 0.75$ $\quad h_o = 0.5$ ft.

Test	S_o ppt	L_i ft	Q_{fo} ft^3/sec	u_o ft/sec	$\bar{D}$ $ft^2/sec \times 10^{-3}$	$\bar{K}$ $ft^2/sec \times 10^{-3}$	$\bar{C}_1$	$\bar{C}_2$	$\bar{C}_3$
11	26.4	140.	.021	.43	.31	.13	32.8	1.3	.13
14	29.7	180.	.0075	.70	.26	.39	111.2	14.2	.029
16	29.2	160.	.0075	.43	.25	.19	119.5	6.1	.047

Table 4.12 b

Computation of Correlation Constants for Delft Tests

$g = 9.8\ m^2/sec$ $\quad b_o = .672\ m$ $\quad \bar{C}_1 = \dfrac{\alpha g S_o h_o^4 b_o}{Q_{fo} L_i \bar{D}}$ $\quad \bar{C}_2 = \dfrac{\bar{K} L_i b_o}{Q_{fo} h_o}$ $\quad \bar{C}_3 = \dfrac{U_{fo}}{u_o}$

$\alpha = 0.75$ $\quad h_o = .216\ m$

Test	S_o ppt	L_i m	Q_{fo} m^3/sec	u_o m/sec	$\bar{D}$ $m^2/sec \times 10^{-4}$	$\bar{K}$ $m^2/sec \times 10^{-4}$	$\bar{C}_1$	$\bar{C}_2$	$\bar{C}_3$
117	30.	51.	.0029	.142	.66	.17	32.8	1.2	.14
116	30.	51.	.0029	.130	.74	.20	29.2	1.1	.15
121	30.	54.	.00145	.106	.88	.11	45.8	1.4	.09
122	30.	51.	.00181	.108	.77	.13	44.2	1.1	.11

Table 4.12 c

Computation of Correlation Constants for James River Survey

$g = 9.8\ m^2/sec$ $\quad b_o = 3000\ m$ $\quad \bar{C}_1 = \frac{\alpha g S_o h_o^4 b_o}{Q_{fo} L_1 \bar{D}}$ $\quad \bar{C}_2 = \frac{\bar{K} L_1 b_o}{Q_{fo} h_o}$ $\quad \bar{C}_3 = \frac{U_{fo}}{u_o}$

$\alpha = 0.75$ $\quad h_o = 8\ m$

Date	S_o ppt	L_1 m	Q_{fo} m^3/sec	u_o m/sec	$\bar{D}$ $m^2/sec \times 10^{-4}$	$\bar{K}$ $m^2/sec \times 10^{-4}$	$\bar{C}_1$	$\bar{C}_2$	$\bar{C}_3$
18-23 June	24	90,900.	124.	.6	7.5	2.1	361.	58.	.0085
26 June-7 July	24	94,130	104.	.6	6.5	3.1	272.	105.	.007
17-21 July	24	90,900	130.	.6	6.5	2.1	313.	55.	.009

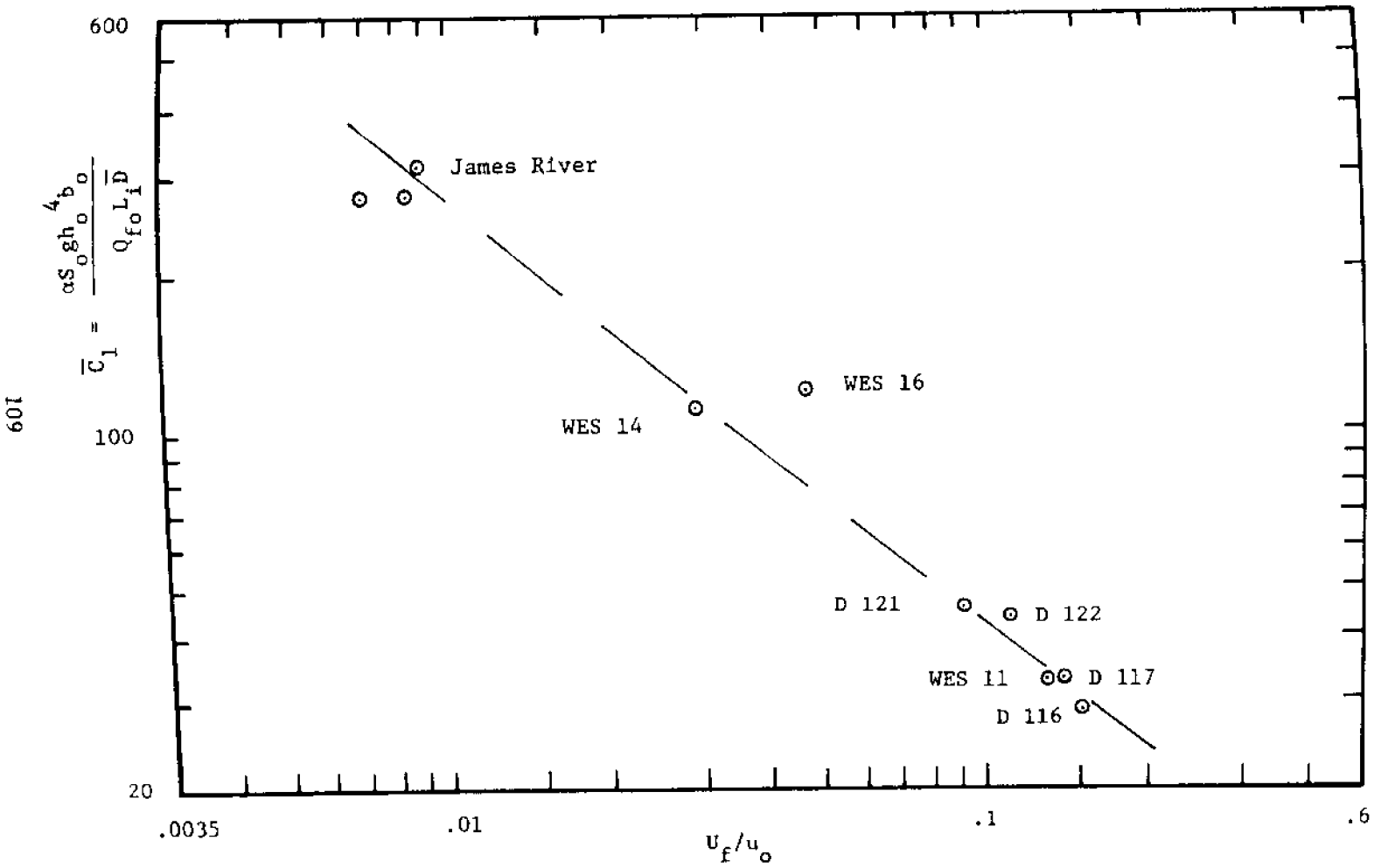

Figure 4.15 Correlation of $\overline{D}$

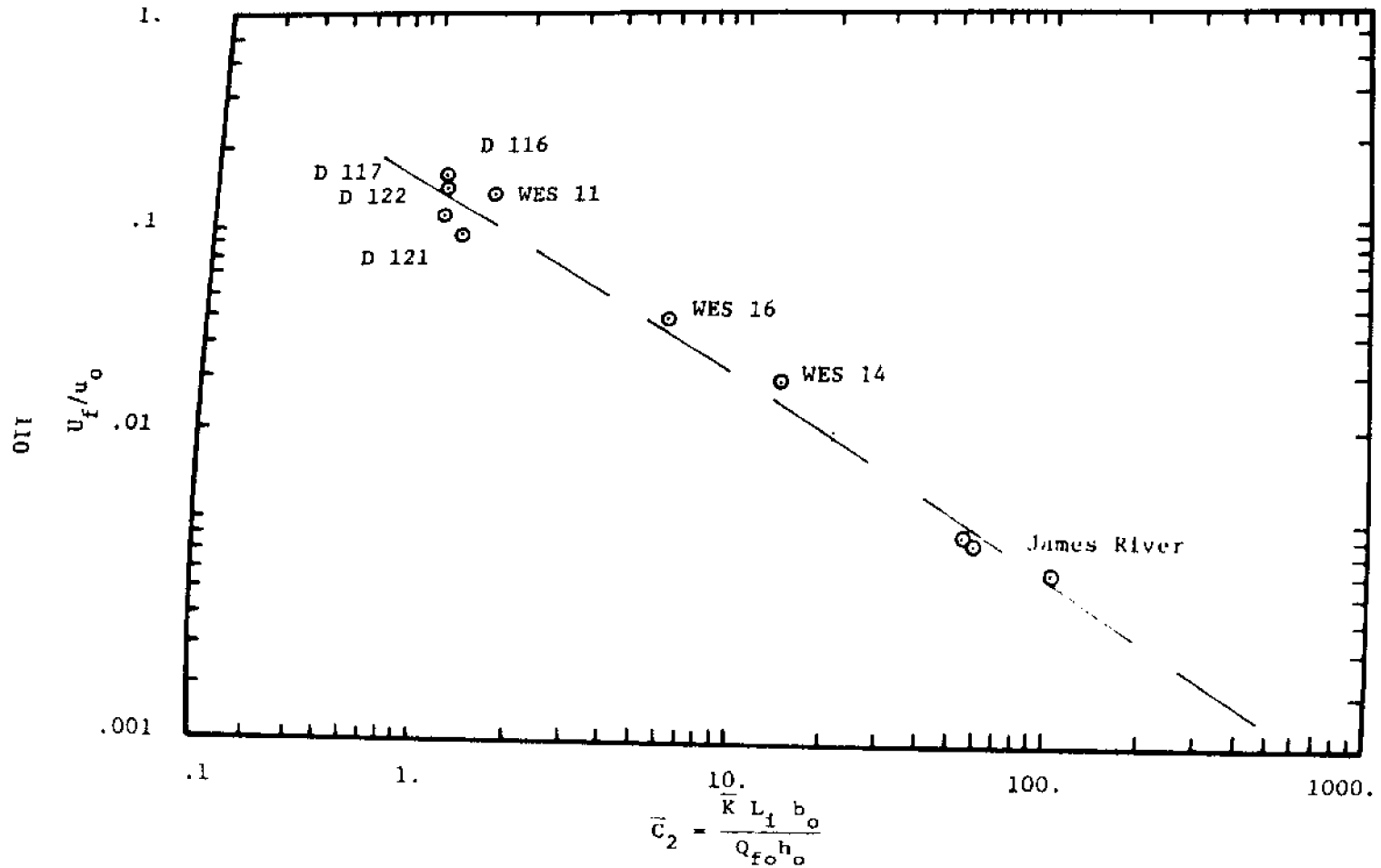

Figure 4.16 Correlation of $\bar{K}$

$$\bar{C}_2 = \frac{\bar{K} L_i b_o}{Q_{fo} h_o} = \left(\frac{\bar{K}}{u_o h_o}\right)\left(\frac{u_o}{U_{fo}}\right)\left(\frac{L_i}{h_o}\right) \qquad 4.7$$

These latter groupings more clearly show that the dynamics of the net circulation and net salinity distribution are dependent upon scale ratios, $\left(\frac{h_o}{L_i}\right)$, a densimetric tidal Froude number, $\frac{\alpha S_o g h_o}{u_o^2}$, and eddy coefficients, $\frac{\bar{K}}{u_o h_o}$ and $\frac{\bar{D}}{u_o h_o}$.

V Analysis of Transient Flume Study Using Coupled One and Two Dimensional Models

5.1 Description of Transient Test Procedure

The WES salinity flume described in Chapter IV has been used to evaluate the transient behavior of estuaries as well as the steady-state conditions discussed previously. WES test 42 was conducted with a transient freshwater inflow, decreased in discrete steps for 25 consecutive tidal cycles, starting from a steady-state initial condition. All other flume variables, including tidal amplitude and ocean salinity were maintained constant during the course of the test, as indicated in table 5.1

Table 5.1

Summary of Flume Conditions for WES Transient Test 42

depth, msl	.5 ft.
width	.75 ft.
length	327. ft.
tidal amplitude	.05 ft.
tidal period	600. sec
roughness (side wall), n	.02 $ft.^{1/6}$
initial freshwater discharge	.025 $ft.^3/sec$
final freshwater discharge	.00652 ft^3/sec

The test was begun by running 23 cycles at a freshwater inflow of .025 ft^3/sec and thus permitting an equilibrium initial condition to be reached. For the following 25 cycles, the freshwater inflow was decreased .00077 ft^3/sec at the end of each cycle. Measurements of velocity were

made for cycle 1 (last steady-state cycle prior to decreasing inflow) and cycle 25 for three depths, .05, .25, and .45 ft., at five stations, 5, 40, 80, 120 and 160 ft. from the ocean end at one minute intervals for both cycles. Similar times, depths and stations were used in measuring salinities for cycles 1, 6, 14 and 24.

5.2 Discussion of One-Dimensional Numerical Model and Results for Transient Test

The numerical computation of the one-dimensional longitudinal salinity distribution was carried out with a model presented by Thatcher and Harleman (1972). This model is a real-time simultaneous solution of the one-dimensional (longitudinal) equations of momentum, continuity, state, and salt conservation. Real-time refers to time variations within a tidal period, unlike the analytical two-dimensional model, which is averaged over a tidal period. Since the numerical model can handle boundary conditions which change with successive tidal cycles, e.g., tidal amplitude, freshwater inflow, etc., it can compute the transient or natural behavior of real estuaries. Finally, the numerical model has been developed for variable area estuaries, a condition which is not required for the constant width salinity flume considered in this discussion.

The governing equations for the numerical model are:

continuity equation

$$b \frac{\partial h}{\partial t} + \frac{\partial \bar{Q}}{\partial x} - q = 0 \qquad 5.1$$

momentum equation

$$\frac{\partial \bar{Q}}{\partial t} + \bar{U}\frac{\partial \bar{Q}}{\partial x} + \bar{Q}\frac{\partial \bar{U}}{\partial x} + g\frac{\partial h}{\partial x}A + g\frac{Ad_c}{\rho} + g\frac{\bar{Q}|\bar{Q}|}{AC^2R_h} = 0 \qquad 5.2$$

where

d_c = distance from the surface to the centroid of the cross-section

b = channel width

h = mean water level depth

$\bar{Q}$ = discharge, averaged over the cross-section

q = lateral inflow per unit length

$\bar{U}$ = longitudinal velocity, averaged over the cross-section

A = cross-sectional area

g = acceleration of gravity

R_h = hydraulic radius = $\dfrac{A}{b + 2(h + \bar{\eta})}$

$\bar{\eta}$ = surface elevation relative to local mean water level

C = chezy coefficient

salt equation

$$\frac{\partial A\bar{S}}{\partial t} + \frac{\partial \bar{Q}\bar{S}}{\partial x} = \frac{\partial}{\partial x}\left(EA\frac{\partial \bar{S}}{\partial x}\right) \qquad 5.3$$

where

$\bar{S}$ = salinity, averaged over the cross-section

E = coefficient of longitudinal dispersion

equation of state

$$\rho = 0.75\ \bar{S} + 1{,}000. \qquad 5.4$$

where

S = salinity in parts per thousand

ρ = density in kg/m^3.

The coefficient of longitudinal dispersion E is related by Thatcher and Harleman to the local longitudinal salinity gradient $\frac{\partial \bar{S}}{\partial x}$,

$$E(x,t) = K_1 \left| \frac{\partial \overset{0}{S}}{\partial \overset{0}{x}} \right| + E_T \qquad 5.5$$

where $\overset{0}{S} = \frac{\bar{S}}{S_o}$ and $\overset{0}{x} = x/L$, S_o being the ocean salinity and L the length of the estuary. E_T is the dispersion coefficient applicable to a completely mixed region, where $\frac{\partial \bar{S}}{\partial x} = 0$ or to the freshwater tidal region upstream of the limit of salinity intrusion,

$$E_T = 77\ n\ \bar{U}\ R_h^{5/6} \qquad 5.6$$

where n is the Manning's coefficient.

Thatcher and Harleman have found a correlation for the dispersion parameter K and the stratification as represented by the estuary number E_D,

$$E_D = \frac{P_T F_D^{\ 2}}{\bar{Q}_f\ T} \qquad 5.7$$

where P_T is the tidal prism defined as the volume of water entering on the flood tide. F_D is the densimetric Froude number, $\frac{u_o}{\sqrt{gh\,\Delta\rho/\rho}}$,

wherein u_o is the maximum flood velocity at the entrance and $\Delta\rho$ is the change in density over the entire length of the estuary.

The dispersion parameter K_1 is normalized by the maximum flood velocity and the length of the estuary $\frac{K_1}{U_o L}$. The correlation of $\frac{K_1}{U_o L}$ with the estuary number E_D includes data from five WES steady-state flume tests, and several studies of variable area estuaries for both quasi-steady-state and transient conditions. Figure 5.1 shows this correlation. Since all parameters except K_1 can be computed directly, this correlation can be used to compute the changing value of the dispersion parameter K_1, and therefore the dispersion coefficient $E(x,t)$ for the transient study.

Using boundary conditions of known tidal amplitude and flood tide salinity at the ocean end, the numerical model computes the elevations $\bar{\eta}$, discharges $\bar{Q}$ and salinities $\bar{S}$ for discrete time steps at discrete points along the flume length. Finite difference techniques are used to find the numerical solution, combining both explicit and implicit methods.

Table 5.2 summarizes the flume conditions which are the input to the numerical model.

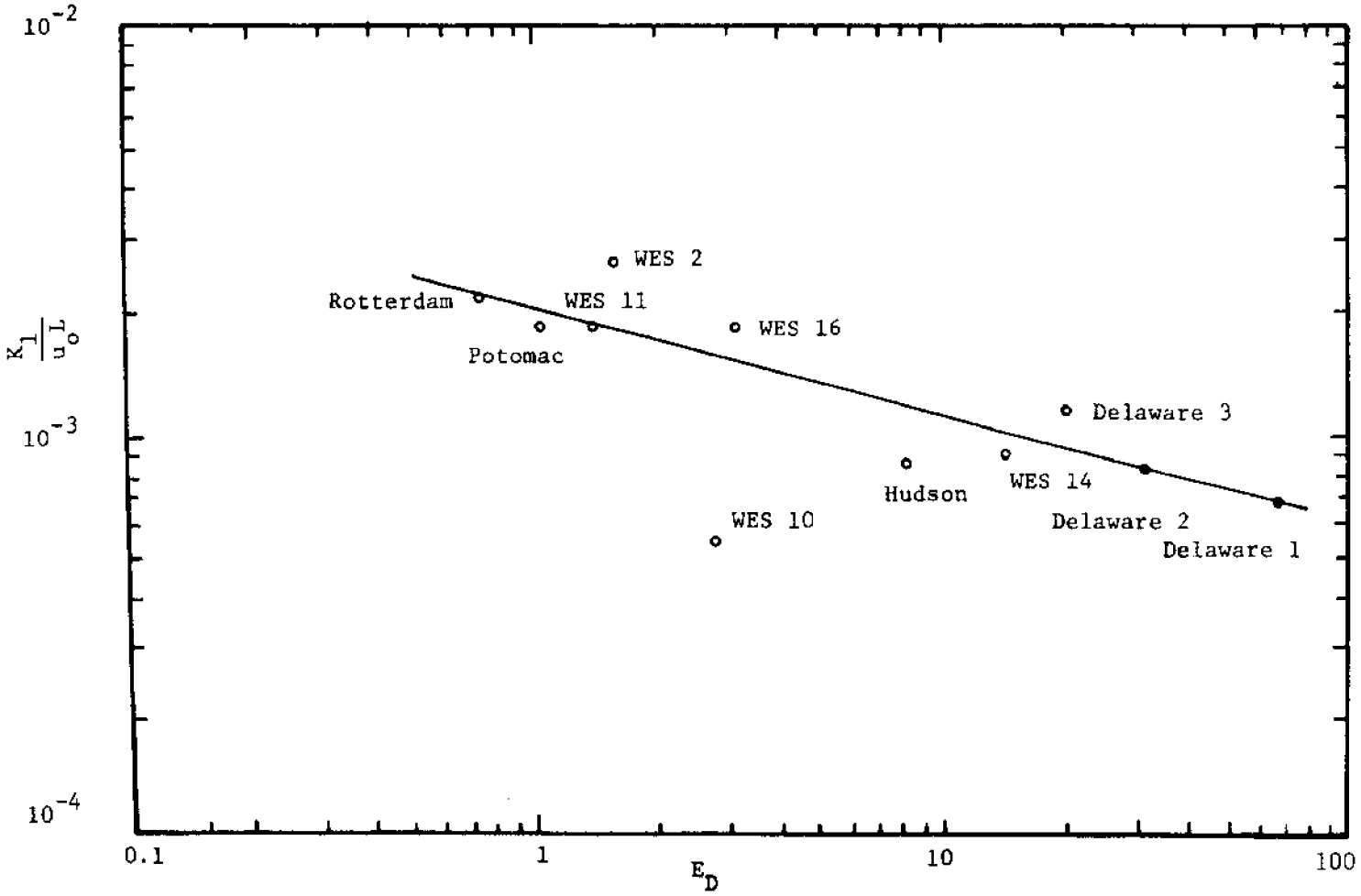

Figure 5.1 Correlation of Dispersion Parameter to Degree of Stratification (from Thatcher and Harleman 1972)

Table 5.2

W.E.S. Transient Test 42 Flume Conditions

tidal period	600 sec.
flume length	327 ft.
width	0.75 ft.
depth, msl	0.05 ft.
Manning's n	.02 $ft.^{1/6}$
ocean salinity	29.0 ppt
tidal amplitude	.05 ft.

The value for the freshwater inflow varied from the initial discharge of 0.025 ft^3/sec to a final value at the 25th cycle of .00652 ft^3/sec as discussed. The dispersion parameter K_1 was taken from figure 5.1 which yielded a value of .31 for cycle 1 and a value of .21 for cycle 25. Figures 5.2, 5.3 and 5.4 illustrate the numerical solution for the one-dimensional salinities at stations 40, 80 and 120 for the 25 transient cycles of WES test 42. The very good agreement between experimental data (the crosses) and the computed salinities shows the capabilities of the numerical program. These figures, 5.2 - 5.4 also show the effect of a decreasing freshwater inflow on the distribution of salinity in the flume. A steady increase in salt level and length of salinity intrusion is seen to be a result of this type of freshwater hydrograph. The effects of this flow pattern on the vertical profiles of velocity and salinity as well as its influence on sediment transport are examined in the following sections of this chapter.

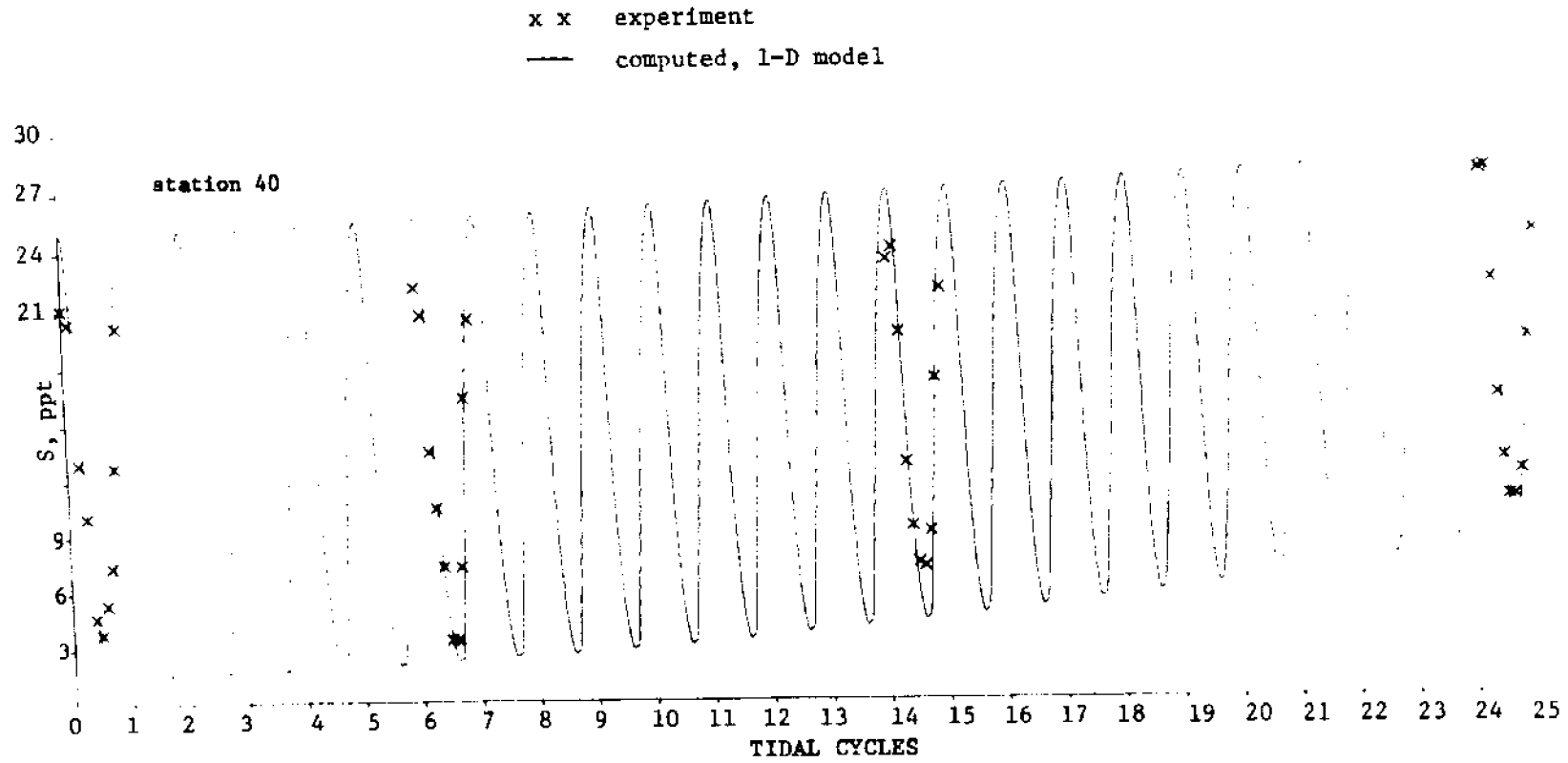

Figure 5.2 Tidal salinity verification, station 40. WES 42

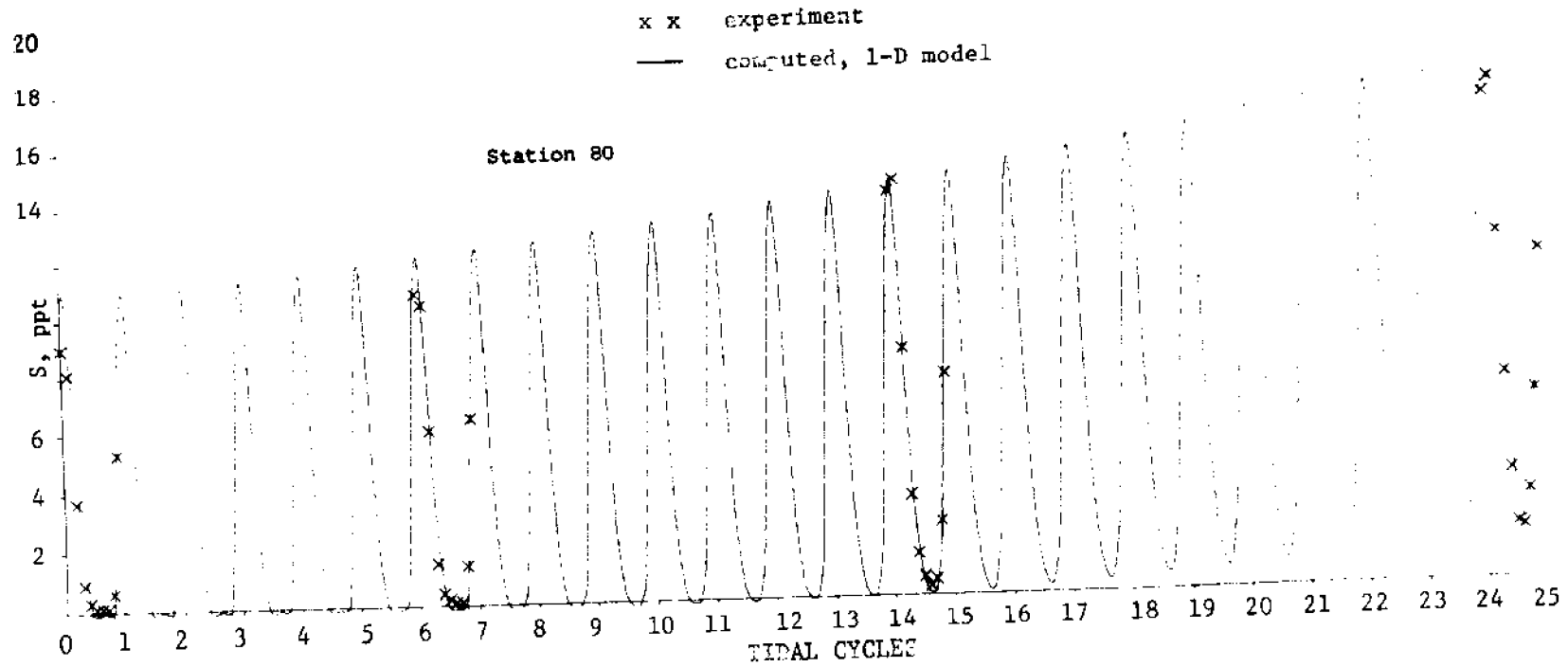

Figure 5.3 Tidal salinity verification, station 80, WES 42

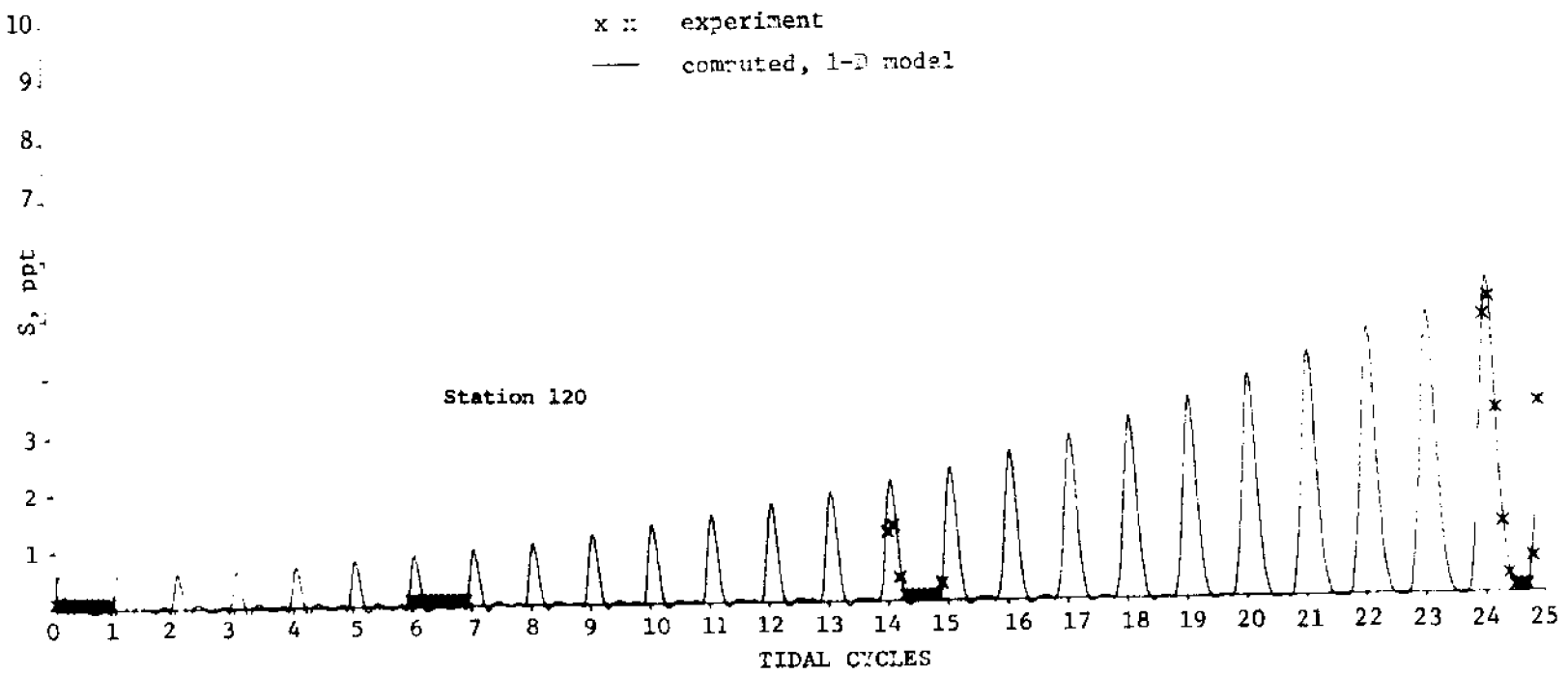

Figure 5.4 Tidal salinity verification, station 120, WES 42

5.3 Analytical Solution for Unsteady Flow Conditions

The analytical model presented in Chapter III was developed for estuaries in a steady-state condition, i.e., influencing factors such as tidal amplitude and freshwater inflow remain constant for successive tidal cycles. For the analysis of the transient flume test, or for more realistic natural conditions, an additional term is included in the equation of salt conservation, 3.32

$$\frac{\partial S}{\partial t} + U \frac{\partial S}{\partial x} + V \frac{\partial S}{\partial y} = K \frac{\partial^2 S}{\partial y^2} \qquad 5.8$$

where $\frac{\partial S}{\partial t}$ is the average over a single tidal period of the temporal change in salinity $S(x,y,t)$. For steady-state conditions, $\frac{\partial S}{\partial t}$ is zero, but this is not the case for transient conditions, since it varies by definition from one cycle to the next. The other model equations are unchanged with the note that the freshwater discharge Q_f is now a variable and has a different value with each tidal cycle. However, the momentum equations remain the same as for the steady state because both temporal and convective accelerations can be neglected.

In order to solve this modified set of model equations, an assumption is introduced for the $\frac{\partial S}{\partial t}$ term which is similar to that made for the $\frac{\partial S}{\partial x}$ term in equation 5.8. Since it has been shown reasonable to assume that $\frac{\partial S}{\partial x} \neq f(y)$, this same substitution, $\frac{\partial S}{\partial t} \neq f(y)$ (and thus $\frac{\partial S}{\partial t}$ can be replaced with $\frac{\partial S_d}{\partial t}$) is introduced,

$$\frac{\partial S_d}{\partial t} + U \frac{\partial S_d}{\partial x} + V \frac{\partial S}{\partial y} = K \frac{\partial^2 S}{\partial y^2} . \qquad 5.9$$

Equation 5.9 is non-dimensionalized with the same terms used in the steady-state analysis with the addition of the tidal period T, $\tau = t/T$.

$$\frac{L_i bh}{Q_f T} \frac{\partial \Theta_d}{\partial \tau} - \frac{\partial \psi}{\partial \eta} \frac{\partial \Theta_d}{\partial \xi} + \frac{\partial \psi}{\partial \xi} \frac{\partial \Theta}{\partial \eta} = \frac{KL_i b}{Q_f h} \frac{\partial^2 \Theta}{\partial \eta^2} . \qquad 5.10$$

Using the same boundary conditions and solution technique discussed in Chapter III, the unsteady model, including equation 5.10 yields the following expression for the two-dimensional salinity,

$$\Theta(\xi,\eta) = \int f(\xi,\eta)\, d\eta + \Theta_d - \int_0^1 \int f(\xi,\eta)\, d\eta d\eta \qquad 5.11$$

where

$$f(\xi,\eta) = \exp\left(\int \frac{\partial \phi}{\partial \xi} \frac{1}{C_2}\, d\eta\right) \int \left\{\left(C_4 \frac{\partial \Theta_d}{\partial \tau} - \frac{\partial \phi}{\partial \eta} \frac{\partial \Theta_d}{\partial \xi}\right) \frac{1}{C_2} \exp\left(\int - \frac{\partial \phi}{\partial \xi} \frac{1}{C_2} d\eta\right)\right\} d\eta \qquad 5.12$$

and

$$C_4 = \frac{L_I bh}{Q_f T} .$$

The equation for the stream function is unchanged.

5.4 Two-Dimensional Experimental and Analytical Results for Transient Flume Study

As with the analysis of the steady-state flume tests discussed in Chapter IV, the application of the analytical model to this transient flume study begins with the computation of the one-dimensional longitudinal salinity distribution. In this case, to illustrate the predictive possibilities of the coupled one-and two- dimensional models, the Thatcher

and Harleman (1972) numerical model is used to compute this needed distribution. The values for salinity from the real-time model are averaged over each of the 25 transient tidal cycles. This same technique is employed to find the change in mean salinity $\frac{\partial S_d}{\partial t}$. Figure 5.5 illustrates the experimental and computed time-averaged, one-dimensional salinity distribution for cycles 1, 14 and 24. Except at station 5, where flume entrance effects are present, the agreement between the averaged numerical results and the averaged experimental data is very good, a further confirmation of the numerical model. As with the previous flume analysis, the first and second spacial derivatives of this mean salinity are determined with the spline technique outlined in appendix 2.

The other necessary inputs to the analytical model include the flume dimensions, intrusion lengths, and eddy coefficients $\bar{D}$ and $\bar{\bar{K}}$. These latter terms were taken from the steady-state correlation shown in figures 4.15 and 4.16. Table 5.3 summarizes the inputs to the two-dimensional model for cycles in which experimental data are available. Figures 5.6 and 5.7 illustrate the comparison between experimental and computed velocities for cycles 1 and 25. The circled crosses indicate experimental points which are probably inaccurate and should be discounted. In general, the analytical results, using values for $\bar{D}$ taken from the steady-state correlations, yield very acceptable results for this transient test. Figure 5.8 shows the comparison of salinity profiles. Again, using values of $\bar{\bar{K}}$ from the steady-state correlations appears to give quite good fits of the distributions of salinity.

As discussed in section 5.3, the analytical model for the transient

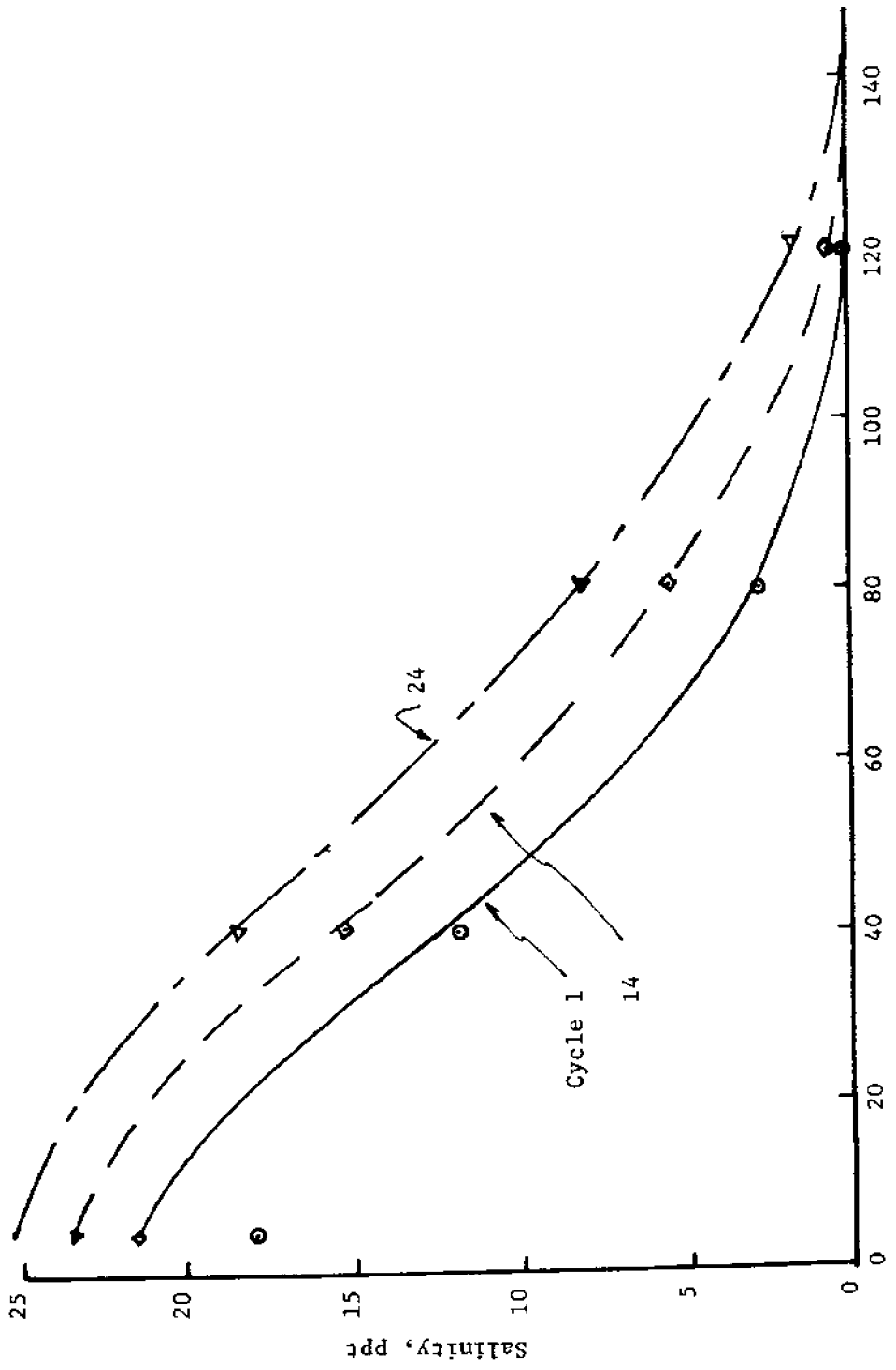

Figure 5.5 Longitudinal salinity distribution, WES 42

Table 5.3

Summary of Inputs to Two-Dimensional Model for WES Transient Test 42

h = 0.5 ft. b = 0.75 ft. S_o = .29 ppt

Cycle	max. flood velocity, u_o, ft/sec	U_f/u_o	L_1, ft	Q_f/ft^3/sec	$\bar{D}$,x10^{-3}ft^2/sec	$\bar{R}$,x10^{-3}ft^2/sec
1	.41	.16	110.	.025	.41	.14
6	.41	.13	112.	.021	.41	.15
14	.41	.10	120.	.015	.41	.16
24	.42	.05	145.	.0073	.39	.19
25	.42	.04	150.	.0065	.37	.20

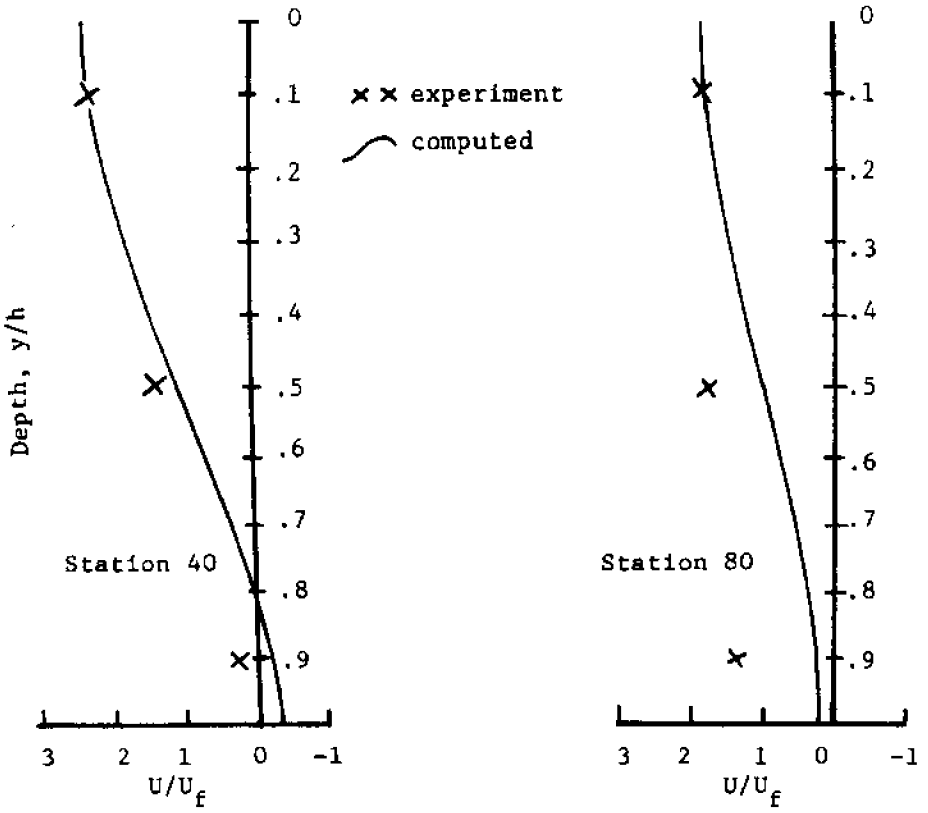

Figure 5.6 Horizontal velocity profiles, WES 42, cycle 1

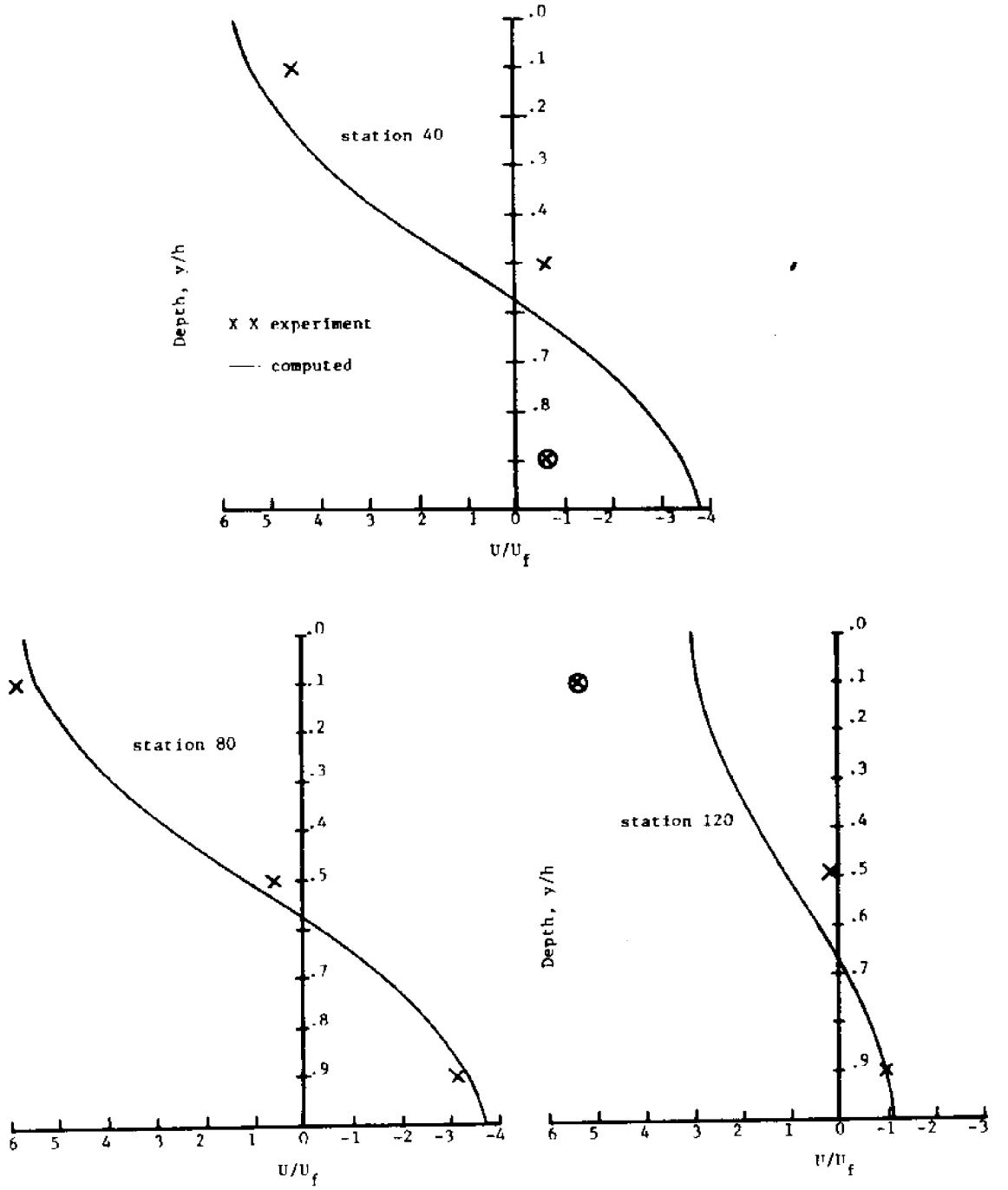

Figure 5.7 Horizontal velocity profiles, WES 42, cycle 25

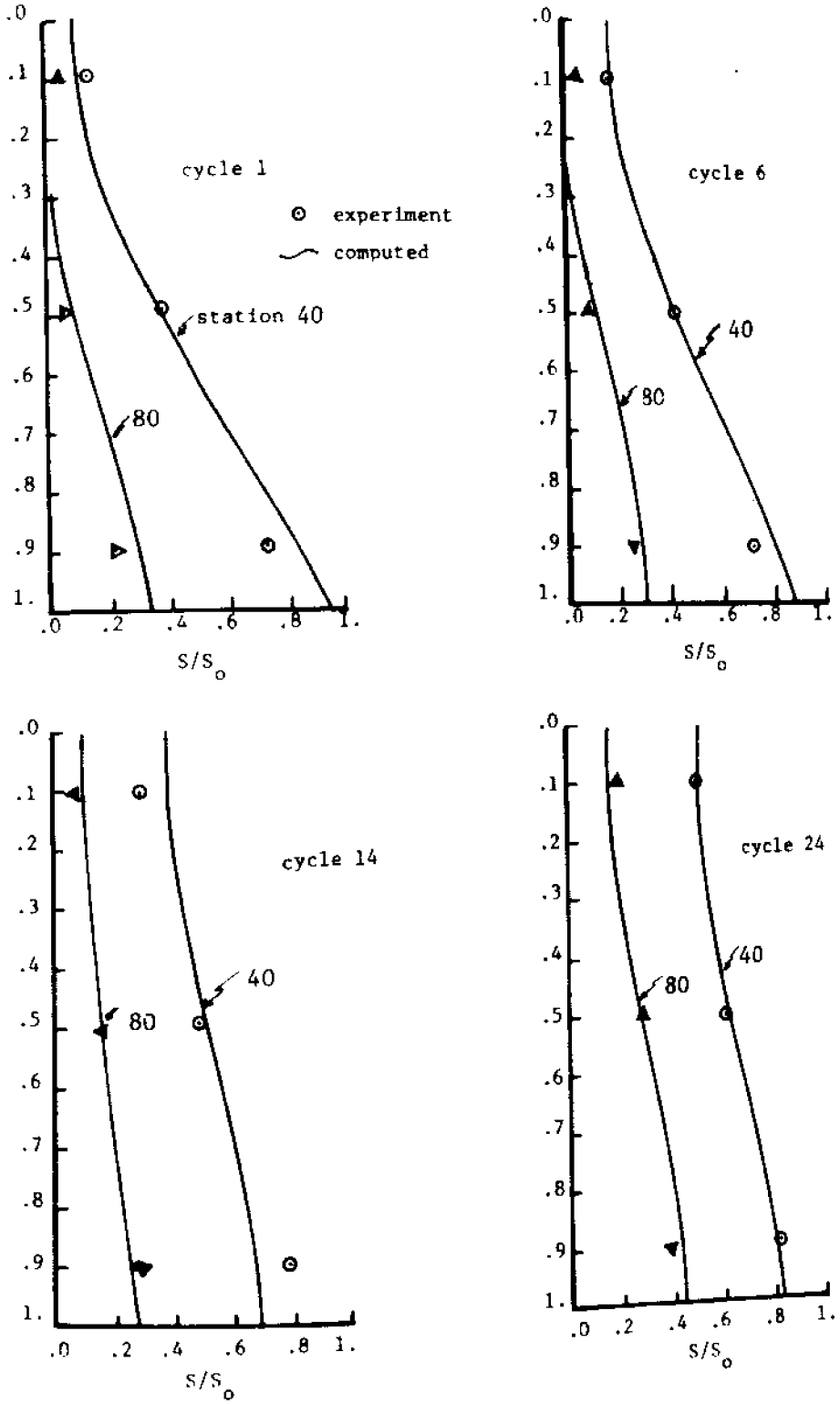

Figure 5.8 Salinity profiles, WES 42

flume conditions includes a $\frac{\partial S}{\partial t}$ term in the salt balance equation. It is interesting to examine the importance of including this term in the model, at least with regard to the scales found in a laboratory flume. Table 5.4 lists the computed values of the salinities for cycle 6 at station 40 for model solutions with and without the unsteady term.

Table 5.4

Effect of $\frac{\partial S}{\partial t}$ Term in Salt Balance

WES 42 Station 40 Cycle 6

Depth, y/h	S, ppt (with $\frac{\partial S}{\partial t}$)	S, ppt ($\frac{\partial S}{\partial t}$ neglected)
0	5.17	5.28
.2	6.42	6.51
.4	9.86	9.92
.6	14.75	14.74
.8	20.20	20.10
1.	25.52	25.30

The maximum difference of .22 ppt is not a significant quantity considering the model assumptions and other departures from the natural system. Thus, it would seem that perhaps the steady-state salt balance equation could be used to model this transient salinity phenomenon. However, it should be noted that this flume test has a 70 per cent change in freshwater discharge in 25 cycles, and the Delaware estuary can have the same change in about 10 tidal cycles. Without additional analysis, it is therefore uncertain as to whether the unsteady terms

can be neglected for applications of this model to real estuaries.

5.5 Influence of Transient Flume Conditions on Shoaling Characteristics

An important feature of the two-dimensional modeling of the time-averaged velocity profiles is the identification of the longitudinal position where the net bottom velocity changes direction and goes through a zero value. This point is commonly called the "null-point", and has been shown by Simmons (1965), and others, to be a zone of high rates of shoaling in estuarine channels, as previously discussed in Chapter II. Figure 5.9 illustrates the features of this null-point and shows that it is equivalent to the point where the net landward flow of salt water ceases.

Since the vertical structure of the net velocity field is strongly dependent upon the magnitude of freshwater inflow, the null-point must also exhibit a dependence on these discharges. Figure 5.10 shows how the null-point, as determined from the analytical model, moves upstream as the freshwater inflow is decreased over the 25 cycles of the transient flume study. The null-point can be found analytically from the equation for the horizontal velocity,

$$\frac{U}{U_f} = - \frac{\partial \Theta_d}{\partial \xi} \frac{C_1}{24} \{ - 4\eta^3 + 6\eta^2 - 1 \} - 1 \qquad 3.64$$

At the bottom, $\eta = 1$, a condition of zero velocity must satisfy an equation which states that

$$1 = - \frac{\partial \Theta_d}{\partial \xi} \frac{C_1}{24}$$

where $\frac{\partial \Theta_d}{\partial \xi}$ is the non-dimensional one-dimensional salinity gradient, and

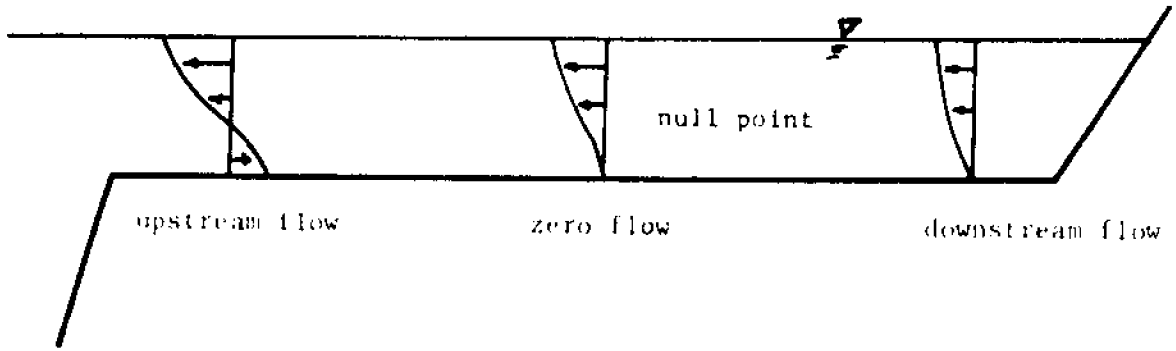

Figure 5.9 Schematic illustration of null point

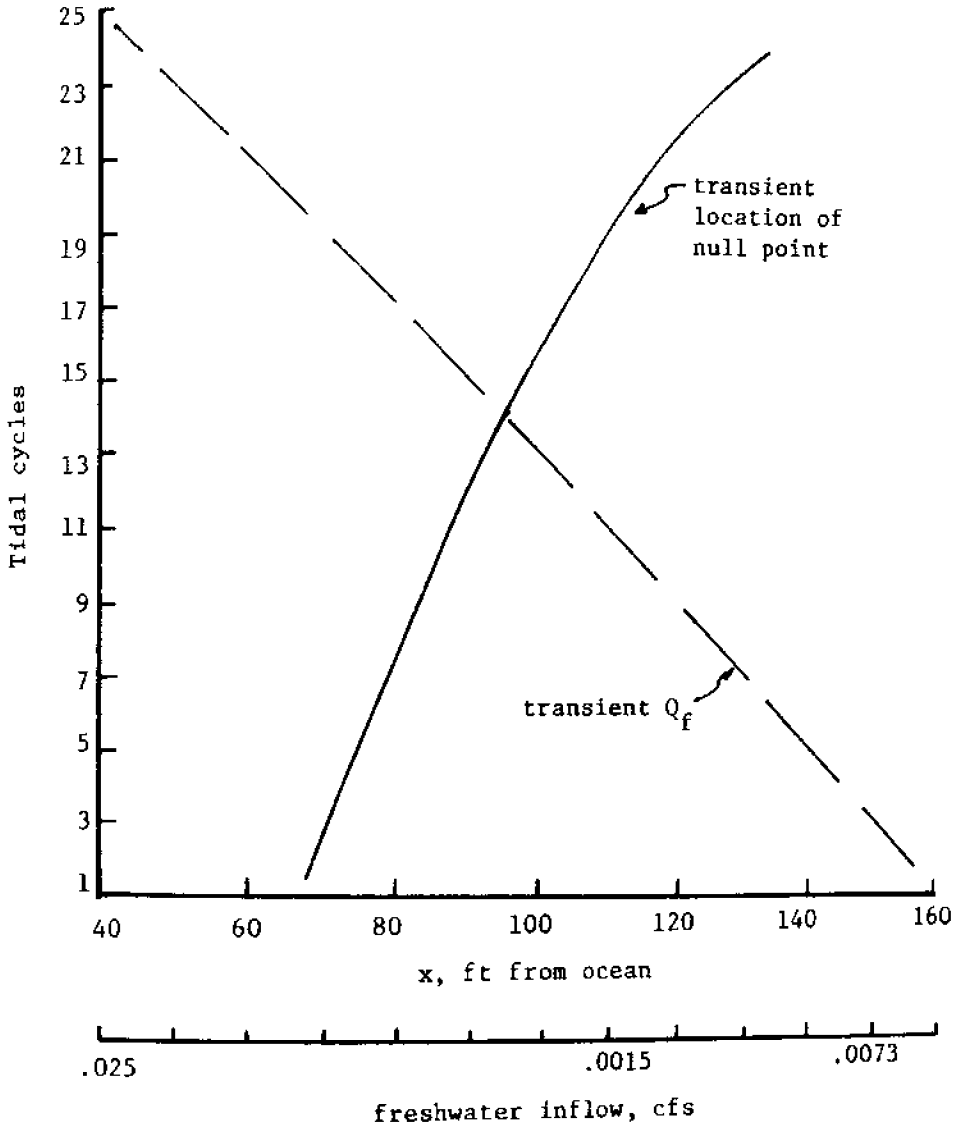

Figure 5.10 Relationship between null point and freshwater
WES 42

$$C_1 = \frac{\alpha\, S_o g h^4 b}{L_i\, Q_f\, \bar{D}} .$$

The fact that U/U_f is zero implies that the net density current is just equal and opposite to the freshwater velocity, since U contains both of these components in its definition.

VI The Savannah Estuary - An Analytical Investigation of Estuarine Shoaling

The shoaling problems of the Savannah Estuary have been carefully reviewed by Simmons (1965) and Harleman and Ippen (1969). Both hydraulic models and field investigations have shown a relationship between the longitudinal location of maximum shoaling and a null point as indicated in figure 6.1. Figure 6.2 is a location map for the estuary. From these figures it is seen that immediately downstream of Savannah Harbor, between stations 120 and 130, a zone of very high shoaling is located by comparison with the rest of the estuary. In addition, for the model data shown in figure 6.1, with a freshwater flow equal to 7,000 cfs, the null point also occurs between these two stations.

In their report, Harleman and Ippen present the time-and depth-averaged longitudinal salinity distributions from the model for freshwater flows of 7,000 cfs and 16,000 cfs, shown in figure 6.3 (their figure 13). With these curves, and the correlation for eddy coefficients presented in Chapter IV, it is possible to apply the analytical model developed in Chapter III to this estuary and thus further investigate the null point dependence on freshwater flow rates.

Table 6.1 summarizes the data input to the analytical model for both the 7,000 cfs and 16,000 cfs freshwater flow rates. Following the arguments of Harleman and Ippen, the discharge through the navigation channel is estimated at three-fourths of the total freshwater discharge, i.e., 5250 cfs and 12,000 cfs respectively. The value of 2 knots for the maximum flood velocity is taken from the Coast and Geodetic Tidal Current Tables.

The values for the spacial derivatives of the one-dimensional longitudinal salinity distribution were computed using the spline program

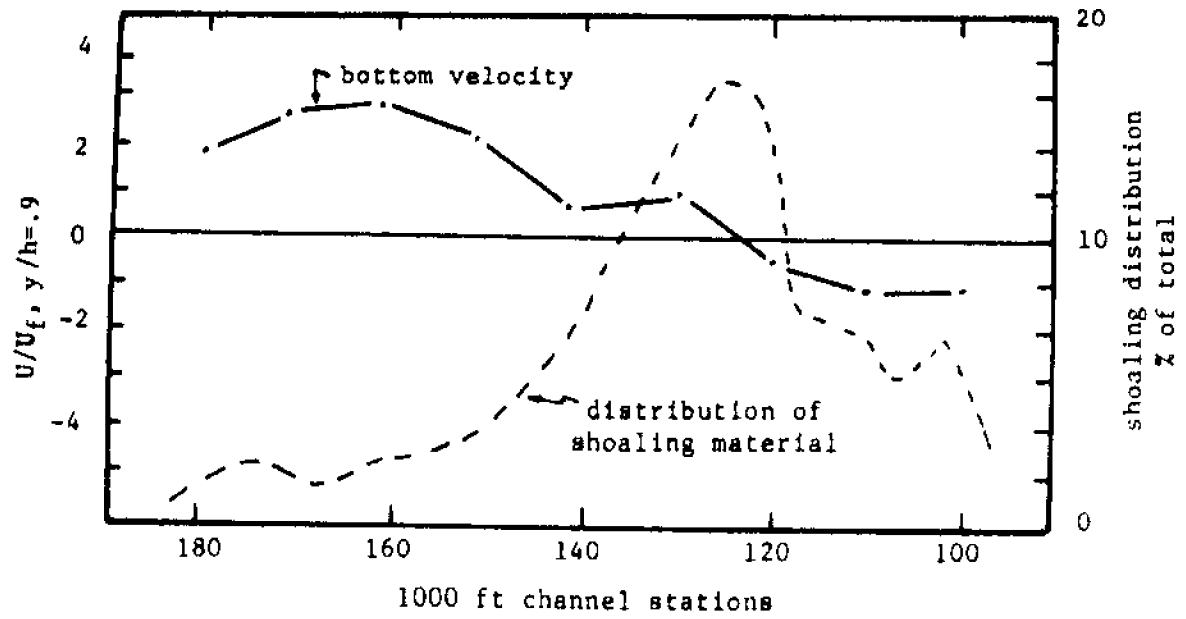

Figure 6.1 Longitudinal location of maximum shoaling in relation to null point for Savannah estuary, Q_f=7000 cfs (from Harleman and Ippen 1969)

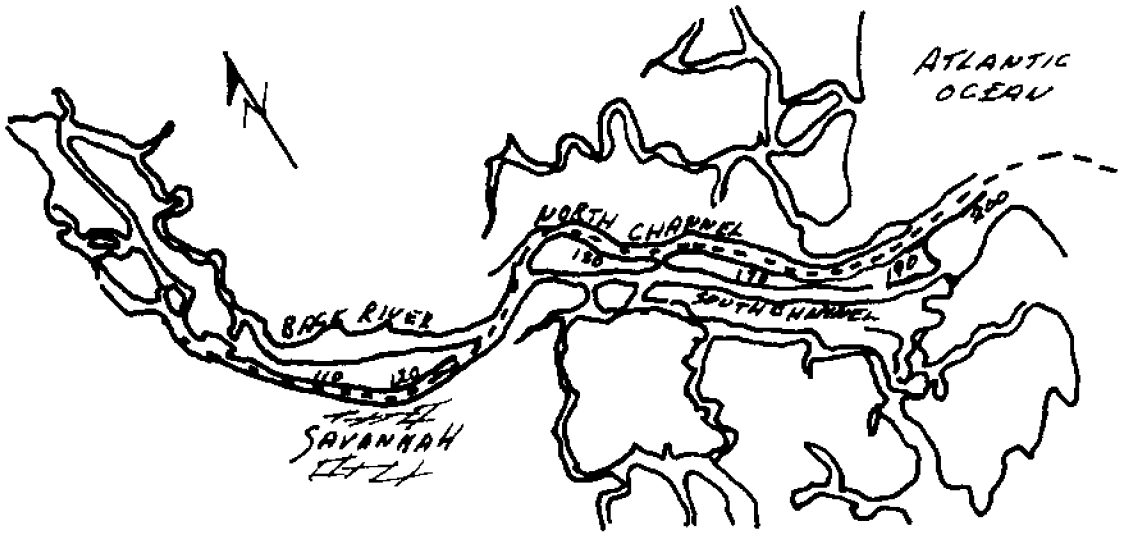

Figure 6.2 Location map, Savannah estuary
(from Simmons 1965)

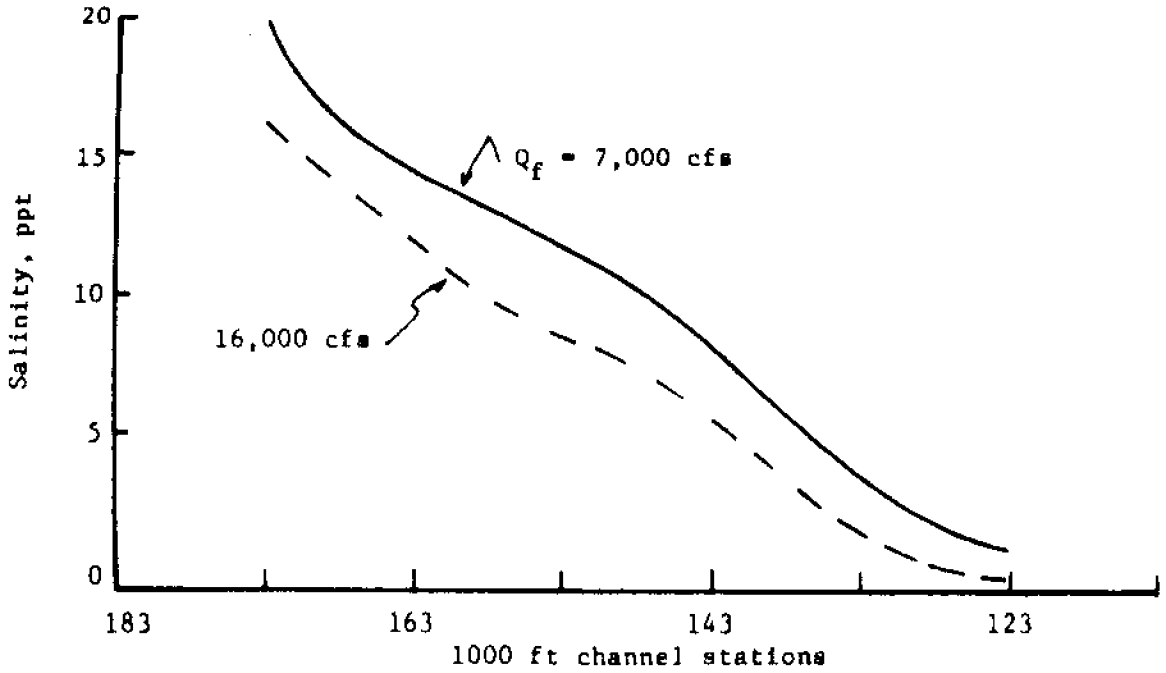

Figure 6.3 Effects of Q_f on longitudinal salinity distribution, Savannah estuary (from Harleman and Ippen 1969)

outlined in appendix 2.

Figure 6.4 illustrates the analytical results for the null point for the two freshwater flows. The connected circles are the computed values and the crosses are the hydraulic model data, as reported by Harleman and Ippen. The fairly close agreement between computed and experimental values indicates that the Savannah estuary prototype scales and conditions do not seriously violate the assumptions of the analytical model.

In figure 6.4 it is seen that the null point shifts downstream about 1,000 feet when the freshwater discharge is increased to 16,000 cfs. Qualitative results of this nature illustrate the usefulness of the analytical model in the analysis of the many factors which determine the circulation patterns in estuaries. When used in conjunction with a numerical model, as discussed in Chapter V, or a hydraulic model, as in the present illustration, this analytical model should prove to be a valuable aid to engineering analysis.

Table 6.1

Savannah Estuary & Inputs to Analytical Model

S_o = 30 ppt	h_o = 27 ft.
u_o - 2 knots	b_o = 2,000 ft.

Q_f = 16,000 cfs	Q_f = 7,000 cfs
L_i = 85,000 ft.	L_i = 100,000 ft.
U_f/u_o = .066	U_f/u_o = .029
$\bar{D}$ = 12.2 x 10^{-3} ft^2/sec	$\bar{D}$ = 12.8 x 10^{-3} ft^2/sec

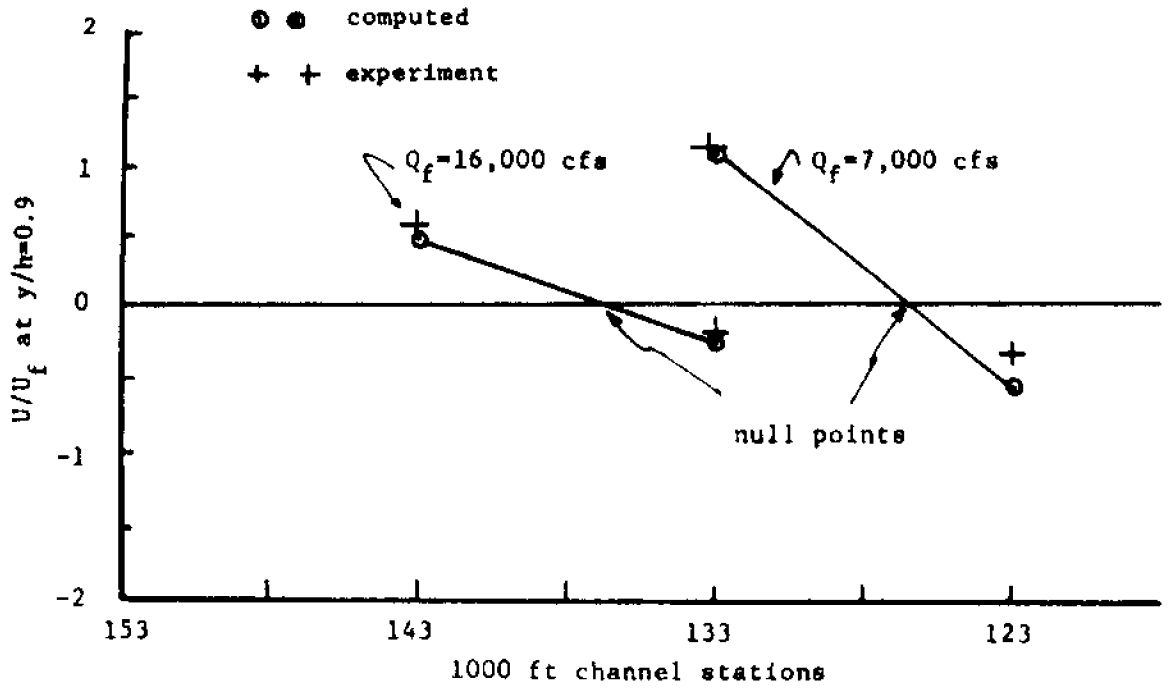

Figure 6.4 Null point location for Savannah estuary

VII Summary and Conclusions

7.1 Objectives

The importance of estuaries in the complex schemes of the natural environment demands that man gain a more fundamental understanding of the dynamics of these water bodies. The ecological stress threatening estuaries as a result of increasing coastal development can only be answered with the knowledge derived from intensive research and analysis. A small part of this needed understanding can be realized from the development of mathematical models of estuarine circulation and dynamics. The development of a mathematical model requires the understanding of the physics of the natural system being modeled. Thus, the record of these model developments is in fact the history of man's increasing knowledge of these coastal systems.

The present study seeks a method of predicting the patterns of circulation and salinity distribution for the somewhat restrictive condition resulting from time-averaging these processes over a tidal period. Longitudinal and vertical variations only, are considered, and thus lateral spacial averaging is also implied. Although these limiting conditions exclude the modeling of the tidal varying properties characteristic of estuaries, several important problems can be examined with such a model. An interesting example of this latter set of model applications is the occurence of zones of shoaling and of turbidity in estuarine channels as a consequence of the modification of the natural freshwater inflow patterns. The coupled growth in mathematical model development and physical understanding through physical models and field work has made serious engineering

analysis possible which can be applied successfully to this problem.

7.2 Summary

The model of the time-averaged longitudinal and vertical distributions of velocity and salinity developed in this study employs an analytical solution to the four basic equations describing these parameters.

1. Equations of motion. These equations state the conservation of longitudinal and vertical momentum. The assumption is made that, for the mean force balance, averaged over a tidal period, the only important terms are the following: the pressure gradient and buoyancy for the vertical equation, and the balance between the pressure gradient and the vertical flux of momentum for the longitudinal equation of motion.

2. Equation of water conservation. The continuity equation for an incompressible fluid is used in the model.

3. Equation of salt conservation. The two-dimensional equation of the conservation of dissolved salt is included in the model in which the horizontal and vertical convection is balanced by the vertical eddy diffusion only. Thus, the transport by horizontal eddying has been neglected.

4. Equation of state. The relationship between density and salinity is approximated by a linear function which neglects temperature effects.

In seeking an analytical solution to the above set of equations, several additional assumptions are introduced. The longitudinal salinity gradient has been shown by field and laboratory analysis to be nearly independent of depth. This observation is included in the model by replacing the actual longitudinal salinity gradient $\frac{\partial S}{\partial x}(x,y)$ with the

gradient of the depth averaged salinity $\frac{\partial S_d}{\partial x}(x)$. The second important assumption is that the mean vertical eddy coefficients of momentum $D_y(x,y)$ and salt $K_y(x,y)$ may be replaced with effective coefficients independent of depth, D(x) and K(x).

With the above assumptions and a set of generally accepted boundary conditions, an analytical solution is found using simple methods of numerical intergration. This solution is studied with data from several flume tests and three field studies. A result of this analysis is that accurate profiles of velocity and salinity can be obtained when the eddy coefficients D(x) and K(x) are assumed as constants, $\bar{D}$ and $\bar{K}$, independent of both x and y. These modified coefficients have been correlated with the ratio of freshwater velocity and maximum flood tide velocity at the entrance of the estuary, incorporating two dimensionless terms which may be derived from the governing equations.

The model, including the correlations for the eddy coefficients, has been successfully applied to a transient flume study wherein the freshwater inflow varied over a period of 25 tidal cycles. In this regard, the model was coupled with the results from a one-dimensional non-time-averaged numerical model of salinity intrusion. Used in this manner, the two models represent an important combined approach to the analysis of estuarine systems.

Finally, the two-dimensional analytical model has correctly described the relationship known to exist between the zones of shoaling and levels of freshwater inflow for the Savannah estuary.

7.3 Future Work

The present model is neither the first attempt, nor should it be the final answer to the mathematical formulation of the physics governing estuarine circulation and diffusion. Immediate improvements and refinements might best be directed towards a more sophisticated approach to the determination of the eddy coefficients, rather than the essentially empirical technique of the present study. A significant improvement in the details of the vertical structure of velocity and salinity is directly dependent on the more accurage representation of these coefficients.

Ultimately, a real-time two-dimensional, or even three-dimensional model, may be developed, using numerical methods with large, high speed computers. For the proper evaluation of these models of the future, as well as the present analytical schemes, much more laboratory, and especially, field data are needed. The present oceanographical data banks are often collections of observations which do not lend themselves to direct comparison to mathematical models. A greater feedback between model builder and field observer must be iniated to promote rapid progress in this study of estuaries.

BIBLIOGRAPHY

Abbott, M. R. (1960) "Salinity Effects in Estuaries", Journal of Marine Research, Vol. 18, No. 2, 1960.

Bowden, K. F. (1960) "Circulation and Mixing in the Mersey Estuary", International Association of Scientific Hydrology, Pub. No. 51, 1960.

Bowden, K. F. (1963) "The Mixing Precesses in a Tidal Estuary", International Journal of Air and Water Pollution, Vol. 7, 1963.

Bowden, K. F. (1967) "Circulation and Diffusion", in Estuaries, G. H. Lauff ed., American Assn. Advancement Sci., Washington, D.C., 1967.

Bowden, K. F. & Gilligan, R. M. (1971) "Characteristic Features of Estuarine Circulation as Represented in the Mersey Estuary", Limnology & Oceanography, Vol. 16, No. 3, 1971.

Delft Hydraulics Laboratory (1970) "Flume Study on Salinity Intrusion in Estuaries", M 896-X, 1970.

Hansen, D. V., and Rattray, M., Jr. (1965) "Gravitational Circulation in Straits and Estuaries", Journal of Marine Research, Vol. 23, No. 2, 1965.

Hansen, D. V. (1967) "Salt Balance and Circulation in Partially Mixed Estuaries", in Estuaries, G. H. Lauff ed., American Assn. Advancement Sci., Washington, D. C., 1967.

Harleman, D. R. F. and Ippen, A. T. (1967) "Two-Dimensional Aspects of Salinity Intrusion in Estuaries: Analysis of Salinity and Velocity Distributions", T. B. No. 13, Committee on Tidal Hydraulics, U. S. Army Corps of Engineers, 1967.

Harleman, D. R. F. and Ippen, A. T. (1969) "Salinity Intrusion Effects in Estuary Shoaling", Journal of the Hydraulics Division, ASCE, Vol. 95, No. HY 1, Proc. Paper 6340, 1969.

Inglis, Sir Claude and Allen, F. H. (1957) "The Regimen of the Thames Estuary as Affected by Currents, Salinities, and River Flow", Institution of Civil Engineers March, 1957.

Ippen, A. T. and Harleman, D. R. F. (1961) "One-Dimensional Analysis of Salinity Intrusion in Estuaries", T.B. No. 5, Committee on Tidal Hydraulics, U.S. Army Corps of Engineers, 1961.

Kent, R. E. and Pritchard, D. W. (1959) "A Test of Mixing Length Theories in a Coastal Plain Estuary", Journal of Marine Research, Vol. 18, No. 1, 1959

Lee, C. H. (1970) One-Dimensional, Real-Time Model for Estuarine Water Quality Predictions, Ph.D. Thesis, Department of Civil Engineering, Massachusetts Institute of Technology.

McGregor, P. D. (1971) "The Influence of Topography and Pressure Gradient on Shoaling in a Tidal Estuary", Geophysical Journal Royal Astronomical Soc., 25, 1971.

Montgomery, R. B. (1943) "Generalization for Cylinders of Prandtl's Linear Assumptions for Mixing Length", Ann. N Y Acad. Sci., Vol. 44, 1943.

Munk, W. H. and Anderson, E. R. (1948) "Notes on a Theory of the Thermocline", Journal of Marine Research, Vol. 7, No. 3, 1948.

Pritchard, D. W. (1952) "Salinity Distribution and Circulation in the Chesapeake Bay Estuarine System", Journal of Marine Research. Vol. 11, No. 2, 1952.

Pritchard, D. W. and Kent, R. E. (1953) "The Reduction and Analysis of Data from the James River Operation Oyster Spat", Tech. Report VI, Chesapeake Bay Institute, The Johns Hopkins University, Ref. 53-12, 1953.

Pritchard, D. W. (1954) "A Study of the Salt Balance in a Coastal Plain Estuary", Journal of Marine Research, Vol. 13, No. 1, 1954.

Pritchard, D. W. (1956) "The Dynamic Structure of a Coastal Plain Estuary", Journal of Marine Research, Vol. 15, No. 1, 1956.

Pritchard, D. W. (1960) "The Movement and Mixing of Contaminants in Tidal Estuaries", in Waste Disposal in the Marine Environment, Pergamon Press, 1960.

Simmons, H. B. (1965) "Channel Depth as a Factor in Estuarine Sedimentation", Tech. Bull No. 8, Comm. on Tidal Hyd., U. S. Army, Corps of Engineers, Vicksburg, Miss., 1965.

Thatcher, M. L. and Harleman, D. R. F. (1972) "A Mathematical Model for the Prediction of Unsteady Salinity Intrusion in Estuaries", Tech. Report No. 144, Ralph M. Parsons Laboratory, Department of Civil Engineering, Massachusetts Institute of Technology, 1972.

TRACOR (1971) Estuarine Modeling: An Assessment, Environmental Protection Agency, Washington, D. C., 1971.

U.S. Army Engineer Waterways Experiment Station (1955) Investigation of Salinity and Related Phenomena (Interim Report on Flume Control Tests), Vicksburg, Miss., 1955.

Wylie, C. R. (1960) Advanced Engineering Mathematics, McGraw-Hill Book Company, Inc., 1960

APPENDICES

Appendix 1

The Computer Program for Two-Dimensional Analytical Estuary Model

The analytical solutions for velocity and salinity development in Chapter III include several complex integrals which are evaluated by numerical intergration techniques. From a computational point of view, the model is very simple and requires only a limited amount of time and storage. Both an IBM 370/155 using Fortran IV, G level, Mod 3 and a HP 2114B using HP Basic have been employed in this study. To illustrate the relative simplicity of the computational scheme, the HP Basic program is presented in this appendix.

Program inputs:

S,M,N — the normalized one-dimensional salinity and its first and second derivatives. These parameters are usually determined from the SPLINE program described in appendix 2.

D,K — the eddy coefficients, normally taken from the correlations presented in Chapter IV.

U1 — the freshwater velocity, Q_f/bh (constant for constant b and h).

H1 — the depth of msl.

Sϕ — the ocean salinity.

L1 — the salinity intrusion length.

For each longitudinal station, the model begins with the computation of the dimensionless groups C1 and C2. Then, at each discrete depth a horizontal and vertical velocity is found. With these parameters known, the numerical intergration of the salinity function is carried out, a computation requiring four nested integrals. Finally, the salinity is computed and printed with the horizontal and vertical velocities.

In HP basic, the program is as follows:

```
620  DIM S[5],M[5],N[5],K[5],D[5],A[11],B[11],H[11]
650  MAT  READ S
652  MAT  READ M
654  MAT  READ N
656  MAT  READ K
658  MAT  READ D
660  READ U1,H1,S0,L1
670  FOR J=1 TO 5
672  LET C2=K[J]*L1/(U1*H1↑2)
674  LET C1=1.00000E-03*.75*S0*32.2*H1↑3/(L1*D[J]*U1)
676  FOR I=1 TO 11
678  LET Y=.1*(I-1)
680  LET A[I]=(M[J]*(1+C1*M[J]/24*(4*Y↑3-6*Y↑2+1)))/C2
682  LET B[I]=(-C1*N[J]/24*(Y↑4-2*Y↑3+Y))/C2
690  NEXT I
691  PRINT
692  PRINT
693  PRINT "Y/H","  U/UF","  V/UF","  S/S0"
694  PRINT "-----------------------------------------------
695  PRINT
700  LET T2=T4=T6=T8=H3=0
702  FOR I=2 TO 11
704  LET T1=T2
706  LET T2=T2+5.00000E-02*(B[I]+B[I-1])
708  LET T3=T4
710  LET T4=T4+5.00000E-02*(A[I]*EXP(-T2)+A[I-1]*EXP(-T1))
712  LET T5=T6
714  LET T6=T6+5.00000E-02*(EXP(T2)*T4+EXP(T1)*T3)
716  LET H[I-1]=T5
718  LET T7=T8
720  LET T8=T8+5.00000E-02*(T6+T5)
722  NEXT I
730  LET H[11]=T6
750  FOR I=1 TO 11
752  LET Y=.1*(I-1)
760  LET H4=H[I]+S[J]-T8
762  LET H3=H3+H4
768  LET U=A[I]*C2/M[J]
770  LET V=B[I]*C2*H1/L1
780  PRINT Y,U,V,H4
782  NEXT I
784  LET H3=H3/11
786  PRINT H3
790  NEXT J
```

```
820   DATA .81,.66,.37,.13,2.00000E-02
822   DATA -.51,-.97,-1.17,-.69,-.21
824   DATA -1.4,-2.9,1.2,2.6,1.3
826   DATA 2.30000E-04,2.30000E-04,2.30000E-04
827   DATA 2.30000E-04,2.30000E-04
828   DATA 1.40000E-04,1.40000E-04,1.40000E-04
829   DATA 1.40000E-04,1.40000E-04
830   DATA -2.00000E-02,.5,29.7,182
900   END
```

A sample of the output from this program is given below. All values are dimensionless, and y/h = 0 is at the surface.

Y/H	U/UF	V/UF	S/S0
0	4.73864	0	.774508
.1	4.52927	-2.76591E-03	.775924
.2	3.961	-5.23296E-03	.780085
.3	3.12355	-7.16431E-03	.786747
.4	2.10664	-8.39079E-03	.795527
.5	1	-8.81089E-03	.805925
.6	-.106637	-8.39079E-03	.817347
.7	-1.12355	-7.16431E-03	.829136
.8	-1.961	-5.23296E-03	.840626
.9	-2.52927	-2.76591E-03	.851212
1	-2.73864	0	.860432
.810679			

Appendix 2

The Computer Program for Spline Interpolation of One-Dimensional Salinity Gradients

The first and second spacial derivatives of the one-dimensional longitudinal salinity distribution, which are inputs to the analytical model described in appendix 1, are computed with a spline interpolation routine. The spline program, written here in HP Basic, was adapted from the M.I.T. Information Processing Center Program, described in their bulletin AP-72. As stated in AP-72:

> The spline fit curve is a mathematical expression for the shape taken by an idealized spline (a thin wood or metal strip) passing through the given points..... The spline curve is a piecewise cubic with continuous first and second derivatives. Thus, it can give good approximations to the first and second derivatives of the function in addition to the function values.

Program inputs:

Y the 1-D salinities, normalized by the ocean salinity

L the salinity intrusion length, ft.

T the distance between values of salinity, y (T is constant in this case, but can also be a variable.)

S the distance between points where interpolated salinities are to be found.

N the number of points where salinities are given

M the number of points where interpolation is carried out.

```
2  INPUT N,M,S,T,L1
3  DIM X[21],Z[21],A[21],B[21],C[21],D[21],E[21],W[2,21]
4  LET Z[1]=X[1]=0
5  FOR I=2 TO M
6  LET Z[I]=Z[I-1]+S/L1
7  NEXT I
8  DIM Y[5]
9  PRINT "X","MEAN SAL.","DS/DX","D2S/DX2"
10  PRINT "-------------------------------------------------------
11  FOR I=2 TO N
12  LET X[I]=X[I-1]+T/L1
13  NEXT I
14  PRINT
15  MAT  READ Y
16  LET S1=T/L1
17  LET N0=N-1
18  LET W[1,1]=-.5
19  LET W[2,1]=0
20  FOR I=2 TO N0
22  LET F=(Y[I+1]-Y[I])/S1-(Y[I]-Y[I-1])/S1
23  LET S4=S1*.166667
24  LET W2=(S1+S1)*.333333-S4*W[1,I-1]
25  LET W[1,I]=(S1*.166667)/W2
26  LET W[2,I]=(F-S4*W[2,I-1])/W2
27  NEXT I
36  LET E[N]=(.5*W[2,N0])/(1+.5*W[1,N0])
40  FOR I=2 TO N
45  LET K=N+1-I
50  LET E[K]=W[2,K]-W[1,K]*E[K+1]
55  NEXT I
60  FOR I=1 TO M
65  LET Z1=Z[I]
70  LET K=2
75  IF (Z1-X[1])<0 THEN 80
76  IF (Z1-X[1])=0 THEN 300
77  IF (Z1-X[1])>0 THEN 85
80  IF Z1<(1.1*X[1]-.1*X[2]) THEN 400
82  GOTO 300
85  LET K=N
87  IF (Z1-X[N])<0 THEN 96
88  IF (Z1-X[N])=0 THEN 300
90  IF (Z1-X[N])>0 THEN 93
93  IF Z1>(1.1*X[N]-.1*X[N-1]) THEN 400
94  GOTO 300
```

```
96  LET M2=2
100  LET M3=N
110  REM
111  LET K=(M3+M2)/2
115  IF (M3>(M2-.1)) AND (M3<(M2+.1)) THEN 300
120  IF (Z1-X[K])<0 THEN 125
121  IF (Z1-X[K])=0 THEN 300
122  IF (Z1-X[K])>0 THEN 130
125  LET M3=K
126  GOTO 110
130  LET M2=K+1
135  GOTO 110
300  REM
301  LET X2=X[K]-Z1
305  LET X3=X2↑2
310  LET Z3=Z1-X[K-1]
315  LET Z4=Z3↑2
320  LET S2=S1*2
325  LET S3=S1*.166667
330  LET E1=E[K]
335  LET E2=E[K-1]
340  LET Y1=Y[K]/S1
345  LET Y2=Y[K-1]/S1
350  LET A[I]=(E2*X3*X2+E1*Z4*Z3)*.166667/S1
351  LET A[I]=A[I]+(Y1-E1*S3)*Z3+(Y2-E2*S3)*X2
355  LET B[I]=(E1*Z4-E2*X3)/S2+Y1-Y2-(E1-E2)*S3
360  LET C[I]=(E2*X2+E1*Z3)/S1
365  NEXT I
371  FOR I=1 TO M
373  LET Z[I]=Z[I]*L1
375  PRINT Z[I],A[I],B[I],C[I]
376  NEXT I
377  GOTO 500
400  PRINT " OUT OF RANGE, X=";Z1
410  GOTO 300
452  DATA .91,.77,.532,.2,4.00000E-02,0
500  END
```

An example of the spline program output is given below. The values of x are in feet, and the other terms are dimensionless.

```
?5,5,40,40,160
X              MEAN SAL.       DS/DX          D2S/DX2
-------------------------------------------------------

 0             .91             -.441          -.714
 40            .77             -.70875        -1.428
 80            .532            -1.26          -2.982
 120           .2              -1.09125        4.332
 160           4.00000E-02     -.278999        2.166

READY
```

Appendix 3

Tables of Computed and Experimental Velocity and Salinity Distributions

The following tables present the comparison of computed and experimental velocity and salinity distributions for the flume tests and field data evaluated in Chapter IV. The units of the eddy coefficients D and K are as stated in the table; all other terms are dimensionless.

TABLE A1

COMPUTED AND EXPERIMENTAL VELOCITY AND SALINITY DISTRIBUTIONS

WES TEST 11

X/LI = 0.04

S MEAN= 0.66 DS/DX MEAN= -1.29 D2S/DX2 MEAN= 0.713

D= 0.39E-03 SQ FT/SEC K= 0.17E-03 SQ FT/SEC

Y/H	EXP U/UF	COMP U/UF	EXP S/S	COMP S/S
0.000	2.55	2.40	0.37	0.44
0.100	2.26	2.32	0.39	0.44
0.200	1.90	2.11	0.45	0.47
0.300	1.60	1.80	0.53	0.51
0.400	1.30	1.41	0.59	0.57
0.500	1.01	1.00	0.67	0.63
0.600	0.75	0.59	0.75	0.70
0.700	0.48	0.20	0.82	0.78
0.800	0.18	-0.11	0.87	0.85
0.900	-0.12	-0.32	0.90	0.93
1.000	-0.42	-0.40	0.92	1.00

TABLE A2

COMPUTED AND EXPERIMENTAL VELOCITY AND SALINITY DISTRIBUTIONS

WES TEST 11

X/LI = 0.29

S MEAN= 0.367 DS/DX MEAN= -1.022 D2S/DX2 MEAN= 1.425

D= 0.31E-03 SQ FT/SEC K= 0.13E-03 SQ FT/SEC

Y/H	EXP U/UF	COMP U/UF	EXP S/S0	COMP S/S0
0.000	3.08	2.40	0.12	0.15
0.100	2.82	2.32	0.14	0.16
0.200	2.20	2.11	0.16	0.19
0.300	1.62	1.79	0.20	0.23
0.400	1.24	1.41	0.28	0.28
0.500	0.78	1.00	0.37	0.34
0.600	0.56	0.59	0.46	0.41
0.700	0.25	0.21	0.53	0.48
0.800	-0.10	-0.11	0.57	0.55
0.900	-0.42	-0.32	0.60	0.62
1.000	-0.68	-0.40	0.61	0.68

TABLE A3

COMPUTED AND EXPERIMENTAL VELOCITY AND SALINITY DISTRIBUTIONS

WES TEST 11

X/LI = 0.57

S MEAN= 0.124 DS/DX MEAN= -0.717 D2S/DX2 MEAN= [illegible].713

D= 0.22E-03 SQ FT/SEC K= 0.17E-03 SQ FT/SEC

Y/H	EXP U/UF	COMP U/UF	EXP S/SO	COMP S/S[illegible]
0.000	2.18	2.38	0.03	[illegible]
0.100	2.16	2.30	0.03	[illegible].11
0.200	2.10	2.09	0.04	[illegible].12
0.300	1.97	1.78	0.[illegible]4	0.[illegible]4
0.400	1.64	1.41	0.[illegible]5	[illegible].07
0.500	1.20	1.00	0.06	0.11
0.600	0.76	0.59	0.08	0.15
0.700	0.32	0.22	0.18	0.19
0.800	-0.12	-0.09	0.26	0.23
0.900	-0.49	-0.30	0.29	0.27
1.000	-0.74	-0.38	0.30	0.30

TABLE A4

COMPUTED AND EXPERIMENTAL VELOCITY AND SALINITY DISTRIBUTIONS

WES TEST 14

X/LI = [illegible].22

S MEAN= [illegible].760 dS/DX MEAN= -0.838 D2S/DX2 MEAN= -[illegible].837

D= [illegible].20E-03 SQ FT/SEC K= [illegible].38E-03 SQ FT/SEC

Y/H	EXP U/UF	COMP U/UF	EXP S/S[illegible]	COMP S/S
[illegible]	5.50	5.3[illegible]	0.72	[illegible].72
[illegible]	5.1[illegible]	5.[illegible]6	[illegible].72	0.73
[illegible]	4.50	4.40	0.73	[illegible].73
[illegible]	3.6[illegible]	3.44	0.74	0.74
[illegible]	2.5[illegible]	2.27	0.75	[illegible].75
[illegible]	1.3[illegible]	1.[illegible]0	0.76	[illegible].76
[illegible]	0.2[illegible]	-0.27	[illegible].77	.77
[illegible]	-1.[illegible]	-1.44	0.78	[illegible].78
[illegible]	-2.4[illegible]	-2.4[illegible]	0.79	[illegible].79
[illegible]	-3.4[illegible]	-3.06	0.80	[illegible].8[illegible]
[illegible]	-4.2[illegible]	-3.30	0.8[illegible]	[illegible].81

TABLE A5

COMPUTED AND EXPERIMENTAL VELOCITY AND SALINITY DISTRIBUTIONS

WES TEST 14

x/LI = 0.44

S MEAN= 0.528 dS/DX MEAN= -1.397 D2S/DX2 MEAN= -4.256

D= 0.28E-03 SQ FT/SEC K= 0.52E-03 SQ FT/SEC

Y/H	EXP U/UF	COMP U/UF	EXP S/S'	COMP S/S'
0.000	6.40	6.12	0.45	0.48
0.100	6.10	5.83	0.46	0.48
0.200	5.20	5.06	0.49	0.48
0.300	3.80	3.91	0.50	0.49
0.400	2.10	2.52	0.53	0.51
0.500	0.60	1.05	0.54	0.52
0.600	-0.80	-0.52	0.55	0.54
0.700	-2.00	-1.91	0.56	0.56
0.800	-2.90	-3.06	0.57	0.57
0.900	-3.20	-3.83	0.58	0.59
1.000	-3.30	-4.12	0.58	0.60

TABLE A6

COMPUTED AND EXPERIMENTAL VELOCITY AND SALINITY DISTRIBUTIONS

WES TEST 14

X/LI = 0.66

S MEAN= 0.198 DS/DX MEAN= -1.242 D2S/DX2 MEAN= 5.663

D= 0.30E-03 SQ FT/SEC K= 0.28E-03 SQ FT/SEC

Y/H	EXP U/UF	COMP U/UF	EXP S/S'	COMP S/S'
0.000	5.60	5.25	0.13	0.14
0.100	5.30	5.01	0.14	0.14
0.200	4.60	4.37	0.15	0.15
0.300	3.30	3.41	0.16	0.16
0.400	2.00	2.26	0.17	0.18
0.500	1.00	1.00	0.20	0.20
0.600	-0.50	-0.26	0.22	0.22
0.700	-1.50	-1.41	0.23	0.23
0.800	-2.30	-2.37	0.25	0.25
0.900	-2.60	-3.01	0.26	0.26
1.000	-2.90	-3.25	0.27	0.27

TABLE A7

COMPUTED AND EXPERIMENTAL VELOCITY AND SALINITY DISTRIBUTIONS

WES TEST 16

X/L I = 0.25

S MEAN= 0.656 DS/DX MEAN= -0.371 D2S/DX2 MEAN= -2.359

D= 0.246-03 SQ FT/SEC K= 0.185-03 SQ FT/SEC

Y/H	EXP U/UF	COMP U/UF	EXP S/SO	COMP S/SO
0.000	6.40	5.44	0.52	0.53
0.100	6.00	5.38	0.53	0.54
0.200	5.00	4.68	0.55	0.55
0.300	3.50	3.44	0.57	0.57
0.400	2.00	2.37	0.60	0.60
0.500	0.50	1.00	0.64	0.64
0.600	-0.70	-0.37	0.68	0.68
0.700	-1.80	-1.64	0.72	0.72
0.800	-2.60	-2.68	0.77	0.77
0.900	-3.10	-3.39	0.80	0.81
1.000	-3.20	-3.66	0.84	0.84

TABLE A8

COMPUTED AND EXPERIMENTAL VELOCITY AND SALINITY DISTRIBUTIONS

WES TEST 16

X/LI = 0.50

S MEAN= 0.347 DS/DX MEAN= -1.155 D2S/DX2 MEAN= 1.275

D= 0.24E-03 SQ FT/SEC K= 0.17E-03 SQ FT/SEC

Y/H	EXP U/UF	COMP U/UF	EXP S/SO	COMP S/SO
0.000	7.20	5.15	0.24	0.23
0.100	6.50	5.07	0.25	0.25
0.200	5.20	5.00	0.26	0.26
0.300	3.50	3.93	0.28	0.29
0.400	1.80	2.53	0.31	0.32
0.500	0.30	1.00	0.35	0.36
0.600	-1.00	-0.53	0.39	0.40
0.700	-2.00	-1.93	0.43	0.44
0.800	-3.00	-3.09	0.47	0.48
0.900	-3.40	-3.87	0.52	0.50
1.000	-3.50	-4.16	0.54	0.52

TABLE A9

COMPUTED AND EXPERIMENTAL VELOCITY AND SALINITY DISTRIBUTIONS

WES TEST 16

X/LI = 0.75

S MEAN= 0.121 DS/DX MEAN= -0.690 D2S/DX2 MEAN= 2.558

D= 0.24E-03 SQ FT/SEC K= 0.21E-03 SQ FT/SEC

Y/H	EXP U/UE	COMP U/UE	EXP S/SO	COMP S/SO
0.000	4.40	4.30	0.09	0.08
0.100	4.10	4.12	0.08	0.09
0.200	3.60	3.61	0.10	0.09
0.300	2.90	2.97	0.10	0.10
0.400	1.90	1.96	0.11	0.11
0.500	1.00	1.00	0.13	0.13
0.600	0.10	0.02	0.15	0.14
0.700	-0.90	-0.87	0.15	0.15
0.800	-1.60	-1.41	0.16	0.16
0.900	-2.20	-2.12	0.17	0.17
1.000	-2.30	-2.30	0.19	0.18

TABLE A10

COMPUTED AND EXPERIMENTAL VELOCITY AND SALINITY DISTRIBUTIONS

DELFT TEST 117

X/LI = 0.29

C MEAN= 0.503 DS/DX MEAN= -0.030 D2S/DX2 MEAN= 0.840

E= 0.56E-04 SQ M/SEC K= 0.15E-04 SQ M/SEC

Y/H	EXP U/UF	COMP U/UF	EXP S/SO	COMP S/SO
0.077	2.66	2.45	0.09	0.20
0.154	2.45	2.31	0.21	0.22
0.231	2.01	2.09	0.31	0.26
0.308	1.40	1.92	0.40	0.31
0.385	1.82	1.61	0.46	0.37
0.462	1.47	1.17	0.53	0.44
0.539	1.26	0.83	0.59	0.51
0.615	1.02	0.49	0.65	0.59
0.693	0.78	0.18	0.74	0.66
0.770	0.15	-0.09	0.80	0.74
0.847	-0.23	-0.31	0.86	0.81
0.924	0.60	-0.45	0.89	0.88

TABLE A11

COMPUTED AND EXPERIMENTAL VELOCITY AND SALINITY DISTRIBUTIONS

DELFT TEST 117

X/L = 0.43

S MEAN= 0.375 DS/DX MEAN= -0.012 D2S/DX2 MEAN= -0.627

D= 0.60E-04 SQ M/SEC K= 0.19E-04 SQ M/SEC

Y/H	EXP U/UF	COMP U/UF	EXP S/SO	COMP S/SO
0.077	2.47	2.32	0.04	0.07
0.154	2.37	2.19	0.06	0.10
0.231	2.03	2.00	0.14	0.13
0.308	1.61	1.75	0.24	0.17
0.385	1.77	1.46	0.33	0.23
0.462	1.56	1.16	0.39	0.29
0.539	1.38	0.84	0.45	0.36
0.616	1.10	0.53	0.51	0.44
0.693	0.41	0.25	0.58	0.52
0.770	0.23	-0.00	0.64	0.61
0.847	-0.20	-0.20	0.71	0.70
0.924	-0.68	-0.32	0.78	0.78

TABLE A12

COMPUTED AND EXPERIMENTAL VELOCITY AND SALINITY DISTRIBUTIONS

DELFT TEST 117

X/LI = 0.57

S MEAN= 0.249 DS/DX MEAN= -0.914 D2S/DX2 MEAN= 1.970

D= 0.69E-04 SQ M/SEC K= 0.13E-04 SQ M/SEC

Y/H	EXP U/UF	COMP U/UF	EXP S/SO	COMP S/SO
0.077	2.55	2.05	0.02	-0.00
0.154	1.76	1.94	0.03	0.02
0.231	1.57	1.79	0.04	0.05
0.308	1.33	1.59	0.08	0.10
0.385	1.09	1.37	0.16	0.15
0.462	1.[illegible]	1.12	0.24	0.20
0.539	1.36	0.87	0.31	0.26
0.615	1.20	0.63	0.36	0.32
0.693	0.[illegible]7	0.40	0.42	0.38
0.770	0.[illegible]6	0.21	0.46	0.43
0.847	0.08	0.05	0.51	0.49
0.924	-0.[illegible]4	-0.05	0.58	0.54

TABLE A13

COMPUTED AND EXPERIMENTAL VELOCITY AND SALINITY DISTRIBUTIONS

DELFT TEST 117

X/LT = 0.71

S MS/N= 0.14[illegible] DS/DX MEAN= -0.6[illegible] D2S/DX2 MEAN= 0.102

D= 0.[illegible]E-0 SQ M/SEC K= 0.19E-04 SQ M/SEC

Y/H	EXP U/UF	COMP U/UF	EXP S/SO	COMP S/SO
0.077	2.08	1.91	0.01	-0.03
0.154	2.00	1.82	0.02	-0.02
0.231	1.[illegible]	1.[illegible]	0.02	0.00
0.308	1.[illegible]	1.52	0.03	0.03
0.385	1.32	1.32	0.05	0.0[illegible]
0.462	1.10	1.11	0.10	0.10
0.539	0.[illegible]	0.89	0.17	0.14
0.616	0.[illegible]	0.68	0.21	0.18
0.693	0.[illegible]	0.48	0.25	0.23
0.770	0.[illegible]	0.31	0.30	0.28
0.847	0.[illegible]	0.18	0.34	0.33
0.924	0.10	0.0[illegible]	0.39	0.39

TABLE A14

COMPUTED AND EXPERIMENTAL VELOCITY AND SALINITY DISTRIBUTIONS

RELIEF TEST 117

X/LI = 0.85

< MEAN= 0.050 DS/DX MEAN= -0.603 D2S/DX2 MEAN= 2.235

D= 0.943E-04 SQ M/SEC K= 0.225E-04 SQ M/SEC

Y/H	EXP U/UF	COMP U/UF	EXP S/SO	COMP S/SO
0.077	1.54	1.52	0.01	-0.02
0.154	1.64	1.47	0.01	-0.01
0.231	1.52	1.39	0.01	-0.01
0.308	1.[illegible]	1.30	0.01	0.01
0.385	1.[illegible]	1.18	0.01	0.02
0.[illegible]	1.12	1.0[illegible]	0.02	0.0[illegible]
0.[illegible]	1.03	0.[illegible]4	0.0[illegible]	0.0[illegible]
0.[illegible]14	0.[illegible]3	0.92	0.0[illegible]	0.0[illegible]
0.[illegible]3	0.[illegible]7	0.70	0.12	0.10
0.[illegible]70	0.33	0.41	0.14	0.12
0.[illegible]7	0.[illegible]9	0.[illegible]3	0.15	0.14
0.[illegible]24	0.[illegible]8	0.[illegible]5	0.17	0.14

TABLE A15

COMPUTED AND EXPERIMENTAL VELOCITY AND SALINITY DISTRIBUTIONS

DELFT TEST 116

X/L1 = 0.29

S MEAN= 0.461 DS/DX MEAN= -1.038 D2S/DX2 MEAN= -0.386

D= 0.54E-04 SQ M/SEC K= 0.20E-04 SQ M/SEC

Y/H	EXP U/UF	COMP U/UF	EXP S/SO	COMP S/SO
0.077	2.90	2.41	0.06	0.16
0.154	2.60	2.28	0.13	0.19
0.231	2.26	2.07	0.25	0.22
0.308	2.02	1.90	0.34	0.28
0.385	1.66	1.50	0.42	0.32
0.462	1.37	1.17	0.50	0.39
0.539	1.12	0.83	0.55	0.45
0.616	0.82	0.50	0.63	0.53
0.693	0.43	0.20	0.69	0.61
0.770	0.37	-0.03	0.75	0.69
0.847	-0.07	-0.29	0.81	0.78
0.924	-0.35	-0.41	0.95	0.85

TABLE A16

COMPUTED AND EXPERIMENTAL VELOCITY AND SALINITY DISTRIBUTIONS

DELFT TEST 116

X/LI = 0.43

S MEAN= 0.315 DS/DX MEAN= -0.967 D2S/DX2 MEAN= 1.390

H= 0.54E-04 SQ M/SEC K= 0.15E-04 SQ M/SEC

Y/H	EXP U/UF	COMP U/UF	EXP S/SO	COMP S/SO
0.077	2.46	2.32	0.03	0.02
0.154	2.46	2.19	0.04	0.04
0.231	2.23	1.99	0.07	0.08
0.308	1.94	1.75	0.16	0.13
0.385	1.70	1.46	0.25	0.19
0.462	1.36	1.16	0.33	0.25
0.539	1.13	0.84	0.40	0.32
0.616	0.88	0.53	0.45	0.40
0.693	0.61	0.25	0.50	0.47
0.770	0.42	0.00	0.54	0.54
0.847	0.09	-0.19	0.62	0.61
0.924	-0.36	-0.32	0.70	0.67

TABLE A17

COMPUTED AND EXPERIMENTAL VELOCITY AND SALINITY DISTRIBUTIONS

DELFT TEST 116

X/LI = 0.57

S MEAN= 0.194 DS/DX MEAN= -0.735 D2S/DX2 MEAN= 1.883

D= 0.91E-04 SQ M/SEC K= 0.13E-04 SQ M/SEC

Y/H	EXP U/UF	COMP U/UF	EXP S/SO	COMP S/SO
0.077	1.60	1.74	0.01	-0.01
0.154	1.53	1.59	0.02	0.00
0.231	1.43	1.50	0.02	0.03
0.309	1.30	1.43	0.04	0.05
0.385	1.22	1.27	0.09	0.10
0.462	1.06	1.09	0.17	0.15
0.539	1.33	0.91	0.24	0.19
0.616	1.05	0.73	0.30	0.25
0.693	0.74	0.57	0.34	0.30
0.770	0.51	0.42	0.39	0.35
0.847	0.22	0.31	0.42	0.40
0.924	-0.19	0.24	0.48	0.46

TABLE A18

COMPUTED AND EXPERIMENTAL VELOCITY AND SALINITY DISTRIBUTIONS

DELFT TEST 116

X/LI = 0.71

S MEAN= 0.103 DS/DX MEAN= -0.568 D2S/DX2 MEAN= 0.476

D= 0.68E-04 SQ M/SEC K= 0.18E-04 SQ M/SEC

Y/H	EXP U/UF	COMP U/UF	EXP S/SO	COMP S/SO
0.077	1.66	1.73	0.01	-0.01
0.154	1.76	1.69	0.01	-0.02
0.231	1.75	1.55	0.02	-0.00
0.308	1.73	1.41	0.02	0.02
0.385	1.38	1.25	0.03	0.0
0.462	1.21	1.04	0.06	0.07
0.539	1.02	0.91	0.10	0.10
0.616	0.81	0.76	0.15	0.13
0.693	0.73	0.59	0.19	0.17
0.770	0.66	0.49	0.22	0.20
0.847	0.50	0.34	0.25	0.24
0.924	0.34	0.27	0.28	0.28

TABLE A19

COMPUTED AND EXPERIMENTAL VELOCITY AND SALINITY DISTRIBUTIONS

DELFT TEST 116

X/LI = 0.85

S MEAN= 0.032 DS/DX MEAN= -0.387 D2S/DX2 MEAN= 1.935

DX= 0.92E-04 SQ M/SEC K= 0.34E-04 SQ M/SEC

Y/H	EXP U/UF	COMP U/UF	EXP S/SO	COMP S/SO
0.077	1.38	1.38	0.01	-0.01
0.154	1.52	1.34	0.01	-0.01
0.231	1.52	1.28	0.01	-0.00
0.308	1.48	1.21	0.01	0.00
0.385	1.15	1.13	0.01	0.01
0.462	1.18	1.04	0.01	0.02
0.539	1.08	0.95	0.02	0.03
0.614	1.02	0.87	0.03	0.04
0.693	1.04	0.79	0.05	0.05
0.770	0.91	0.72	0.07	0.06
0.847	0.82	0.66	0.09	0.08
0.924	0.41	0.62	0.10	0.09

TABLE A20

COMPUTED AND EXPERIMENTAL VELOCITY AND SALINITY DISTRIBUTIONS

DELFT TEST 121

X/LI = 0.27

S MEAN= 0.552 DS/DX MEAN= -0.949 D2S/DX2 MEAN= 1.627

D= 0.72E-04 SQ M/SEC K= 0.59E-05 SQ M/SEC

Y/H	EXP U/UF	COMP U/UF	EXP S/SO	COMP S/SO
0.077	3.66	3.19	0.18	0.17
0.154	3.44	2.97	0.23	0.21
0.231	2.71	2.65	0.34	0.27
0.308	2.15	2.24	0.44	0.34
0.385	1.72	1.77	0.51	0.43
0.462	1.22	1.26	0.59	0.52
0.539	0.75	0.74	0.68	0.61
0.616	0.27	0.23	0.76	0.69
0.693	-0.14	-0.25	0.83	0.76
0.770	-0.32	-0.65	0.85	0.82
0.847	-0.63	-0.99	0.87	0.88
0.924	-0.98	-1.19	0.89	0.92

TABLE A21

COMPUTED AND EXPERIMENTAL VELOCITY AND SALINITY DISTRIBUTIONS

DELFT TEST 121

X/LI = 0.41

S MEAN= 0.425 DS/DX MEAN= -1.023 D2S/DX2 MEAN= -2.718

D= 0.76E-04 SQ M/SEC K= 0.15E-04 SQ M/SEC

Y/H	EXP U/UF	COMP U/UF	EXP S/SO	COMP S/SO
0.077	3.35	3.23	0.12	0.13
0.154	3.29	3.02	0.13	0.15
0.231	3.05	2.68	0.16	0.19
0.308	2.51	2.27	0.24	0.22
0.385	1.95	1.78	0.33	0.27
0.462	1.35	1.26	0.42	0.33
0.539	0.87	0.73	0.51	0.40
0.616	0.45	0.21	0.60	0.48
0.693	-0.03	-0.27	0.68	0.57
0.770	-0.33	-0.69	0.73	0.66
0.847	-0.78	-1.02	0.76	0.74
0.924	-1.06	-1.23	0.93	0.85

TABLE A22

COMPUTED AND EXPERIMENTAL VELOCITY AND SALINITY DISTRIBUTIONS

DELFT TEST 121

X/LI = 0.54

S MEAN= 0.284 DS/DX MEAN= -0.907 D2S/DX2 MEAN= 4.428

D= 0.84E-04 SQ M/SEC K= 0.59E-05 SQ M/SEC

Y/H	EXP U/UF	COMP U/UF	EXP S/SO	COMP S/SO
0.077	2.41	2.79	0.08	0.05
0.154	2.64	2.62	0.08	0.08
0.231	2.53	2.35	0.10	0.13
0.308	2.20	2.02	0.12	0.18
0.385	2.05	1.53	0.17	0.24
0.462	1.52	1.21	0.24	0.29
0.539	1.04	0.78	0.32	0.34
0.616	0.63	0.37	0.40	0.38
0.693	0.20	-0.02	0.48	0.41
0.770	-0.23	-0.36	0.53	0.43
0.847	-0.53	-0.62	0.57	0.45
0.924	1.04	-0.79	0.60	0.46

TABLE A23

COMPUTED AND EXPERIMENTAL VELOCITY AND SALINITY DISTRIBUTIONS

DELFT TEST 121

X/L1 = 0.68

S MEAN= 0.182 DS/DX MEAN= -0.746 D2S/DX2 MEAN= -2.039

D= 0.90E-04 SQ M/SEC K= 0.15E-04 SQ M/SEC

Y/H	EXP U/UE	COMP U/UE	EXP S/SO	COMP S/SO
0.077	2.41	2.55	0.05	0.02
0.154	2.39	2.40	0.05	0.03
0.231	2.31	2.17	0.05	0.04
0.308	2.22	1.88	0.06	0.07
0.385	1.70	1.54	0.10	0.10
0.462	1.42	1.19	0.14	0.13
0.539	1.06	0.81	0.19	0.17
0.616	0.69	0.45	0.26	0.21
0.693	0.40	0.12	0.31	0.26
0.770	0.09	-0.17	0.35	0.31
0.847	-0.34	-0.40	0.39	0.36
0.924	-0.96	-0.55	0.42	0.42

TABLE A24

COMPUTED AND EXPERIMENTAL VELOCITY AND SALINITY DISTRIBUTIONS

OUTLET TEST 121

X/L1 = 0.81

S MEAN= 0.000 dS/dX MEAN= -0.525 d2S/dX2 MEAN= 3.828

D= 0.11E-03 SQ M/SEC K= 0.10E-04 SQ M/SEC

Y/H	EXP U/UF	COMP U/UF	EXP S/SO	COMP S/SO
0.077	1.73	1.94	0.02	-0.02
0.154	1.79	1.85	0.02	-0.01
0.231	1.76	1.71	0.02	0.00
0.309	1.59	1.53	0.02	0.02
0.386	1.30	1.33	0.03	0.04
0.462	1.19	1.11	0.04	0.07
0.539	1.01	0.89	0.06	0.09
0.616	0.74	0.67	0.10	0.11
0.693	0.73	0.44	0.14	0.13
0.770	0.47	0.29	0.18	0.16
0.847	0.31	0.15	0.20	0.17
0.924	0.17	0.05	0.21	0.20

TABLE A25

COMPUTED AND EXPERIMENTAL VELOCITY AND SALINITY DISTRIBUTIONS

OUTLET TEST 121

X/LI = 0.99

V MEAN= 0.024 DS/DX MEAN= -0.249 D2S/DX2 MEAN= 1.755

D= 0.10E-03 SQ M/SEC K= 0.15E-04 SQ M/SEC

Y/H	EXP U/UF	COMP U/UF	EXP S/SO	COMP S/SO
0.077	1.18	1.41	0.01	-0.00
0.154	1.10	1.37	0.01	-0.00
0.231	1.17	1.31	0.01	0.00
0.308	1.05	1.23	0.01	0.01
0.385	1.07	1.14	0.01	0.01
0.462	1.14	1.05	0.02	0.02
0.539	0.94	0.95	0.02	0.02
0.616	0.83	0.85	0.03	0.03
0.693	0.65	0.77	0.04	0.04
0.770	0.59	0.69	0.05	0.04
0.847	0.44	0.63	0.06	0.05
0.924	0.23	0.59	0.06	0.06

TABLE A26

COMPUTED AND EXPERIMENTAL VELOCITY AND SALINITY DISTRIBUTIONS

DELFT TEST 122

X/LI = 0.29

U MEAN= 0.502 DS/DX MEAN= -1.000 D2S/DX2 MEAN= 1.016

E= 0.72E-01 SQ M/SEC K= 0.10E-04 SQ M/SEC

Y/H	EXP U/UF	COMP U/UF	EXP S/SO	COMP S/SO
0.077	3.31	2.95	0.13	0.15
0.154	2.89	2.74	0.16	0.19
0.231	2.45	2.47	0.27	0.23
0.308	2.00	2.11	0.37	0.29
0.385	1.81	1.68	0.44	0.36
0.462	1.31	1.23	0.52	0.43
0.539	0.91	0.74	0.61	0.52
0.616	0.40	0.31	0.69	0.61
0.693	0.03	-0.11	0.78	0.69
0.770	-0.24	-0.48	0.82	0.77
0.847	-0.48	-0.76	0.85	0.84
0.924	-0.83	-0.95	0.87	0.90

TABLE A27

COMPUTED AND EXPERIMENTAL VELOCITY AND SALINITY DISTRIBUTIONS

DELFT TEST 122

X/LI = 0.43

S MEAN= 0.361 DS/DX MEAN= -1.022 D2S/DX2 MEAN= -1.323

D= 0.75E-04 SQ M/SEC K= 0.15E-04 SQ M/SEC

Y/H	EXP U/UF	COMP U/UF	EXP S/SO	COMP S/SO
0.077	3.23	2.99	0.08	0.05
0.154	2.94	2.70	0.09	0.07
0.231	2.73	2.42	0.10	0.10
0.308	2.36	2.07	0.17	0.15
0.385	1.84	1.66	0.25	0.20
0.462	1.34	1.22	0.34	0.27
0.539	0.96	0.77	0.43	0.35
0.616	0.58	0.33	0.50	0.43
0.693	0.07	-0.08	0.61	0.52
0.770	-0.22	-0.43	0.67	0.61
0.847	-0.52	-0.71	0.71	0.70
0.924	-0.92	-0.89	0.74	0.79

TABLE A28

COMPUTED AND EXPERIMENTAL VELOCITY AND SALINITY DISTRIBUTIONS

DELFT TEST 122

X/LI = 0.57

E MEAN= 0.220 DS/DX MEAN= -0.922 D2S/DX2 MEAN= 4.124

E= 0.73E 04 SQ M/SEC K= 0.60E-05 SQ M/SEC

Y/H	EXP U/UE	COMP U/UE	EXP S/SO	COMP S/SO
0.077	2.39	2.52	0.04	-0.01
0.154	2.33	2.37	0.05	0.02
0.231	2.26	2.15	0.05	0.07
0.303	2.21	1.86	0.07	0.12
0.385	2.06	1.53	0.10	0.18
0.462	1.71	1.19	0.16	0.23
0.538	1.32	0.82	0.23	0.27
0.615	0.82	0.46	0.30	0.31
0.693	0.42	0.14	0.39	0.34
0.770	0.07	-0.15	0.45	0.37
0.847	-0.31	-0.37	0.49	0.39
0.923	-0.85	-0.52	0.53	0.40

TABLE A29

COMPUTED AND EXPERIMENTAL VELOCITY AND SALINITY DISTRIBUTIONS

DELFT TEST 122

X/LI = 0.71

S MEAN= 0.125 DS/DX MEAN= -0.457 D2S/DX2 MEAN= -1.815

D= 0.843E-04 SQ M/SEC K= 0.185E-05 SQ M/SEC

Y/H	EXP U/UB	COMP U/UB	EXP S/SO	COMP S/SO
0.077	1.70	2.10	0.03	-7.43
0.154	1.73	1.99	0.02	-7.40
0.231	1.71	1.83	0.03	-7.23
0.308	1.74	1.62	0.03	-6.95
0.385	1.63	1.39	0.05	-6.48
0.462	1.37	1.13	0.07	-5.70
0.538	1.12	0.87	0.11	-4.41
0.615	0.87	0.61	0.17	-2.34
0.692	0.60	0.37	0.22	0.49
0.770	0.30	0.17	0.27	3.64
0.847	-0.08	0.01	0.30	12.10
0.924	-0.34	-0.10	0.33	20.11

TABLE A30

COMPUTED AND EXPERIMENTAL VELOCITY AND SALINITY DISTRIBUTIONS

JAMES RIVER 18 JUNE - 23 JUNE

X/LI = [illegible]19

S MEAN= [illegible]767 dS/DX MEAN= -1.419 D2S/DX2 MEAN= -4.148

U= [illegible]E-03 SQ M/SEC K= [illegible]16E-03 SQ M/SEC

SBT

Y/H	EXP U/UF	COMP U/UF	EXP S/S^	COMP S/S
[illegible]	29.21	20.39	[illegible].64	[illegible].64
[illegible]	21.23	19.42	[illegible].64	[illegible].64
[illegible]	14.52	17.62	[illegible].64	[illegible].65
[illegible]	8.71	15.13	[illegible].65	[illegible].65
[illegible]	3.27	12.79	[illegible].66	[illegible].66
[illegible]	-2.36	8.62	[illegible].68	[illegible].68
[illegible]	-8.17	4.88	[illegible].71	[illegible].69
[illegible]	-13.97	1.[illegible]	[illegible].73	[illegible].7[illegible]
[illegible]	-16.51	-2.88	[illegible].74	[illegible].72
[illegible]	-19.63	-6.62	[illegible].74	[illegible].73
[illegible]	-16.33	-10.78	[illegible].75	[illegible].75
[illegible]	-15.67	-13.13	[illegible].75	[illegible].76
[illegible]	-13.43	-15.62	[illegible].76	[illegible].77
[illegible]	-16.70	-17.42	[illegible].76	[illegible].78

TABLE A31

COMPUTED AND EXPERIMENTAL VELOCITY AND SALINITY DISTRIBUTIONS

JAMES RIVER 18 JUNE - 23 JUNE

X/LI = [illegible]

S MEAN= [illegible] dS/DX MEAN= -2.080 D2S/DX2 MEAN= -8.295

D= [illegible] SQ M/SEC K= [illegible] SQ M/SEC

Y/H	EXP U/UF	COMP U/UF	EXP S/S0	COMP S/S0
[illegible]	16.49	14.36	[illegible].46	[illegible].46
[illegible]	13.50	13.69	[illegible].46	[illegible].46
[illegible]	10.52	12.45	[illegible].46	[illegible].46
[illegible]	7.25	11.74	[illegible].46	[illegible].47
[illegible]	4.55	8.64	[illegible].46	[illegible].48
[illegible]	1.42	6.25	[illegible].47	[illegible].49
[illegible]	-2.13	3.68	[illegible].50	[illegible].51
[illegible]	-5.69	1.09	[illegible].51	[illegible].52
[illegible]	-8.67	-1.67	[illegible].56	[illegible].54
[illegible]	-10.19	-4.25	[illegible].57	[illegible].55
[illegible]	-10.09	-6.64	[illegible].57	[illegible].56
[illegible]	-9.95	-8.73	[illegible].58	[illegible].58
[illegible]	-10.80	-10.45	[illegible].58	[illegible].59
[illegible]	-11.86	-11.69	[illegible].59	[illegible].60

TABLE A32

COMPUTED AND EXPERIMENTAL VELOCITY AND SALINITY DISTRIBUTIONS

JAMES RIVER 18 JUNE - 23 JUNE

X/LI = 0.42

S MEAN= 0.214 DS/DX MEAN= -2.851 D2S/DX2 MEAN= -4.148

D= 0.12E-02 SQ M/SEC K= 0.35E-03 SQ M/SEC

Y/H	EXP U/UF	COMP U/UF	EXP S/S0	COMP S/S
0.10	17.16	8.99	0.17	0.16
0.17	7.44	8.59	0.17	0.17
0.23	1.98	7.85	0.17	0.17
0.30	-1.19	6.82	0.17	0.18
0.37	-3.27	5.57	0.18	0.18
0.43	-5.16	4.14	0.18	0.19
0.50	-6.45	2.60	0.20	0.20
0.57	-7.24	1.00	0.22	0.21
0.63	-7.74	-0.60	0.24	0.22
0.70	-7.94	-2.14	0.24	0.23
0.77	-7.94	-3.57	0.25	0.24
0.83	-7.94	-4.82	0.25	0.25
0.90	-7.94	-5.85	0.25	0.26
0.97	-7.94	-6.59	0.26	0.27

TABLE A33

COMPUTED AND EXPERIMENTAL VELOCITY AND SALINITY DISTRIBUTIONS

JAMES RIVER 26 JUNE - 7 JULY

X/LI = 0.19

S MEAN= 0.713 DS/DX MEAN= -1.342 D2S/DX2 MEAN= -5.311

D= 0.35E-03 SQ M/SEC K= 0.26E-03 SQ M/SEC

Y/H	EXP U/UF	COMP U/UF	EXP S/S0	COMP S/S
0.16	35.70	28.15	0.66	0.67
0.17	28.56	26.79	0.67	0.67
0.23	21.42	24.28	0.67	0.67
0.30	13.63	20.79	0.67	0.68
0.37	4.11	16.52	0.68	0.69
0.43	-5.41	11.67	0.68	0.69
0.50	-11.92	6.44	0.70	0.70
0.57	-16.01	1.00	0.72	0.71
0.63	-18.82	-4.43	0.73	0.72
0.70	-21.20	-9.67	0.74	0.73
0.77	-22.72	-14.51	0.75	0.74
0.83	-24.23	-18.78	0.75	0.75
0.90	-25.16	-22.27	0.75	0.75
0.97	-25.75	-24.79	0.76	0.76

TABLE A34

COMPUTED AND EXPERIMENTAL VELOCITY AND SALINITY DISTRIBUTIONS

JAMES RIVER 26 JUNE - 7 JULY

X/LI = [illegible].29

S MEAN= [illegible].538 DS/DX MEAN= -2.159 D2S/DX2 MEAN= -1[illegible].622

D= [illegible].65E-03 SQ M/SEC K= [illegible].31E-03 SQ M/SEC

Y/H	EXP U/UF	COMP U/UF	EXP S/S[illegible]	COMP S/S
[illegible]	20.51	19.43	[illegible].48	0.48
[illegible].17	17.12	18.51	[illegible].49	[illegible].49
[illegible].25	13.56	16.8[illegible]	0.49	[illegible].49
[illegible].30	[illegible].66	14.43	[illegible].49	[illegible].50
[illegible].37	5.93	11.54	[illegible].5[illegible]	[illegible].5[illegible]
[illegible].43	1.53	8.24	[illegible].51	[illegible].51
[illegible].50	-2.54	4.69	[illegible].52	[illegible].52
[illegible].57	-5.93	1.[illegible]0	[illegible].54	[illegible].54
[illegible].63	-8.64	-2.68	[illegible].56	[illegible].55
[illegible].70	-11.86	-6.24	[illegible].57	[illegible].56
[illegible].77	-15.59	-9.53	[illegible].57	[illegible].57
[illegible].83	-18.47	-12.43	[illegible].57	[illegible].58
[illegible].90	-19.83	-14.8[illegible]	[illegible].58	[illegible].59
[illegible].97	-19.49	-16.51	0.59	[illegible].59

TABLE A35

COMPUTED AND EXPERIMENTAL VELOCITY AND SALINITY DISTRIBUTIONS

JAMES RIVER 26 JUNE - 7 JULY

K/LI = 0.41

S MEAN= 0.216 DS/DX MEAN= -3.113 D2S/DX2 MEAN= -5.311

D= 0.11E-02 SQ M/SEC K= 0.45E-03 SQ M/SEC

Y/H	EXP U/UF	COMP U/UF	EXP S/S	COMP S/S
0.10	20.46	11.48	0.18	0.17
0.17	11.12	10.96	0.18	0.17
0.23	3.19	9.99	0.18	0.18
0.30	-1.89	8.64	0.18	0.18
0.37	-5.09	6.99	0.18	0.19
0.43	-6.50	5.12	0.19	0.20
0.50	-6.86	3.19	0.20	0.21
0.57	-6.98	1.[illegible]	0.22	0.21
0.63	-7.10	-1.10	0.23	0.22
0.70	-7.81	-3.12	0.24	0.23
0.77	-9.93	-4.99	0.24	0.24
0.83	-12.06	-6.64	0.25	0.25
0.90	-13.01	-7.98	0.25	0.25
0.97	-13.01	-8.96	0.25	0.26

TABLE A36

COMPUTED AND EXPERIMENTAL VELOCITY AND SALINITY DISTRIBUTIONS

JAMES RIVER 17 JULY - 21 JULY

X/LI = [illegible]

S MEAN= [illegible] dS/DX MEAN= -1.216 D2S/DX2 MEAN= -4.746

D= [illegible] SQ M/SEC K= [illegible] SQ M/SEC

Y/H	EXP U/UF	COMP U/UF	EXP S/SC	COMP S/SC
[illegible]	29.94	25.02	[illegible]	[illegible]
[illegible]	23.71	23.82	[illegible]	[illegible]
[illegible]	16.44	21.60	[illegible]	[illegible]
[illegible]	9.52	18.51	[illegible]	[illegible]
[illegible]	3.63	14.73	[illegible]	.66
[illegible]	-1.90	10.44	[illegible]	[illegible]
[illegible]	-7.96	5.81	[illegible]	[illegible]
[illegible]	-12.81	1.[illegible]	[illegible]	[illegible]
[illegible]	-2[illegible]	-3.8[illegible]	[illegible]	[illegible]
[illegible]	-21.98	-8.44	[illegible]	[illegible]
[illegible]	-2[illegible]	-12.73	[illegible]	[illegible]
[illegible]	-19.56	-16.5[illegible]	[illegible]	[illegible]
[illegible]	-19.04	-19.59	[illegible]	[illegible]
[illegible]	-19.04	-21.82	[illegible]	[illegible]

TABLE A37

COMPUTED AND EXPERIMENTAL VELOCITY AND SALINITY DISTRIBUTIONS

JAMES RIVER 17 JULY - 21 JULY

X/LI = 0.31

S MEAN= 0.520 DS/DX MEAN= -1.980 D2S/DX2 MEAN= -9.491

D= 0.65E-03 SQ M/SEC K= 0.21E-03 SQ M/SEC

Y/H	EXP U/UF	COMP U/UF	EXP S/S0	COMP S/S0
0.10	17.76	15.14	0.45	0.44
0.17	14.51	14.43	0.46	0.45
0.23	16.71	13.12	0.46	0.45
0.30	7.05	11.31	0.46	0.46
0.37	4.20	9.08	0.47	0.47
0.43	1.49	6.56	0.47	0.48
0.50	-1.90	3.83	0.51	0.50
0.57	-4.88	1.00	0.53	0.51
0.63	-6.91	-1.83	0.55	0.53
0.70	-8.95	-4.56	0.56	0.55
0.77	-10.71	-7.08	0.57	0.56
0.83	-12.20	-9.31	0.57	0.58
0.90	-13.15	-11.12	0.57	0.59
0.97	-13.42	-12.43	0.58	0.61

TABLE A38

COMPUTED AND EXPERIMENTAL VELOCITY AND SALINITY DISTRIBUTIONS

JAMES RIVER 17 JULY - 21 JULY

X/LI = [illegible]0.43

S MEAN= [illegible]0.21[illegible] dS/DX MEAN= -2.872 D2S/DX2 MEAN= -4.746

D= [illegible].[illegible]0E-[illegible]2 SQ M/SEC K= 0.50E-[illegible]3 SQ M/SEC

Y/H	EXP U/UF	COMP U/UF	EXP S/S[illegible]	COMP S/S[illegible]
[illegible].1[illegible]	17.5[illegible]	1[illegible].3[illegible]	[illegible].17	[illegible].17
[illegible].17	9.56	9.84	[illegible].17	[illegible].17
[illegible].23	[illegible].74	8.97	[illegible].17	[illegible].17
[illegible].30	-1.51	7.78	[illegible].17	[illegible].18
[illegible].37	-4.26	6.32	[illegible].17	[illegible].18
[illegible].43	-6.06	4.66	[illegible].18	[illegible].19
[illegible].50	-7.29	2.86	[illegible].19	[illegible].20
[illegible].57	-8.33	1.[illegible]	[illegible].21	[illegible].21
[illegible].63	-8.99	-[illegible].86	[illegible].22	[illegible].22
[illegible].70	-9.65	-2.65	[illegible].23	[illegible].23
[illegible].77	-10.03	-4.32	[illegible].24	[illegible].23
[illegible].83	-10.22	-5.78	[illegible].24	[illegible].24
[illegible].90	-10.31	-6.97	[illegible].24	[illegible].25
[illegible].97	-10.31	-7.84	[illegible].25	[illegible].25